Australian Government
Department of Defence
Defence Science and
Technology Organisation

A Review of Australian and New Zealand Investigations on Aeronautical Fatigue During the Period April 2005 to March 2007

Graham Clark

Air Vehicles Division
Defence Science and Technology Organisation

DSTO-TN-0747

ABSTRACT

This document has been prepared for presentation to the 30th Conference of the International Committee on Aeronautical Fatigue scheduled to be held in Naples, Italy, 14th and 15th May 2007. Brief summaries and references are provided on the aircraft fatigue research and associated activities of research laboratories, universities, and aerospace companies in Australia and New Zealand during the period April 2005 to March 2007. The review covers fatigue–related research programs as well as fatigue investigations on specific military and civil aircraft.

Published by

Air Vehicles Division
DSTO Defence Science and Technology Organisation
506 Lorimer St
Fishermans Bend, Victoria 3207 Australia

Telephone: (03) 9626 7000
Fax: (03) 9626 7999

AR-013-873
April 2007

APPROVED FOR PUBLIC RELEASE

A Review of Australian and New Zealand Investigations on Aeronautical Fatigue During the Period April 2005 to March 2007

Executive Summary

The Australasian delegate to the International Committee on Aeronautical Fatigue (ICAF) is responsible for preparing a review of aeronautical fatigue work in Australia and New Zealand for presentation at the biennial ICAF conference. The Defence Science and Technology Organisation (DSTO) supports the Australasian delegate to ICAF by publishing the review as a DSTO document. This document later forms a chapter of the ICAF conference minutes published by the conference host nation. The format of the review reflects ICAF requirements.

Contents

8. Australasian Review

8.1 INTRODUCTION

This document presents a review of Australian and New Zealand work in fields relating to aeronautical fatigue in the period 2005 to 2007, and is made up from inputs from the organisations listed below. The author acknowledges these contributions with appreciation. Enquiries should be addressed to the person identified against the item of interest.

DSTO	Defence Science and Technology Organisation, 506 Lorimer Street, Fishermans Bend VIC 3207, Australia
ADFA	Australian Defence Force Academy, University of New South Wales, Canberra, Australia
CASA	Civil Aviation Safety Authority, 16 Furzer St., Phillip, ACT 2606, Australia.
DTA	Defence Technology Agency, Auckland Naval Base, New Zealand
CRC-ACS	Cooperative Research Centre for Advanced Composite Structures. 506 Lorimer Street, Fishermans Bend, VIC 3207, Australia.
Aerostructures Australia	Level 3, 210 Kings Way, South Melbourne, VIC 3205, Australia.
Structural Monitoring Systems Ltd	Level 1, 5/15 Walters Drive, Osborne Park, Western Australia, 6017, Australia.
DGTA	Director General Technical Airworthiness, RAAF Williams, Laverton Vic 3027, Australia
Boeing Australia Limited	363 Adelaide St, PO Box 767, Brisbane QLD 4001, Australia
University of Newcastle	Dept of Civil Engineering, Univ. Of Newcastle, Newcastle, NSW, Australia
Monash University	Dept of Mechanical Engineering, PO Box 72, Monash University, VIC 3800, Australia.

8.2 FATIGUE INVESTIGATIONS ON MILITARY AIRCRAFT

8.2.1 Using Full-Scale Fatigue Testing Results to Life Aircraft Fleets (L.Molent, S.Barter and M.McDonald, DSTO) – Paper to be presented at ICAF 2007 Symposium

Paper to be presented at ICAF 2007 Symposium:

The ability to understand and predict fatigue lives remains a key technical factor affecting modern aircraft fleets which are required to operate safely up to their design lives and sometimes beyond. An essential element of the airframe design and certification process is the full-scale fatigue test, where an airframe is subjected to realistic variable amplitude loads which are predicted to be representative of those that occur over the life-of-type. The results from these fatigue tests are then applied to the lifing of aircraft fleet whose usage may sometime vary considerably from the test spectrum. Therefore a tool capable of interpolating between fleet and test spectra is required.

Experience has shown that traditional fatigue prediction tools do not always perform well in predicting the lives of modern highly optimised airframes. This paper summarises some recent semi-empirical models that appear to be capable of producing more accurate fatigue life predictions for many full-scale fatigue test results. Instead of relying on constant amplitude crack growth data the models use variable amplitude data obtained experimentally under more directly relevant conditions. The models are founded on the observation that for cracks in typical aircraft structural details, as a first approximation the lead cracks grow such that the log of the crack depth is proportional to number of cycles or spectrum loading blocks. The implications of this exponential growth are discussed leading to a reconciliation of a Paris-type growth model with that of the earlier Frost and Dugdale stress-cubed growth relationship.

8.2.2 Flaw Identification through the Application of Loading (FINAL Program) (B.Dixon, DSTO)

A teardown of ex-service F/A-18 wing attachment centre barrels is being conducted. Prior to teardown, each centre barrel is cycled in a test rig until failure in order to increase the amount of representative damage that can be found with Non-Destructive Testing during teardown. Thus far, six centre barrels have been cycled to failure. Three of these have been completely inspected and the defects found on them have been fully documented, while two more are in the process of final assessment. Typically, fatigue cracks have been found in over sixty locations on each centre barrel.

Quantitative fractography has been conducted on the failure locations of the first four centre barrels cycled, as well as at other areas of interest for the maintenance of RAAF F/A-18 structural integrity. The crack growth during the cycling at DSTO has generally been approximately exponential. However, some cracks have been observed to slow relative to their original, approximately exponential rate. This is thought to have been the result of a change in the effective stress field caused by measures such as cold expansion and ring pad coining at holes, see Figure 1 for examples of cracking from cold expanded holes where the process was applied, and also where it was inadvertently not applied.

Quantitative fractography has yielded information about the types of discontinuities from which cracks grow in fleet service (see and the rate of crack growth that occurs at these critical locations. This information is being used to validate repairs that are being applied to the fleet for life extension. Damage has also been introduced into a number of the centre barrels at critical locations to gain more information about the degree of importance of these locations and the measures necessary to gain the most life out of these locations in the future.

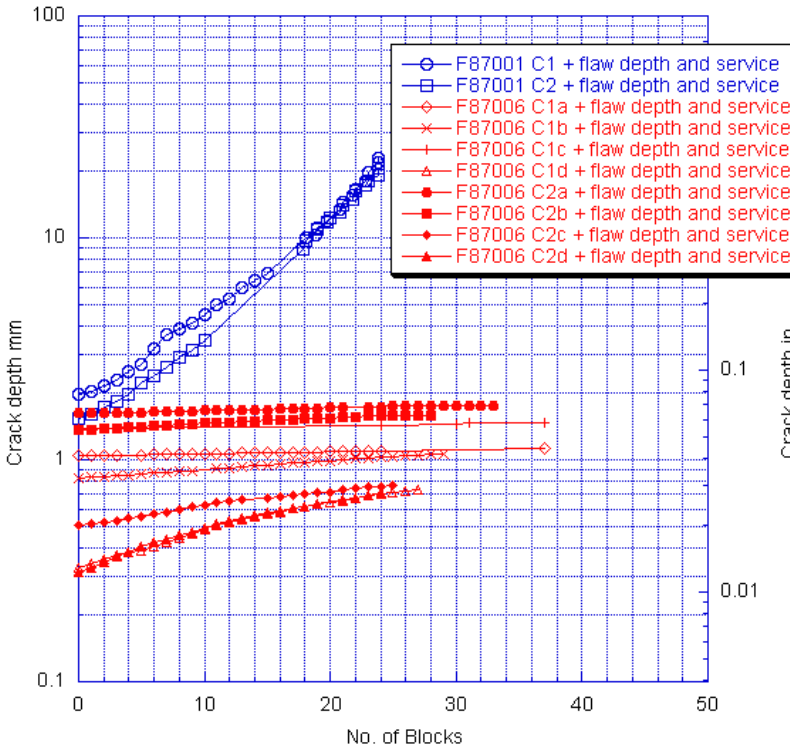

Figure 1: Crack growth from a hole in the centre barrel, with (lower slope) and without (higher slope) the effects of cold-expansion

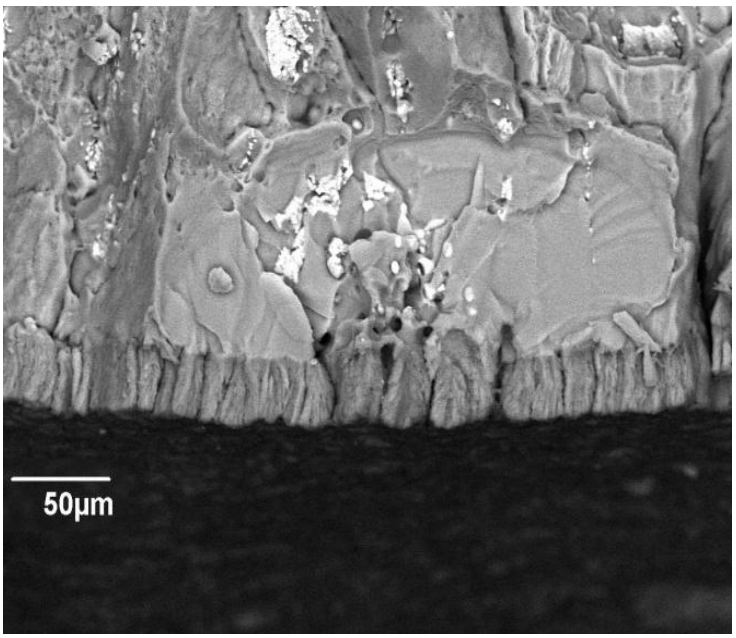

Figure 2: A view of one of the fatigue crack origins from the fifth centre barrel cycled (Scanning Electron Micrograph). Here the small crack grew from etched out inclusions beneath the Ion Vapour Deposited coating

References

1. Dixon, B. and Molent, L., "Ex-Service F/A-18 Centre Barrel Fatigue Flaw Identification Test Plan", DSTO-TR-1426, May 2003.
2. Dixon, B., Molent, L., Barter, S. and Mau, V., "Flaw Identification through the Application of Loads: Teardown of the F/A-18 Centre Barrel from CF-18 188747", DSTO-TR-1660, Dec. 2004.
3. Molent, L, Dixon, B., Barter, S. A., Medved, J. and Nguyen, Q. The *FINAL* Program of Enhanced Teardown for a Fighter Aircraft. proc. ICAF 2005 Hamburg, Jun 8-10, 2005.
4. Dixon, B., Molent, L., Barter, S. and Mau, V., "Flaw Identification through the Application of Loads: Teardown of the F/A-18 Centre Barrel from USN F/A-18D BuNo 163507", DSTO-TR-1740, Jul. 2005.

8.2.3 The Effective Block Approach to Crack Growth Modelling (L.Molent, M.McDonald, S.Barter, P.White, DSTO)

Accurate fatigue prediction tools are essential for fatigue life management. In the case of the RAAF F/A-18 there is a wealth of crack growth data generated through quantitative fractography (QF). Unfortunately conventional damage models (eg. AFGROW, Fastran etc) provided poor representations of these data [5], and this prompted the development of a predictive method tailored to variable amplitude data.

A key concept used is one where a repeating "block" of loading is applied throughout the fatigue life, sufficiently often that the blocks can be treated in a similar manner to single cycles in constant-amplitude loading. This characteristic approach to fatigue life prediction was first proposed by Paris [6]. The basic hypothesis is that the variations of the crack tip fields are describable in terms of some characteristic stress-related measure, for example, Root Mean Squared (RMS) of the stress intensity factor range (ΔK_{RMS}) (or the peak value).

Analysis of fatigue cracking over many decades has provided DSTO with a capability to produce detailed crack growth information for variable-amplitude loading under service conditions or laboratory conditions which closely resemble real service conditions. The methods being developed capitalize on the quality of this data and are aimed at providing useful tools for fatigue management. They have been reviewed in detail [7,9], and this approach has been used successfully on F/A-18 representative titanium coupon specimens at different stress levels to life a fracture critical component [8].

One simple formulation is to use the well-known Paris equation and apply it to variable amplitude loading:

The first step in the process was to derive a crack growth resistance relationship based on the quantitative fractography (QF) coupon data for several fighter aircraft load sequences. To do this, the crack growth gradient (da/dB where B= spectrum blocks) and ΔK_{Peak} ($=\beta\ \Delta\sigma_{Peak}\ \sqrt{(\pi a)}$) were calculated for each consecutive QF data point. In this way the "average" crack growth *per block* is captured, thus accounting for any inherent sequence effects. Typical results for titanium coupons and a complex F/A-18 spectrum are shown in Figure 3. Note that the x-axis was plotted as crack depth *a* here. Here the slope (equivalent to a Paris CA exponent m) was found to be 2 and the intercept (C) varied with the spectrum and stress level (with material and geometry constant). A Paris exponent of approximately two has been found to hold for a large range of variable amplitude spectra and materials [10].

A key outcome from this analysis is that by determining C and m, it appears to be possible to use these parameters, determined using one particular fighter sequence, to predict behaviour under a different sequence. This involves coupon-derived data similar to that in Figure 3, derived for just one sequence, and the use of conventional fatigue prediction models – which can be fairly inaccurate in direct prediction – simply as a transfer tool. The extent to which this approach (described in [7,11]) may be applied (eg. over what type of VA sequence) has not yet been established, and will be the subject of further work. However, the current lifing of the RAAF F-111 is based on the effective Block Approach (EBA) [12].

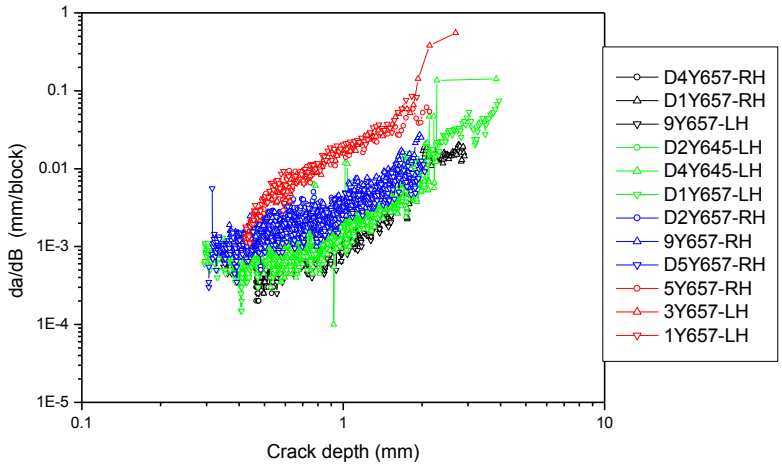

Figure 3: Crack growth rates plotted versus crack depth for un-notched Ti coupons under 4 peak load levels of an F/A-18 manoeuvre plus buffet spectrum

References.

5. Pell, R.A., Molent, L., and Green, A.J., The Fractographic Examination of F/A-18 Aluminium Alloy 7050-T7451 Bulkhead Representative Coupons Tested Under Two Service Spectra and Two Stress Levels, DSTO-TR-1629, Oct 2004.
6. Paris P.C., The Growth of Cracks due to Variation in Loads, Ph.D. Thesis, Lehigh University, Bethlehem, Pennsylvania, 1960.
7. M. McDonald, L. Molent and A. Green, Assessment of Fatigue Crack Growth Prediction Models for F/A-18 Representative Spectra and Material, DSTO-RR-0312, Apr 2006.
8. W. Zhuang, S.A. Barter, M. McDonald and L. Molent, Fatigue Crack Growth Life Assessment of the F/A-18 Aft Fuselage Frames (Y645 and Y657), DSTO-TR-1826, Feb 2006.
9. W. Zhuang, S. Barter and L. Molent, Flight-by-flight fatigue crack growth life assessment. Proceedings International Conference on Fatigue Damage of Structural Materials VI, Hyannis, USA, September 2006. Accepted Feb 2007 International Journal of Fatigue.
10. Molent, L, Jones, R, Barter, S and Pitt, S. Recent developments in fatigue crack growth assessment, Int J. of Fatigue, Vol 28/12 (2006) 1759-1768.
11. Barter, S, McDonald, M and Molent L, Fleet fatigue life interpretation from full-scale and coupon fatigue tests – a simplified approach, USAF ASIP Conference, Memphis, 29 Nov – 1 Dec 2005
12. Walker K, McDonald M, Braemar R and Swanton G. F-WELD fatigue test and associated data interpretation plan – Issue one, DSTO-CR-2006-0035, Oct 2006.

8.2.4 The F/A-18 Fatigue Crack Growth Data Compendium – Update (L.Molent and J.Sun, DSTO)

One of the primary factors that limit the life of metallic aircraft structures is fatigue cracking under variable amplitude cyclic loading. In highly-stressed fighter aircraft, material defects or flaws are often initiators of fatigue cracking, and initial flaws typically 0.01mm in size are widespread. Rarer flaws substantially larger than this (in extreme cases, of mm size) are the ones which need to be considered to provide limits to fatigue life of the fleet aircraft. During the application of flight loads, these fatigue cracks propagate at approximately an exponential rate with time in service.

Various types of ‘fatigue initiating mechanisms’ have been known to commence the fatigue cracking. These include inter-metallic particles; etch pits and material folds due to bead shot peening. The fatigue life of any given metallic structure correlates to what is known as the Equivalent Pre-crack Size (EPS) of these fatigue crack-initiating defects.

A better understanding of the factors that influence EPS has the potential to facilitate more accurate predictions of fatigue life, and thus the potential to extend the safe life of aircraft structures and enhance Australian Defence capability.

Many aluminium alloy 7050-T7451 coupons have been fatigue tested at the Air Vehicles Division of DSTO. During these tests, various F/A-18 representative spectra were repeatedly applied to the coupons, at various stress levels, until failure. In addition, much data are available from cracks in various F/A-18 full-scale structural fatigue tests.

Quantitative fractography was conducted for many of these specimens, producing crack growth data that have been considered useful in fatigue analysis. A completed report presents a collation of DSTO F/A-18 crack growth information known as the F/A-18 Fatigue Crack Growth Data Compendium [1]. Using the data in this compendium, various techniques were used to estimate the EPS. The report presents an assessment of the size of fatigue crack initiating defects and damage types found in these specimens. Further it was determined that the applied stress appeared to have little bearing on the initial defect size or the damage type. However, the surface finish appeared to have decisive influence in governing the type of fatigue damage induced. A key element of further work is to identify the larger flaws which have the potential to give short service lives in fleet aircraft. Recent work has concentrated on the optimal distribution fit for the EPS data [2], see Figure 4 for example.

A sound understanding of the factors influencing the EPS is important to the task of predicting the fatigue life of aircraft structures and thus, the outcome of this investigation is valuable for the enhancement of Australian defence capability. The probabilistic risk assessment method can make use of the data derived within the compendium.

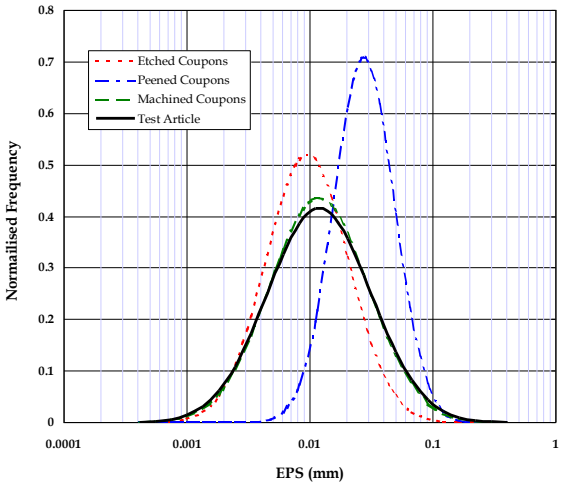

Figure 4: Log-normal curves projected for a given population. Test articles - 97 data points, machined coupon specimens – 96 data points, peened coupon specimens - 20 points, etched coupon specimens - 120 points

References

1. Molent, L, Q. Sun and A. Green, Characterisation of Equivalent Initial Flaw Sizes in 7050 Aluminium Alloy, J. Fatigue and Fracture of Engineering Materials and Structures 29 (2006); 916-937.
2. L. Molent and Q. Sun, Distribution of Equivalent Pre-Crack Size in 7050 Aluminium Alloy, DSTO-TR-1700, March 2006.

8.2.5 F/A-18 Aircraft Structural Integrity Support (J.Moews, Aerostructures)

Aerostructures is undertaking several activities providing support to the management of the RAAF F/A-18 fleet.

8.2.5.1 F/A 18 Fatigue Test Interpretation

The F/A-18 International Follow-On Structural Test Program (IFOSTP) was established to determine the F/A-18 safe life under RAAF usage. With the completion of this program, test interpretation now establishes where critical structure suffered damage and how it can be managed in service.

Aft Fuselage and Empennage Test Interpretation

Using DEF STAN 00-970, Aerostructures developed a fatigue management methodology for the aft fuselage and empennage which combines safe life and safety by inspection methodologies. Critical structure with damage during fatigue testing was the priority.

Mean and safe SN curves, developed in accordance with DEF STAN 00-970, were used to calculate scatter factors that determined whether fatigue test results demonstrated sufficient safe life. Where necessary, residual strength calculations were made to extend the safe life using a simplified crack growth model and fractographic crack growth rates. For inspectable maintenance critical parts with inadequate safe life, inspection intervals were established.

A number of maintenance critical parts (which did not exhibit damage on the fatigue test) were identified, where the test duration was not long enough to clear the structure for full life against DEF STAN 970 requirements. For these candidate locations strain life analyses were performed to determine KtSigma Curves for the given material and spectra. The curves were pegged to the lives of reference locations nearby which suffered fatigue damage during the test. This approach allowed establishing the safe lives of these candidate locations.

Wing Test Interpretation

Based on the requirements DEF STAN 970, a fatigue management methodology for the F/A-18 Inner Wing (IW) structure was developed by the RAAF ASI-DGTA. This methodology proposes the pooling of results from various F/A-18 fatigue tests. Scatter factors were developed IAW DEF STAN 970 safe SN requirements based on the F/A-18 wing root bending moment spectrum and the number of representative tests available for test interpretation.

AeroStructures further expanded this methodology to encompass techniques for analysing all inner wing metallic parts, whether they be dominated by bending or torsion, or be subject to a local load introduction. Under this methodology, the inner wing torque box structure is considered to be a single element for the purpose of demonstrating residual strength.

Test interpretation has commenced recently with the determination of the safe life for the individual parts. Where necessary, residual strength calculations will be performed to extend the safe life using a simplified crack growth model and fractographic crack growth rates. For inspectable maintenance critical parts with inadequate safe life, inspection intervals will be established.

These test interpretation activities allow results of the long running F/A-18 fatigue test program to be applied in support of the RAAF fleet, enabling safe operations to their planned withdrawal date.

8.2.5.2 F/A-18 Hornet UpGrade Project

The RAAF Hornet Upgrade (HUG) project is an undertaking by Australia to maintain and improve the leading edge capability of the F/A-18 aircraft through various systems and structural upgrades and modifications.

HUG 3. Part of that activity includes HUG Phase 3 which is the structural modification and refurbishment program aimed at ensuring the fleet can safely achieve the planned withdrawal date.

Aerostructures was requested to assist the Commonwealth in reviewing engineering issues and making recommendations to the Phase 3 project team. The aim is to provide independent validation that the envisaged technical solutions are sound and represent value for money, or to suggest alternative management strategies.

Aerostructures is supporting the HUG Phase 3 project team by providing engineering support to specific tasks and in a more general sense ensure continuity of engineering knowledge from IFOSTP test interpretation activities through to implementation of management solutions. Activities are underpinned by a methodology for the systematic assessment of damaged structure including test interpretation, review of classification, configuration, accessibility, estimation of expected fleet defects, cost benefit analysis for preventative modifications, technical requirements and impact on operations.

8.2.6 F-111 Sole Operator Program – F-111F Wing Economic Life Determination (T.van Blaricum, DSTO)

The catastrophic failure of the DSTO F-111C Wing Damage Enhancement Test (WDET) article (Wing S/N A15-5) in Feb 2002 was attributed to build quality deficiencies in Taperlok bolt holes in the lower wing skin. This caused the RAAF to source replacement F-111F and F-111D wings from the Aircraft Maintenance and Regeneration Centre (AMARC) as there were concerns that similar flaws could be present in other C model wings. Subsequent investigations identified deficiencies within the structural certification basis of both the F-111 long wing and short wing configurations for the RAAF and USAF operational environments respectively.

As a result of the identified certification basis discrepancies, and significant deviation from the test verification basis evident through assessment of USAF usage data, DSTO was tasked to undertake an additional wing test to determine the economic life of F-111F and F-111D model wings. This test has been titled as the F-111F Wing Economic Life Determination (F-WELD) (see Figure 5) and forms part of the F-111 Sole Operator Program.

The primary objectives of the F-WELD fatigue test are to:

- determine the economic fatigue life of the F-111F and D model wings
- contribute to the development of a revised certification basis and structural management plan for ongoing structural integrity management of F-111F and D model wings through to Planned Withdrawal date PWD, and
- provide an opportunity to conduct Non Destructive Inspection (NDI) procedure development activities utilising an SAIC Ultra Image international UltraSpect-MP automated ultrasonic inspection system

The RAAF have purchased a SAIC[1] automated NDT system and this has been used to inspect the F-WELD test article lower wing skin Taperlok bolt holes to assist in the development of procedures that will help facilitate ongoing management of the wings on the basis of safety-by-inspection.

Testing is being conducted on a short configuration F-111F wing designated A15-80L using a flight-by-flight 1,000 airframe hour spectrum representative of previous USAF in-service operations. The test sequence consists of the application of two blocks of manoeuvre loading followed by Non Destructive Inspection (NDI) followed by the application of Cold Proof Load Test[2] (CPLT) prior to the application of a further two blocks of loading.

Figure 5: F-WELD Test Article Undergoing Cold Proof Load Test

Cannon Air Force Base (AFB) usage is considered to conservatively cover the prior usage of the ex-USAF F-111 D and F wings. The total service hours were therefore converted to an equivalent total of 4,500 Cannon hours to provide a valid starting baseline for the test. As the only available data comprised of Cannon AFB exceedence diagrams a Cannon (AFB) spectrum was derived from a combination of Multi Channel Recorder (MCR) data (used previously in

[1] The UltraSpect-MP system can simultaneously acquire ultrasonic and eddy current data in a single scan. It provides full A-scan capture for all ultrasonic data. This system consists of a laptop computer for software control, a separate Data Acquisition System (DAS), which contains the appropriate inspection hardware, such as ultrasonic cards, eddy current cards, etc. Other inspection techniques integrated into the inspection system include Sonic BondMaster and Phased Array Ultrasonics.

[2] CPLT to design limit load at minus 40 Degrees Celsius forms an integral part of the safety-by-inspection program used to ensure the structural integrity of the F-111 aircraft. CPLT is a safety measure to ensure that any critical size defects in high strength D6ac steel components, which may have been missed during NDI, are detected by actual failure of the component part.

the development of the 4.5g limited DADTA2b spectrum used for the previous wing test) and recorded output from the F-111 Flight Simulator (SIM) to cover manoeuvres of up to 6.5g.

Test Progress to Date

From the starting point of 4,500 Cannon AFB hours the test has progressed in a satisfactory manner although not without incident. There has been a requirement to implement a number of significant repair actions. At 6,500 flying hours a crack was detected at an inspection opening in the rear spar at a location known as Durability and Damage Tolerance (DADTA) item 73; this is a location known to crack in service. The crack had grown from an anchor nut hole (see Figure 6) across the spar web and the low spar cap. Stainless steel doublers were used to restore the spar web and to reinforce the lower wing skin to prevent further cracking of the lower spar cap as shown in Figure 6. The doubler repair has continued to perform well however additional fatigue cracking from Davis nut fastener holes was found at the diagonally opposite corner of the opening. Boron doublers were fitted as shown in the figure to prevent further cracking.

In spite of this the more cracking was found in the lower in board corner of the opening so the decision was taken to remove the remaining Davis nuts and to fit interference fit steel plugs after reaming to remove the crack growth. This strategy has proved to be very successful and has been applied to other regions on the test article where cracking has emanated from Davis nut fastener holes.

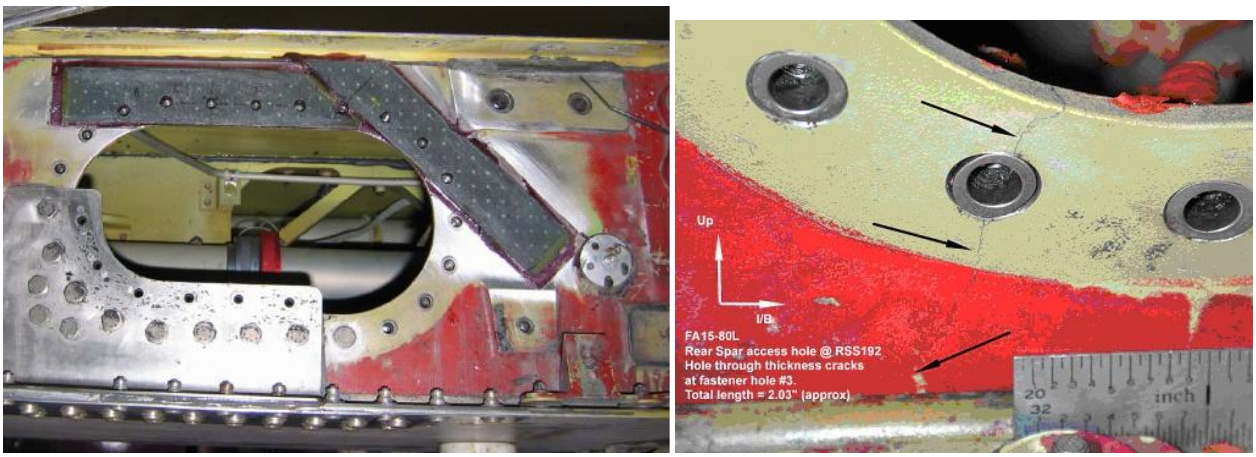

Figure 6: Boron Doublers Fitted to the DI 73 Cut Out to Inhibit Crack Growth

At 18,500 hours fatigue cracking was found at two openings in the upper wing skin. The first of these (Figure 7) known as centre spar station (CSS) 111 provides access to a fuel system pilot valve. The second, known as CSS 115 is known as the gravity re-fuel opening. In both cases cracking had originated from Davis Nut fastener holes.

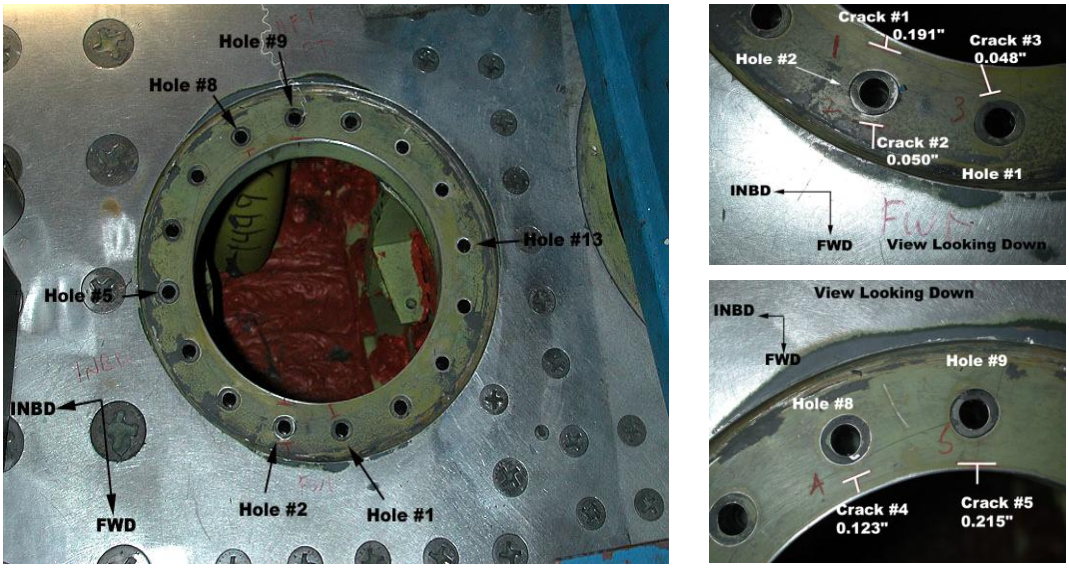

Figure 7: Fatigue Cracking from Davis Nut Fastener Holes at CSS 111

Clearly these cracks could not be tolerated as they would have grown into the upper wing skin causing premature failure of the test article. The decision was taken to implement optimised profile re-works at both locations. These were designed by DSTO. The test wing was mounted on the bed of a large CNC machine to enable the required machining operation to be carried out. The rework for the fuel pilot valve hole is shown in Figure 8. Matching steel plugs were fitted to the re-profiled holes to guard against yielding during subsequent fatigue testing.

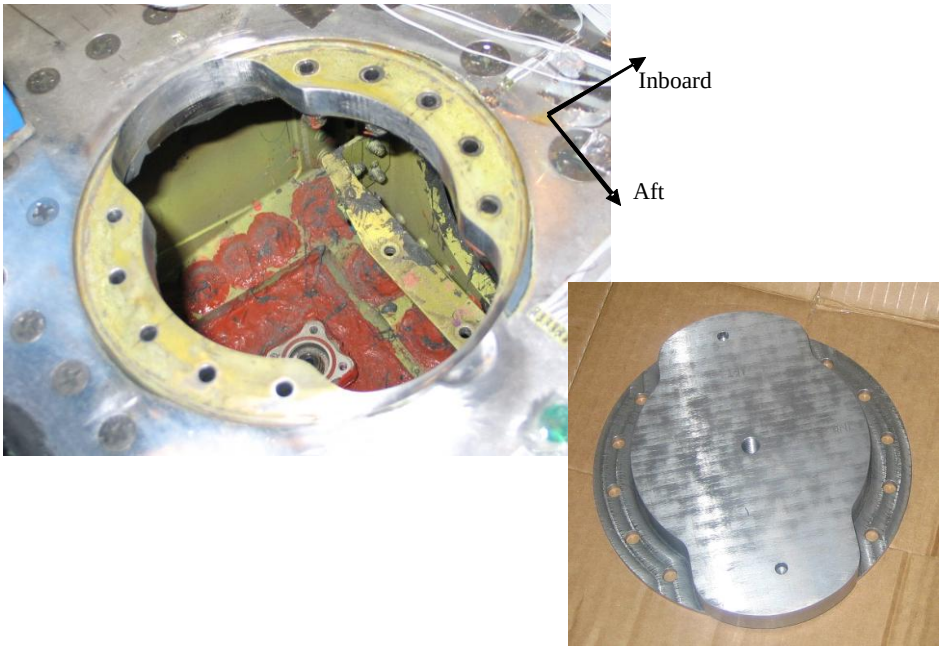

Figure 8: Fuel Pilot Valve Cut Out Rework Showing Matching Steel Plug

Whilst the rework strategy has proved to be successful, the remaining Davis nut fastener holes, especially those in the fuel pilot valve hole, have continued to cause problems with additional fatigue cracking being found at 28,000 test hours. These cracks may have been caused due to secondary bending during up wing loading due to the stiffness difference between the steel plug and the aluminium wing skin. As for the DI 73 cut out the Davis nuts were removed and the holes reamed prior to the fitment of interference fit steel plugs.

At 30,000 test hours inspection revealed the presence of fatigue cracking at an opening in the front spar (Figure 9) at a location known as forward spar station 163 (FSS 163). Once again Davis nut fastener holes were the origin of the problem.

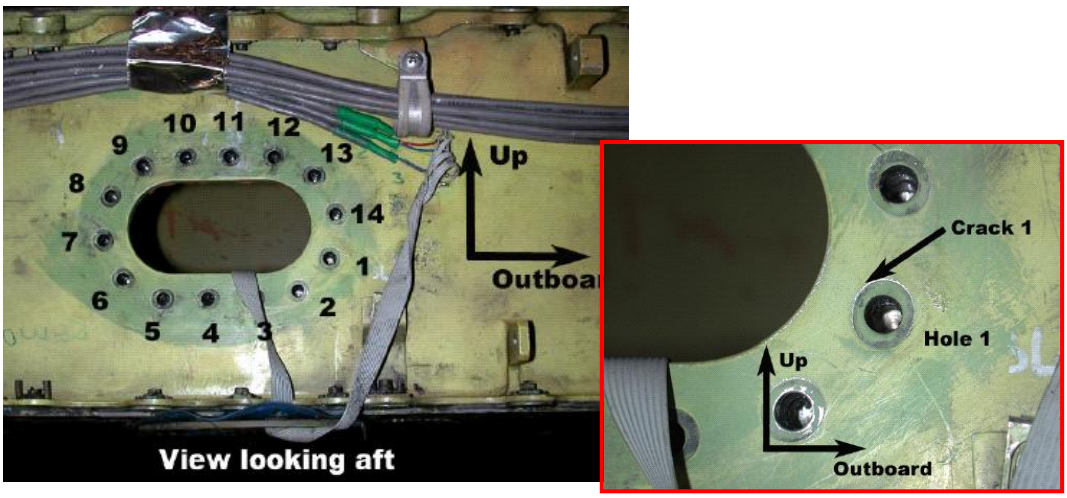

Figure 9: Cracking at Forward Spar FSS 163 Cut-out

The crack emanating from Hole 1 had grown into the cut out, several other holes were also found to contain cracks. To guard against further crack growth the Davis nuts at all four corners were removed and the holes reamed to remove cracking and fitted with interference fit steel plugs. The entire opening was then fitted with a boron doubler as shown in concept in Figure 10.

Figure 10: Boron Doubler Repair at Opening in Forward Spar at FSS 163

The two major milestones associated with the F-WELD test were to first reach 22,400 hours such that the current restriction on wing flight hours can be progressively lifted. The second milestone of 30,000 test hours has now been achieved with the majority of fleet wings cleared to fly until the current planned withdrawal date of the aircraft. Testing will continue until the end of June 2007. The ultimate aim still is to fail the wing in fatigue and then to conduct a comprehensive teardown inspection to identify all fatigue crack locations. That teardown and inspection will assist in the management of the remaining significant issue with F-111 wings, namely build quality concerns – the management approach being pursued is development of appropriate inspection systems and procedures.

The test is progressing (April 2007) beyond the 32,000 hrs point towards 34,000 hours.

8.2.7 The Successful Establishment of In-Country Structural Integrity Support for RAAF F-111 Fleet (K.Walker, and R.Boykett DSTO)

Following a decision announced in 1996, the United States Air Force (USAF) retired their fleet of F-111 aircraft in 1998. This left Australia in the position of being the only operator of the F-111 in the world. Around the time of the 1996 USAF decision, a partnership was formed between the Royal Australian Air Force (RAAF), the Defence Science and Technology Organisation (DSTO) and Australian Industry to create the "F-111 Sole Operator Program". An important context was that support from the original manufacturer of the aircraft, now called Lockheed Martin, was envisaged to become impractical soon after the USAF retirement. The broad aim was to ensure that support for the aircraft could be provided in the new environment. A ten year program was planned. The significant structural aspects included:

a) Conducting full-scale fatigue testing on retired RAAF and USAF wings.
b) Teardown of a retired fuselage and empennage.
c) Development (with Lockheed Martin support) of in-country capabilities for internal and external loads.
d) Development (with Lockheed Martin support) of in-country capabilities for fatigue crack growth analysis and durability and damage tolerance assessment.

The program has now successfully concluded. The activities mentioned were carried out and the capabilities established. Significant outcomes so far include the timely identification (through the full-scale fatigue tests) of hitherto unknown potential lower wing skin fatigue cracking scenarios which, if unchecked, could have led to catastrophic in-flight failures and/or grounding the fleet for extended periods. The in-country capabilities proved to be sufficiently robust to deal with the problem and to develop appropriate management strategies including follow-on testing, substantiated safe lives and new semi-automated non-destructive testing methods.

Figure 11: F111C in RAAF configuration showing critical structural areas

Figure 12: Arrival of the teardown aircraft, and removal of wing carry-through box

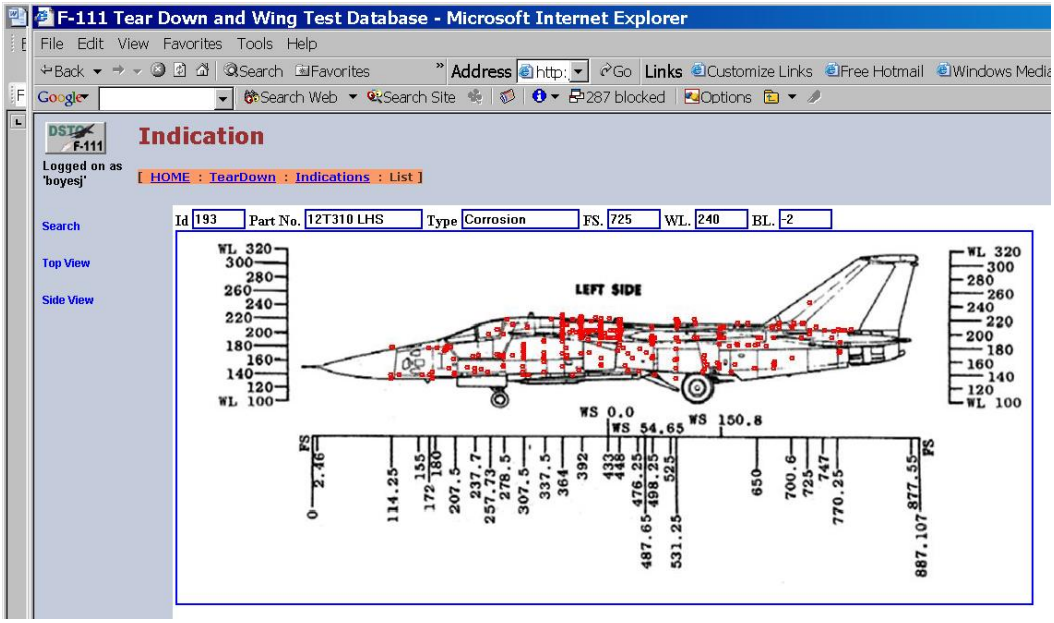

Figure 13:Teardown database screen view showing locations of "indications" discovered during teardown activity

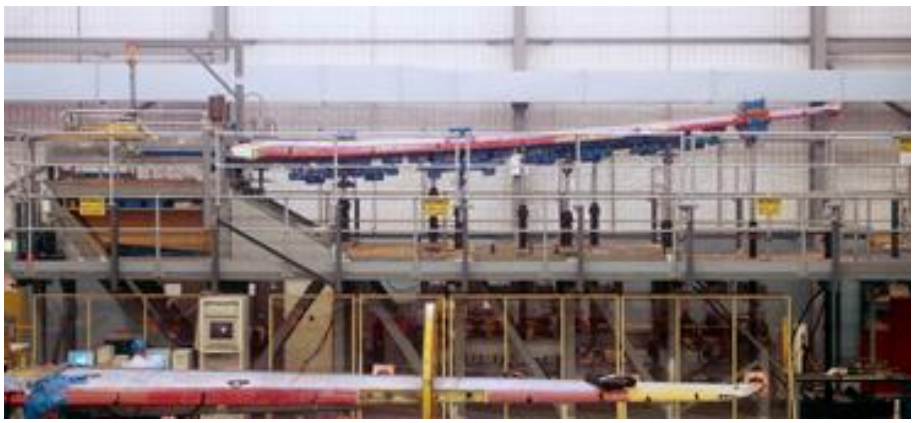

Figure 14: F-111 Wing Fatigue Test Rig

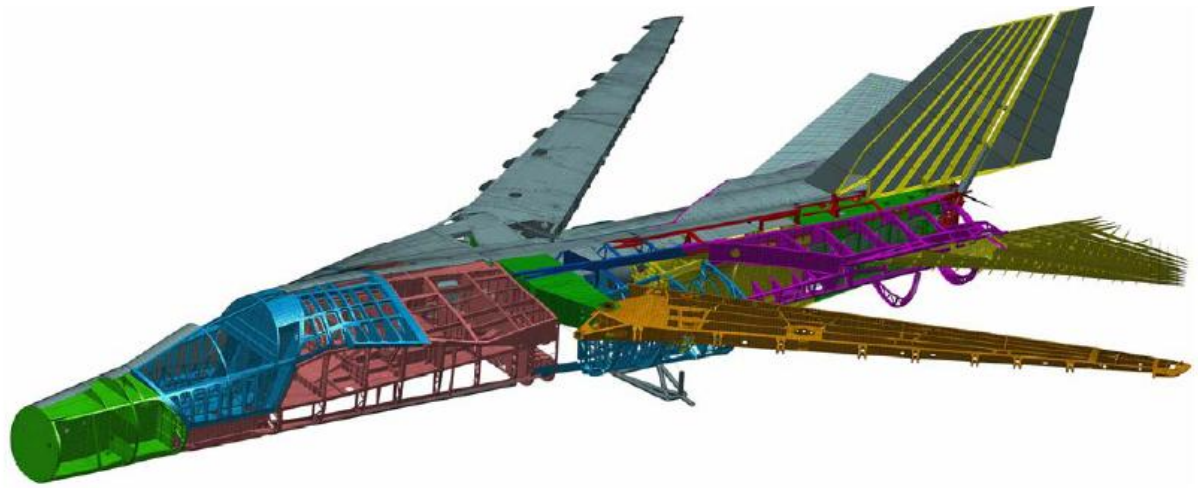

Figure 15: Cutaway view of F-111C finite element model

8.2.8 Review of Structural Integrity Management of RAAF F-111 Over-Wing Longeron (K.Walker [DSTO], M.Ignjatovic and J.Boyes [Aerostructures])

The Over Wing Longeron (OWL) is a critical high strength D6ac steel component in the upper centre fuselage of the F-111 (Figure 16). Structural integrity management for the fatigue sensitive locations in the OWL currently requires a costly and time consuming modification involving re-work and cold expansion of the fastener holes (known as the Cx mod). A comprehensive program of work has been conducted to determine if the Cx mod is required. The work included a review of Royal Australian Air Force and United States Air Force service history, a review of relevant load and stress equations, and several coupon testing programs. The results support the view that the Cx mod is not required, and the area can be managed by regular Cold Proof Load Tests.

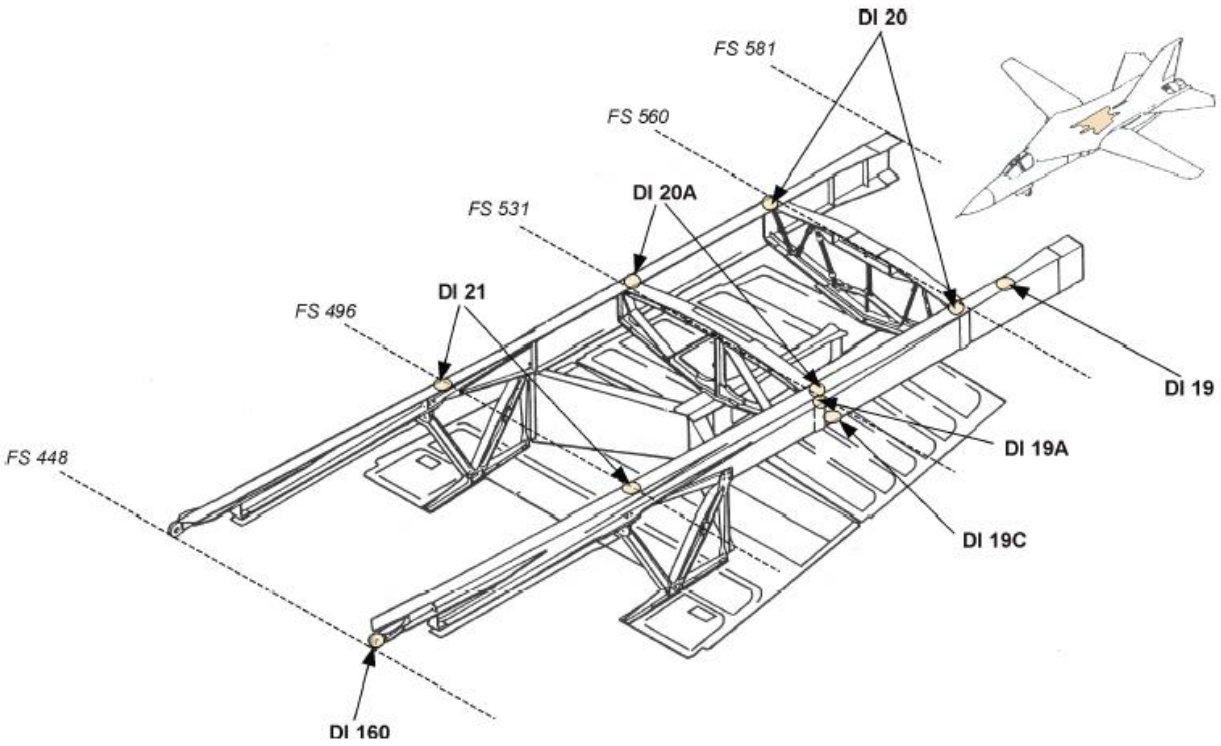

Figure 16: F-111 OWL and DADTA Item Locations

8.2.9 Safety By Inspection Plan Management for the F-111 Pivot Pylons (K.Jackson, Aerostructures)

AeroStructures are presently engaged in a two-year project for the RAAF, the F-111 Aircraft Structural Integrity Program (ASIP) Consolidation Project (F-ACP) which will bring to maturity key elements of the F-111 ASIP using tools and data developed as part of the F-111 Sole Operator Program (SOP). These tasks will be completed in collaboration with various F-111 stakeholders including ASI-DGTA, DSTO, SRSPO and BASC.

The introduction of the AGM-142 store onto the F-111 generated the requirement to assess the effect of AGM-142 carriage. In addition to an investigation into the effect of AGM-142 carriage on airframe fatigue, one of the first tasks undertaken under the F-ACP was the development of a structural integrity management strategy for the F-111 pivot pylons using damage tolerance principles.

Firstly, fatigue critical structural locations on the pivot pylon were selected for Durability and Damage Tolerance Analysis (DADTA) based on OEM fatigue analysis and static strength results along with a survey of RAAF in-service defect findings. In addition, AeroStructures worked with RAAF NDT personnel to develop suitable inspection techniques for critical locations and to establish reasonable estimates for detectable flaw size.

Stress equations for the selected locations where developed in terms of store and pylon aerodynamic and inertia loads. Available OEM wind tunnel data coupled with regression analysis was used to develop expressions for store aerodynamic loads in terms of suitable aircraft flight parameters (Mach number, wing sweep, angles of attack and side slip) and store geometry. Similar wind tunnel data was provided by DSTO and used to characterise AGM-142 aerodynamic loads. Store inertia loads were developed based on aircraft linear and rotational acceleration coupled with store location and mass properties.

Flight Data Recorder (FDR) information from several fleet aircraft was used to generate spectra for the DADTA. Two spectra were developed. The first was representative of operations prior to the introduction of the AGM-142, the second included FDR information from AGM-142 flights. Computer code was developed to process the FDR parameters through the load and stress equations to generate flight by flight stress spectra for each of the locations to be analysed.

DADTA was performed using the OEM linear elastic fracture mechanics code ADAMSYS. Inspection intervals were derived for each location for initial flaws based on durability, inspection at manufacture and in-service inspection by the RAAF. The results were used to quantify the impact of AGM-142 carriage on the F-111 airframe and to develop a Safety-By-Inspection (SBI) management strategy to ensure the F-111 pivot pylons safely reach RAAF Life-Of-Type (LOT) goals.

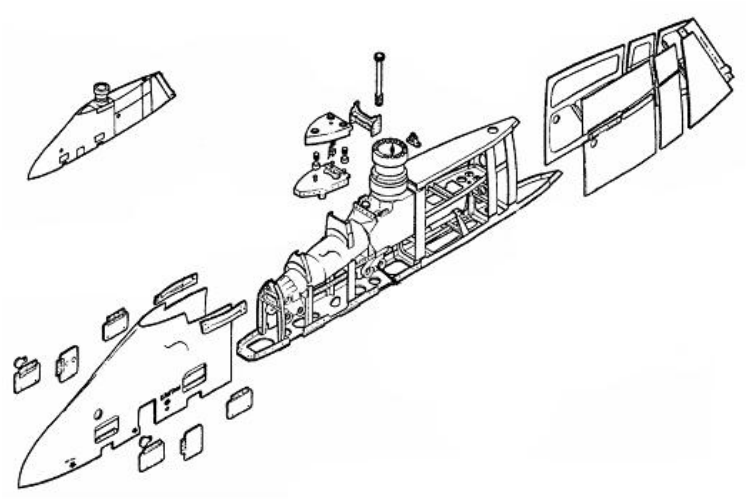

Figure 17: Diagram of F-111 Pivot Pylon Assembly

8.2.10 Support of the ADF F-111 Safety By Inspection Program (R.Kashyap and M.Houston, Aerostructures)

The structural integrity of the F-111 aircraft is managed primarily by a Safety by Inspection (SBI) basis. As the sole operators of the F-111, the Australian Defence Force (ADF) conducted the F-111 Sole Operator Program (SOP) in order to provide tools, data and infrastructure to support the F-111 in the absence of OEM and USAF input. In this endeavour, the ADF was supported by DSTO, Aerostructures and other agencies. Aerostructures continues to support the conduct of the final major activity of the SOP, the F-111F Wing Economic Life Determination (F-WELD) full-scale fatigue test on a retired F-111F wing. Aerostructures' activities include loads and stress sequence development.

8.2.11 Development of a predictive tool for the analysis of fatigue crack growth involving notch plasticity (update) (Weiping Hu, DSTO)

CGAP 1.5 [1] was released and used within the Air Vehicles Division for crack growth analysis on F18, F111 and P3-C, as an alternative tool to the OEM provided software. In addition to fixing a number of bugs, the plasticity module in this version has been verified with the limiting elastic case. The analyses performed [1] show encouraging results for crack growth involving notch plasticity.

To allow the easy conversion of crack growth rate in the form of *da/dN* versus ΔK (with the stress ratio as a parameter) to *da/dN* versus ΔK_{eff}, a user-interface module has been added to CGAP. This allows the easy conversion and use of crack growth data from other material databases. An illustration of the program is shown in the figure below. On the plot of crack growth rates, the *da/dN* curves for $R = 0.1, 0.5, 0.8$ were collapsed on to a single line represented by the yellow, green and red lines, by using ΔK_{eff} as defined in [2].

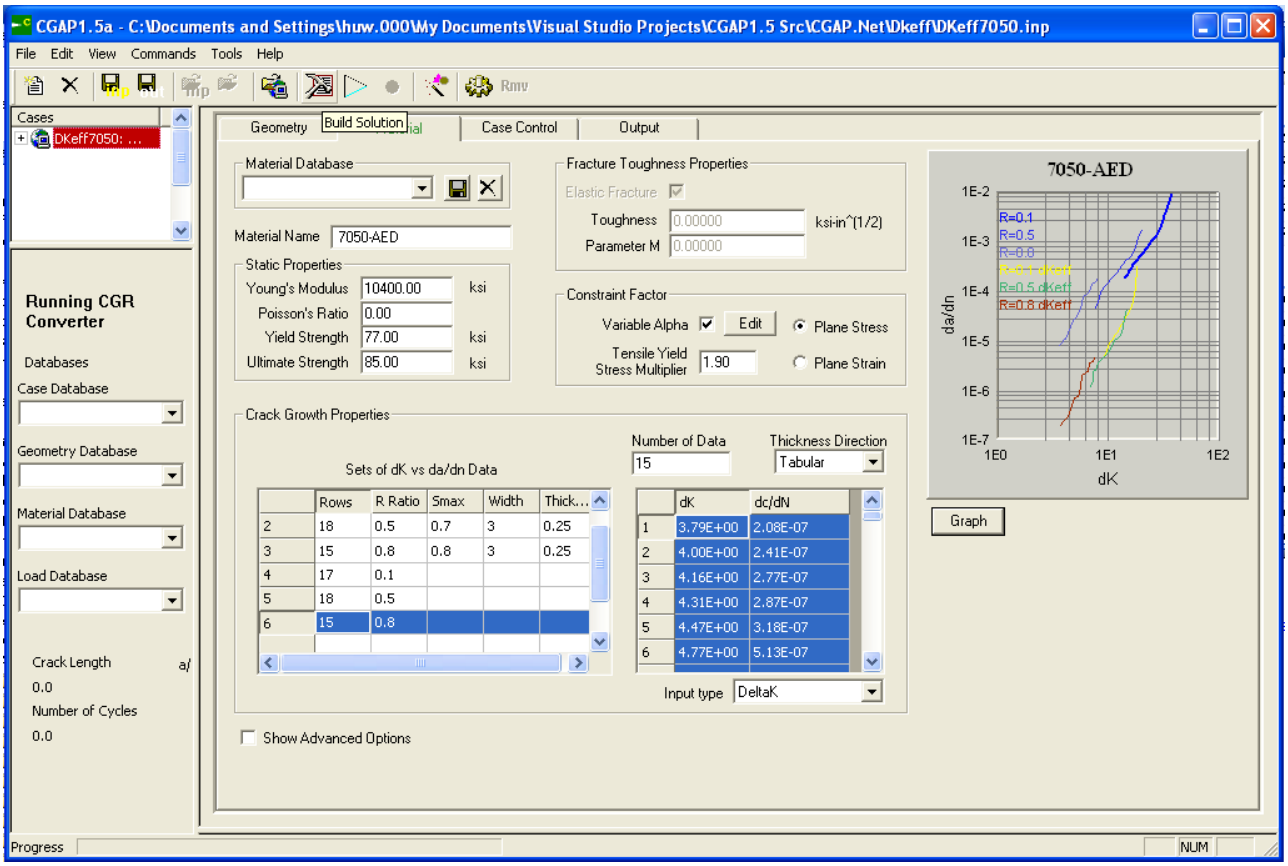

Figure 18: Screen view from CGAP

References

1. Hu, W. and K. F. Walker (2006). Fatigue Crack Growth from a Notch under Severe Overload and Underload. The International Conference on Structural Integrity and Failure, Sydney, Australia.
2. Newman, J. C., Jr. (1992) FASTRAN II - A fatigue crack growth structural analysis program. NASA. NASA TM-104159.

8.2.12 Automated Ultrasonic Inspection for Cracks in F-111 Wing Planks (G.Hugo, C.Harding, S.Bowles, H.Morton, M.Ryan,[DSTO], D.Ward, W.Farley [RAAF NDTSL])

After an F-111C wing failed during full-scale fatigue testing by DSTO, RAAF identified a requirement to nondestructively inspect up to 500 Taper-Lok fastener holes in the lower skin of each F-111 wing for possible fatigue cracks. DSTO and RAAF Non-Destructive Testing Standards Laboratory (NDTSL) subsequently developed automated ultrasonic inspection procedures to perform the required inspections, using 45 degree angle-beam shear wave ultrasonic testing (UT), Figure 19. The procedures use a Westinghouse-AMDATA Intraspect system for ultrasonic data acquisition and motion control, linked to an automated X-Y scanner and a recirculating couplant immersion scanning head, which enables the use of focussed ultrasonic immersion transducers.

- Two characteristics of this inspection problem present unusual challenges, compared to previous applications of automated NDT for crack detection in wing skins:
  a very large variation in skin thickness, from 6 to 30mm, over the regions of the wing requiring inspection, combined with substructure features such as spar web stiffeners which must be accurately interpreted, and
- the fact that it is not feasible to remove and replace individual lower skin Taper-Lok fasteners to confirm, by rotating bolt-hole eddy-current NDT, any indications from the automated UT. (To access lower skin fasteners for removal typically requires the entire upper wing plank to be removed.)

The automated ultrasonic inspections are currently being applied to all F-111 wings in the RAAF fleet to detect any possible fatigue cracks which have initiated from fastener holes with poor build quality (low Taper-Lok fastener interference and/or poor hole surface finish). Given the inconsistent build quality demonstrated for F-111 wings, some rate of possible defect indications from the automated UT is expected due to occasional mechanical damage within the fastener holes. However, the use of an ultrasonic frequency of 15MHz has enabled reliable discrimination between significant fatigue cracks and typical mechanical damage. The capability of the automated UT system to capture and store the full ultrasonic waveform (A-scan) for every point within a scan area has been essential for enabling reliable interpretation of the ultrasonic data through plan-view (C-scan) and elevation cross-section (B-scan) presentations of the data. Holes which are found to contain probable mechanical damage, but don't show evidence of fatigue cracking, will be managed by re-inspection at appropriate intervals to ensure that significant cracks do not develop in service.

The reliability of the automated inspection procedures is being quantified empirically through probability of detection (POD) trials conducted on both (i) retired F-111 wings containing electric-discharge machined (EDM) notches inserted inside the fastener holes, and (ii) test specimens containing fatigue cracks grown at fastener holes using representative F-111 load spectra. A key element of this POD validation is the application of model-assisted POD (MAPOD) methods to account for the differences in ultrasonic sensitivity between genuine fatigue cracks and artificial defects such as EDM notches, particularly the effects of crack closure. The MAPOD methods will enable a realistic assessment of the POD for fatigue cracks in actual wing structure. The automated ultrasonic procedures are also being applied to an F-111F wing undergoing full-scale fatigue testing at DSTO. Comparing the UT results with the final teardown of the wing will establish the limitations of the automated UT procedures for detection of real fatigue cracks.

(a) 

(b) 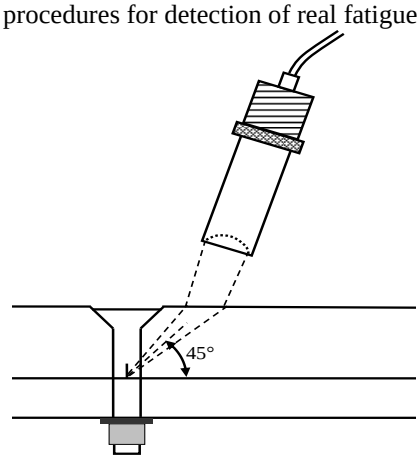

Figure 19: (a) automated ultrasonic inspection of Taper-Lok fastener holes in an F-111C wing using the Intraspect system, and (b) schematic of 45° angle-beam shear-wave inspection using focussed immersion transducers

8.2.13 RAAF C-130H Centre Wing Structural Life Assessment (M.Houston, Aerostructures Australia)

The Royal Australian Air Force (RAAF) operate 12 C-130H aircraft in a tactical and logistic role. In March 2005 Lockheed Martin Aeronautics Company (LM Aero) released SB 82 788 which required a usage review to determine the centre wing Equivalent Baseline Hours (EBH). Centre wings with an EBH above 40000 would be required to undergo an inspection programme to find generalised fatigue cracking and the possible onset of widespread fatigue damage (SB 82 790). Centre wings over 46000 EBH required flight restrictions for the aircraft pending further inspection and assessment.

In parallel with the service bulletin the USAF imposed flight restrictions on all C-130 aircraft with centre wings over 38000 EBH and at 45000 EBH retired or replaced the centre wing.
These changes to the life of the centre wing had ramifications for the RAAF as preliminary work using results from an older Operational Usage Evaluation (OUE) suggested the RAAF C-130H centre wings would reach 40000 and possibly 46000 EBH prior to their Planned Withdrawal Date (PWD).
To address the above possibility, the RAAF undertook a centre wing Structural Life Assessment Study (SLAS). The aims of the SLAS were to determine the current status of the RAAF C-130H centre wings and provide management options for future operations.
The centre wing SLAS was managed by Aerostructures, with support from DSTO, ASI-DGTA and ALSPO and comprised of the following tasks:

- Directed NDT inspections were undertaken on fleet leading aircraft and were in addition to the Safety by Inspection (SBI) programme. The directed inspections aimed to find cracks at locations known to have cracked in other fleets.
- RAAF C-130H usage data was reviewed to refine the previous OUE mission profiles. Nz exceedance data was used to help verify the severity factors obtained from the new OUE.
- RAAF centre wing cracks were compared to those from other operators, the wing durability test and crack growth curves. These comparisons were then used to estimate the age of the RAAF centre wings.
- Corrosion damage found in the centre wing was assessed to determine the cause of corrosion, provide preventative measures and determine the impact on the SBI and maintenance programmes.

Using results from the above tasks predictions were made concerning the remaining centre wing life. These predictions then allowed estimates for when SB 82 790 is required, the future maintenance burden and when refurbishment / replacement programs will be required.

8.2.14 P-3 Durability and Damage Tolerance Testing and Analysis (P.Jackson, DSTO)

From 1999 to 2006 DSTO participated in the full scale testing program of the P-3 Orion maritime Surveillance aircraft known as P-3 Service Life Assessment Program or P-3 SLAP. One of the elements of the program conducted at DSTO was the full scale fatigue test of the empennage and its subsequent durability and damage tolerance analysis. The test is shown in Figure 21. Very early in the test program it was recognised that the stress levels in the principal structural elements would mean that the testing time taken to generate representative failures would be long. Increasing the spectrum load levels would reduce testing time and allow exploration of the UK DEF STAN 00-970 SAFE S-N concepts of variable scatter factor. The test subsequently applied an aircraft usage based load spectrum for two lifetimes in order to expose any early failures resulting from design flaws, followed by the same load spectra significantly augmented but with the peak loads clipped to avoid unrepresentative yielding at critical locations, see Figure 20. The test was reported in ICAF2003 and was successful in generating both early failures and failures of the principle elements to which both DADTA and SAFE S-N analyses could subsequently be applied. See Figure 22 and Figure 23 for examples of failures of structural elements.

The conduct of a DADTA analysis consisting of fatigue life (to initiation) and crack growth calculations as well as the conduct of a SAFE S-N analysis will be presented as a poster in ICAF2007. The full scale fatigue test achieved its aim of producing failures, thus allowing the subsequent analyses to proceed confident that the critical locations and been identified and that crack growth and fatigue life data had been demonstrated by test. The DADTA analysis conducted was compliant with the chosen airworthiness standard for the aircraft, FAR 25.571, including the latest developments with regard to the identification and prevention of Widespread Fatigue Damage. The conduct of the SAFE S-N based

analysis produced values of Safe Life or inspection threshold that were not dissimilar to the same values produced from the DADTA.

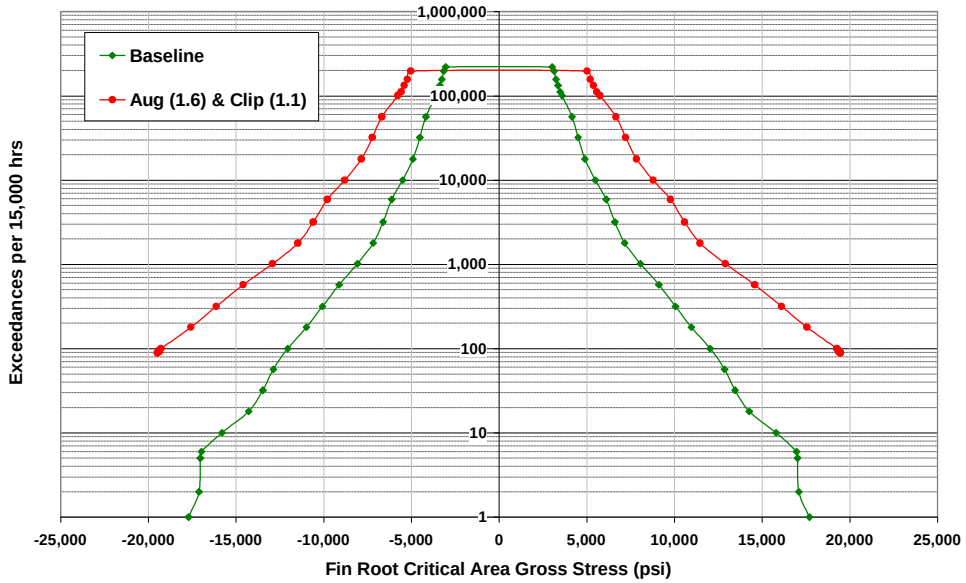

Figure 20: Baseline and Augmented spectra

Figure 21: P-3C Empennage fatigue test at DSTO

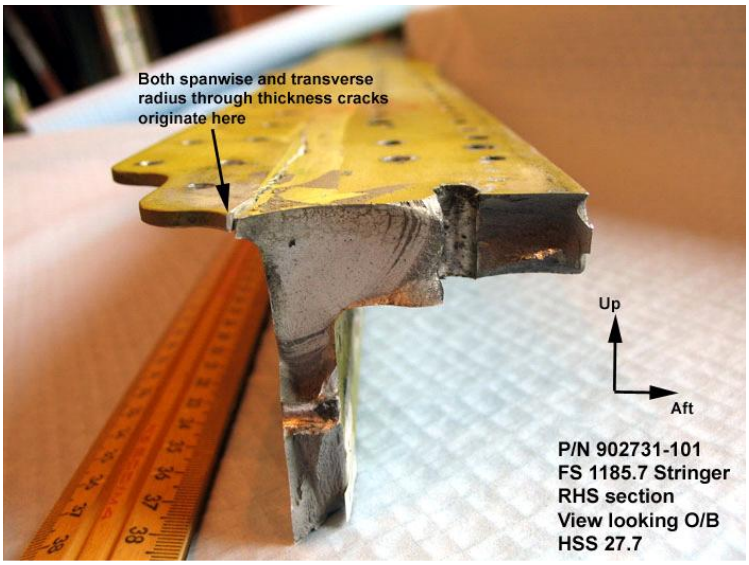

Figure 22: Fatigue cracking after test

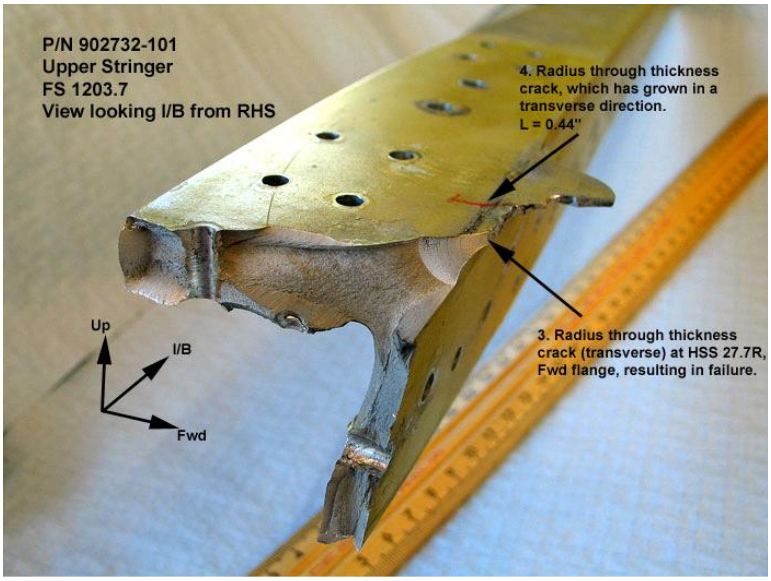

Figure 23: Fatigue cracking after test

8.2.15 Development and Evaluation of Mean Stress Correction Techniques for Improved Fatigue Life Prediction (B.Shah [Lockheed Martin Aeronautics], R.Veul [NLR, Netherlands], P.Jackson and D.Mongru [DSTO]) – Paper to be presented at ICAF 2007 Symposium

Abstract of paper to be presented at ICAF 2007 Symposium:

"Fatigue life predictions of aircraft structure have significant consequences on the life cycle costs and operational readiness of the aircraft fleet. Life prediction approaches are often unique and endemic to an individual organization, and are generally based on empirical parameters that provide the best correlation with the limited tests results that are available. Applicability of these empirical parameters is not universal.

One such current strain-life based approach was used in the international P-3 Service Life Assessment Program (P-3 SLAP) to predict fatigue lives of eight different stress spectra representing two locations on the wing of the Lockheed P-3C Orion aircraft. Two stress spectra for each P-3C fleet operated by the SLAP partners; the US Navy (USN), Royal Australian Air Force (RAAF), Royal Canadian Air Force (CF) and Royal Netherlands Navy RNLN were developed and

tested using notched coupons. The test results showed wide variations against the original analytically predicted fatigue lives. An investigation of the potential cause(s) revealed that method of calculating the mean stress effects of continually varying complex spectra might be the root cause of these variations in the predicted fatigue lives. Furthermore, it is believed that the original strain-life material property data based on smooth specimen simulation under strain control testing may not necessarily be replicating the local strain-stress state at the notches in the coupons, contributing perhaps to a lesser extent to the variations in the predicted life.

This technical paper presents the analytical results of several different approaches to include the effects of continually varying mean stress and improve the correlation with the aforementioned test results. The evaluation shows two promising formulations that provide improved correlation with the P-3C SLAP test results; a modification of a Northrop Corporation originated equation and a Lockheed approach based on a modification of the Walker formulation. Development and use of equivalent strain-life data based on load control tests of coupon specimens with different stress concentrations (notches), under various stress ratios, shows much improved correlation with the test lives than the original life predictions that used a generic mean stress correction equation and strain-life data based on smooth specimen simulation.

The fatigue life estimation effort conducted under the P-3 SLAP showed that generic or legacy formulations for life estimation can fall short of the mark when materials, spectra and stress levels change. At the least, they require careful verification and often modification before being satisfactory applied. The approach presented in the paper, and excellent correlation achieved between test and analysis, provides a platform for re-evaluating tests conducted in the past with a view to further substantiating or improving the applicability of the approaches presented. Use of load control tests of variable notched coupon specimens, under different stress ratios provides equivalent strain-life data with limited testing and expense, and with the potential of better fatigue life predictions. Reduced variability and improved accuracy of fatigue life predictions are crucial for minimizing in-service maintenance actions, and increasing the availability of aircraft for productive engagement."

8.2.16 RAAF P-3C Fatigue Tracking System to Support Safety by Inspection Program (S.Macci, Aerostructures)

The P-3 Orion aircraft is approaching 25 years of service with the Royal Australian Air Force (RAAF). A number of aircraft in the current fleet are fast approaching the P-3C certified Life of Type (LOT), and thus will not reach their planned withdrawal date (PWD) of 2015, without an appropriate structural safety-by-inspection (SBI) program beyond the current maintenance requirements. The current P-3 Certification Structural Design Standard (CSDSTD) for fatigue strength (CAR 4b.270) does not provide a basis for management of the P-3 fleet via a SBI program, and transition to a new CSDSTD for fatigue management of the P-3 is therefore required. Accordingly, FAR 25.571 has been approved as a suitable replacement for fatigue management.

A key component of a SBI program is a Fatigue Tracking System (FTS), which allows the operators to monitor the fatigue life expended on structure of interest via service usage parameters collected for each respective aircraft in the RAAF P-3 fleet. The P-3 is currently operated on a safe life philosophy based on the outputs from the current fatigue tracking system (FTS). A new FTS to support the requirements of the P-3 SBI program is currently under development by the Defence Science and Technology Organisation (DSTO). The system is being validated by Aerostructures and is based on methodologies that are reliant on fleet usage data and data gathered by a collaborative program of testing and analysis, involving the Commonwealth of Australia, known as Service Life Assessment Program (SLAP).

The current FTS was developed as part of the Service Life Evaluation Program (SLEP) II. This system is based on the fatigue tracking program developed for the United States Navy (USN) P-3 fleet and has been updated for the RAAF usage (last done in 1989). The program expresses the portion of the certified safe life expended as a Fatigue Life Index (FLI) which is based on aircraft usage and original fatigue test information (P-3A structure). At a FLI of 110, which represents the certified fatigue life of the P-3, the fatigue life of the airframe would be consumed and the current management philosophy would require revision.

Following collaboration between DSTO and Aerostructures, a Concept of Operations (COps) document was developed to address potential FTSs for the RAAF P-3C fleet. Based on material in the COps document, DSTO was tasked to design an approach to re-baseline the RAAF P-3 fleet, which would form the basis of the FTS for the fleet aircraft.

This revised FTS, called the Structural Life management program Version II (SLMP II) is a result of the data and software tools gained through the SLAP, and it will supersede SLEP-II as the FTS for the RAAF P-3 fleet.

Fatigue Life Measure FLM is used for assessment of life limited structures as a measure of the total fatigue damage accrued. In this regard, the FLM is similar to the FLI used in SLEP-II. The FLM relates individual aircraft fatigue damage accrual to the damage accrued by the FSFT articles at the time at which crack initiation was observed at the tracking location in question. In addition to the assessment of life limited structure, the FLM is used to determine inspection thresholds for SBI structure. The Unit Damage Matrices (UDM) evaluated for the calculation of FLM take account of damage rate due to number of missions, number of landings and number of flight hours.

Unlike SLEP-II, the FTS methodology uses a crack growth Severity Factor (SEF) in addition to the FLM. This crack growth measure is relative to the fleet average usage. The intent is to use the SEF to determine whether individual aircraft usage has deviated sufficiently from the fleet average to warrant revision of inspection intervals.

SLMP-II also includes a means for estimating revised inspection intervals. These are estimated by making use of the fact that post SLAP P-3C inspection intervals are based on fleet average AP-3C usage and that the SEF is a measure of the deviation of individual aircraft usage from the fleet average AP-3C usage.

The FTS methodology categorises RAAF P-3C missions in terms of 7 mission types. These 7 mission types are equivalent to the SLEP-II mission types (SLEP-II mission types 4 and 5 have been combined to represent a single mission type in the FTS methodology) (see Table below). To better align the number and types of missions flown by the P-3 SLAP partners the eight SLEP-II mission profiles were each expanded into a number of sub-mission profiles for use in the UDM development. The usage data was expanded for comparison against the 38 sub mission profiles that were used to generate the USN Full Scale Fatigue Test spectrum.

The DSTO methodology for generating the UDMs and SEFs has been applied to establish the damage and severity figures for one tracking location. The methodology for this tracking location has been reviewed and validated by Aerostructures. In total there are six fatigue tracking locations on each aircraft and at present damage and severity number are being established for these tracking locations. Aerostructures will be reviewing and validating the data related to these tracking location.

Design specification for the SLMP II system has been written and the software development for the FTS has started. The aim is to have the software for the system developed and tested by the middle of 2007. The system should be implemented for use thereafter.

Mission Type	Description	Number of Sub-Missions
1	Crew Training	9
2	Anti-Submarine Warfare (ASW)	12
3	Test Flight	3
4&5	Patrol, Search & Surveillance / Fisheries & Surveillance	8
6	Harpoon	1
7	Transit Ferry	4
8	Air Demonstration	1

Reference

1. RAAF P-3C Fatigue Tracking System to Support Safety by Inspection Program, Shai Macci (Aerostructures) and Emilio Matricciani (DSTO) 12th Australian International Aerospace Congress, March 20, 2007.

8.2.17 Effect of Corrosion on the Safe-Life of P-3C Orion (A.Shekhter, C.Loader and B.R.Crawford, DSTO)

High-Kt specimens of 7075-T6 have been fatigue tested using spectrum loading in corroded and uncorroded states. The shape and morphology of the corrosion pits were then examined using a SEM, and these fractographic data combined with a crack growth model to determine an Equivalent Crack Size (ECS) distribution. A probabilistic approach was used to determine a relationship between a measured corrosion metric and an ECS, which enabled the definition of a safe level of corrosion at fatigue lives calculated using the P-3C Service Life Assessment Program safe life approach.

The material used was thin (3 mm) AA 7075-T6 sheet clad with an approximately 100 μm thick Alclad layer on each face. The experimental program consisted of three parts:

- Establishing a corrosion protocol and corroding fatigue specimens according to this protocol;
- Fatigue testing and fractography of un-corroded and corroded specimens;
- Crack growth modelling of ECS and statistical correlation with pit metrics.

Fatigue testing was conducted using a variable amplitude spectrum at peak stresses of 124 and 140 MPa.

The fatigue life results obtained for 124 and 140 MPa peak stress levels are shown in Figure 24. The reduction in fatigue life due to corrosion is apparent.

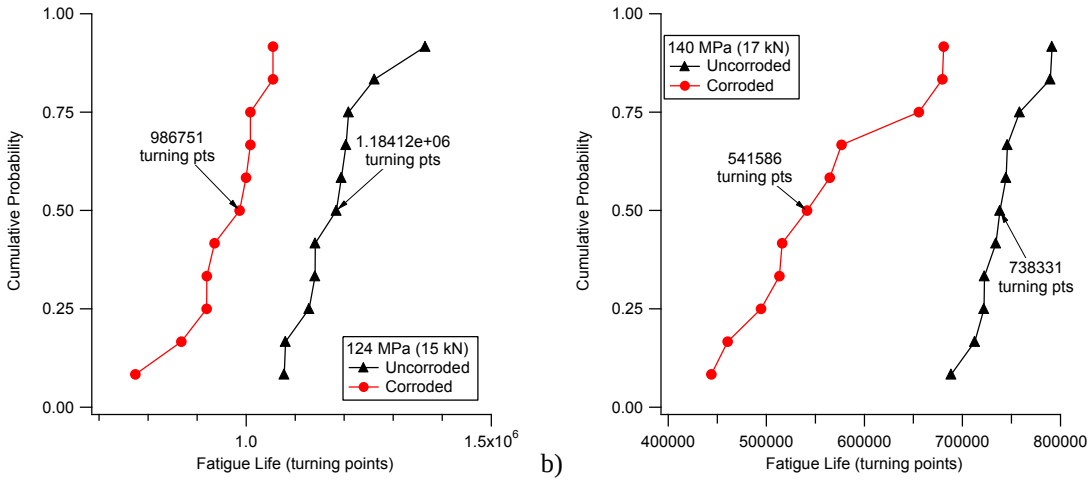

Figure 24: Effect of corrosion on Fatigue Life for (a) 124 MPa and (b) 140 MPa peak stress levels

Fractography

Fractography showed that failure occurred either at the corners of the stress concentrating hole, or from corrosion pits. Corner failures occurred through cracking initiated either within the softer Alclad material from machining defects at the corners or through preferential corrosion of the Alclad.

ECS Results

Analysis showed that pit cross-sectional area was statistically significant with respect to fatigue life. Figure 25 shows the relationship between ECS and the square root of the pit area as a Crack Metric Ratio (CMR). CMR is the ratio between the calculated ECS and the measured metric. (CMR = ECS/metric). Using an analysis of errors, a ‘safe’ CMR relationship was established by shifting data points by three standard deviations, creating a CMR that would only be reached by approximately one in one thousand pits.

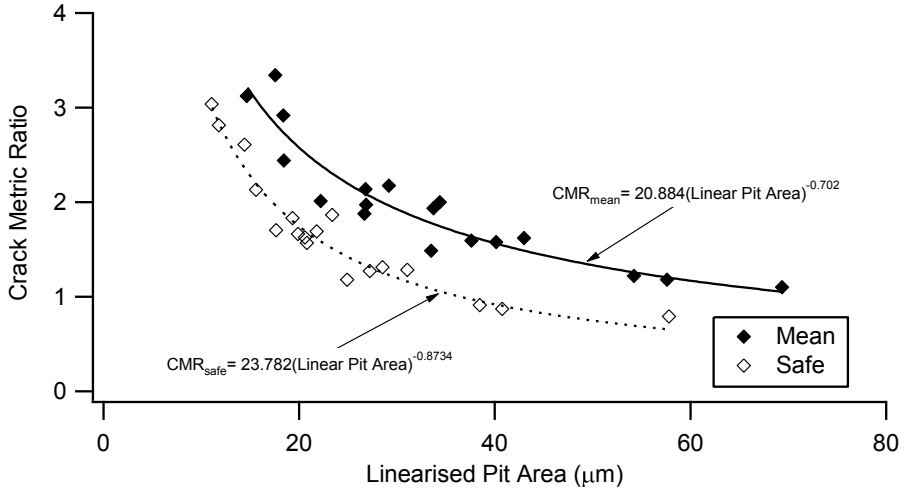

Figure 25: Relationship between crack metric ratio and pit metric

ECS Predictions of Effect of Corrosion on Safe Life.
Fatigue lives predicted for the safe ECS values for both stress levels are shown in Figure 26. This figure also incorporates the crack initiation approach developed for the P-3C SLAP. Threshold life values for both single and multi load-path structures were determined from the baseline fatigue tests using an interval between crack detection (crack reaching a size of 1.25 mm) and failure, provided by a FASTRAN model. As can be seen, at both stress levels, corrosion with a cross sectional area up to 80 μm (6400 μm^2) will not result in failure prior to the threshold lives for both Multi and Single load path structures.

Limitations of the ECS methodology prevent extrapolation beyond the bounds of measured behaviour due to the possibility of a change in mechanism. Additional work would be required to more accurately characterise the upper end of the predicted safe life curves prior to any transition to service.

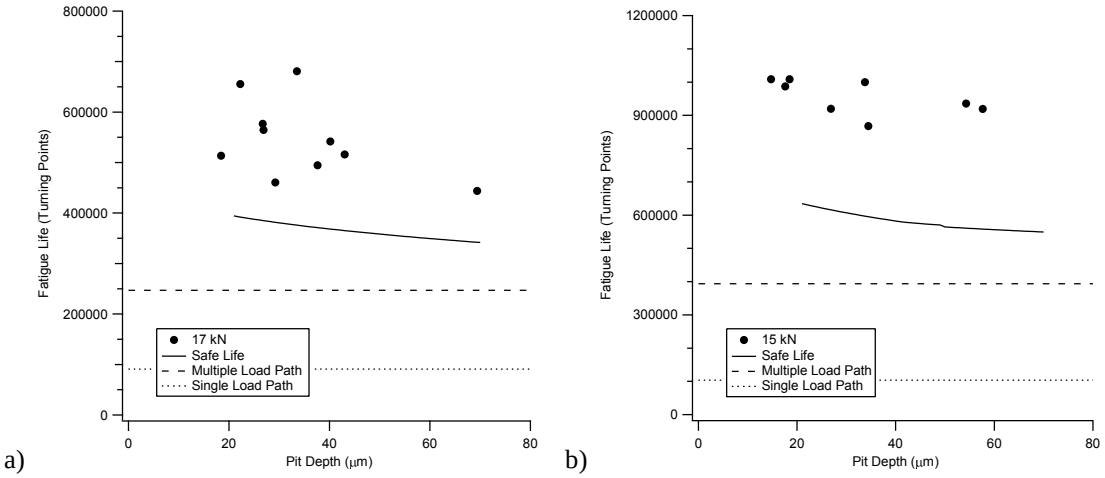

Figure 26: Comparison between the predicted failure lives due to corrosion with the threshold (safe life) values using Crack Initiation predictions for (a) 140 MPa and (b) 124 MPa peak load

Summary
The effect of corrosion on P-3C Safe life was assessed using two methods: crack initiation (CI) and ECS. It should be noted that CI methods can be transferred between load spectra but requires the same corrosion distribution in service. ECS can be used for different corrosion distributions, matching to an in-service distribution determined in the future, but is not readily transferable between load spectrums.

The ECS method has a significant advantage in that corrosion more severe than that which was used in the derivation can be easily incorporated into the model with a very small number of additional tests. Both ECS and CI models

require the in-service corrosion distributions to be determined. Current RAAF practice of corrosion management makes this assessment difficult since corrosion is mostly destroyed once located. Neither model can account for a change in corrosion mode, ie. from pitting to intergranular attack. It was apparent that the use of Alclad sheet prevented pits initiating close to the corners. The effect of the Alclad layer on baseline (un-corroded) lives has not been confirmed.

Following the investigation of the effect of corrosion on P-3C Safe life it was concluded that:

- The ECS analysis has shown that small corrosion pit sizes are unlikely to invalidate the Safe Life method used in the P3 SLAP.
- The CI method can be used in conjunction with the ECS method to assess the effect of corrosion on the Safe Life of the P-3C Orion.

8.2.18 C130J Structural Life (LMeadows, R.Ogden, DSTO)

The Royal Australian Air Force (RAAF) C-130J-30 Hercules fleet was introduced to Commonwealth service in September 1999. Subsequently the FAA certification basis, achieved by Lockheed Martin Aeronautical Systems (LM Aero) for the 382J, (civil variant) was considered inappropriate for the structural certification of the RAAF C-130J-30 fleet. This was due primarily to differences in the intended military operational role and environment.

From an Aircraft Structural Integrity (ASI) management perspective the Commonwealth is currently focused on resolution of the outstanding structural certification issues, and establishment of mature data and system infrastructure to support ongoing management of structural integrity. Key activities aimed at addressing these issues are as follows:

8.2.18.1 Collaborative Wing Fatigue Test
The RAAF has entered into a collaborative arrangement with the UK Ministry of Defence (MoD) to conduct a C-130J full-scale Wing Fatigue Test WFT in the UK. In October 06 agreement was reached on a compromise usage spectrum between the RAF and RAAF. The generation of loads for this spectrum is nearing completion with clipping and truncation studies scheduled to commence in April 07. Test rig commissioning is underway with cycling expected to commence circa August 07.

8.2.18.2 SBI Program
In the absence of WFT results the RAAF has implemented a Safety By Inspection (SBI) program based on Damage Tolerance Analysis conducted by LM Aero. This program accounts for mature, representative RAAF usage measured during the 03/04 timeframe.

8.2.18.3 Structural Health Monitoring
In support of the collaborative WFT program DSTO has developed a system for processing and managing fleet C-130J-30 Structural Health Monitoring System (SHMS) data, (ie. the OEM supplied usage monitoring system). The DSTO developed system, comprising software and database elements has been utilised primarily to characterise RAAF and RAF usage for consideration in the upcoming WFT. The database and an example mission profile plot are show in *Figure 27* and Figure 28.

8.2.18.4 Individual Aircraft Tracking
The RAAF has implemented an Individual Aircraft Tracking (IAT) system to monitor usage, calculate severity factors and evaluate inspection intervals for the C-130J-30 fleet with respect to the baseline SBI program, (ie. DTA). The requirement for this interim system is driven by the uncertified status of the OEM supplied SHMS.

8.2.18.5 Operational Loads Measurement
The RAAF is in the final stages of acquiring and installing an operational load measurement (OLM) system in one RAAF C-130J-30 aircraft. The aircraft is in the installation phase now with ground calibration scheduled to commence in May 07. The OLM, designed by Marshall Aerospace (UK) is required in order to gather loads data for RAAF contribution to, and interpretation of, the collaborative C-130J WFT, see Figure 29.

8.2.18.6 Service Life Prediction Methodologies
DSTO has entered into a collaborative program with the US, UK and Canada under the auspices of TTCP TP4 to examine lifing methodologies related to the C-130 aircraft. Front lower spar caps are being replaced on the RAAF's 12

C-130H aircraft. These will be subject to teardown and detailed fractographic examination to correlate cracking with in service usage. Cracking will also be modeled analytically to determine the most appropriate models for use in interpretation of the C-130J WFT. Examples are shown in Figure 30, Figure 31and Figure 32. Building on recent P3 experience, probabilistic approaches will be investigated for application to C-130 as an alternative to the traditional damage tolerance and fatigue life approaches.

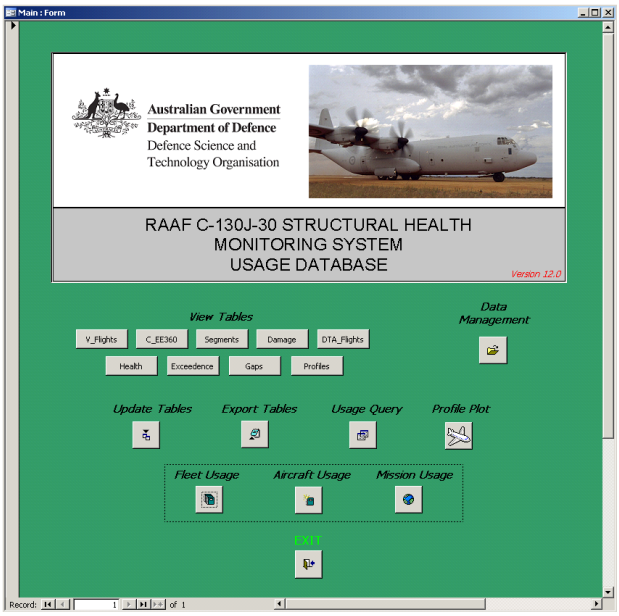

Figure 27: DSTO C-130J-30 Fleet Usage Database

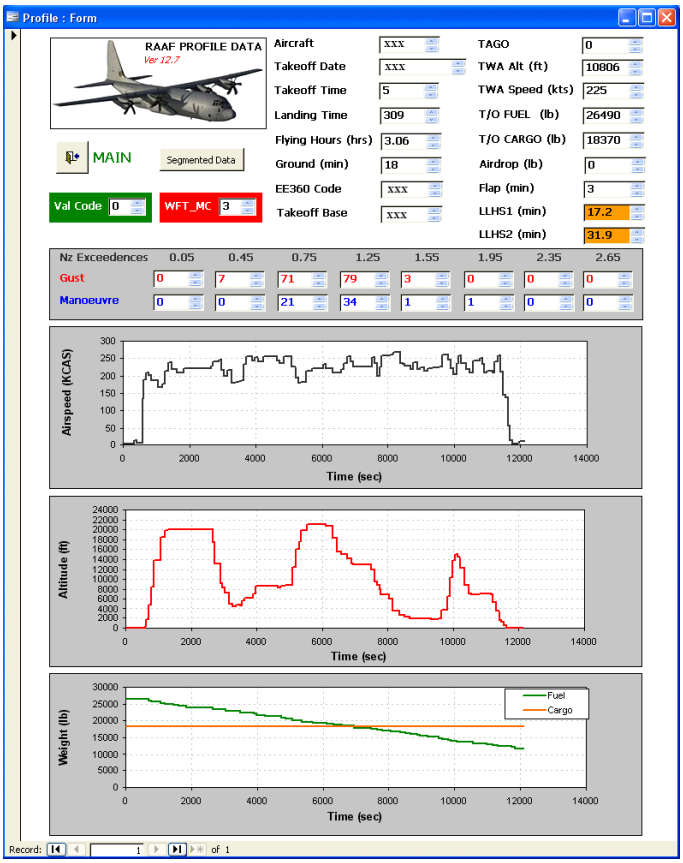

Figure 28: Usage Database – Profile Plot

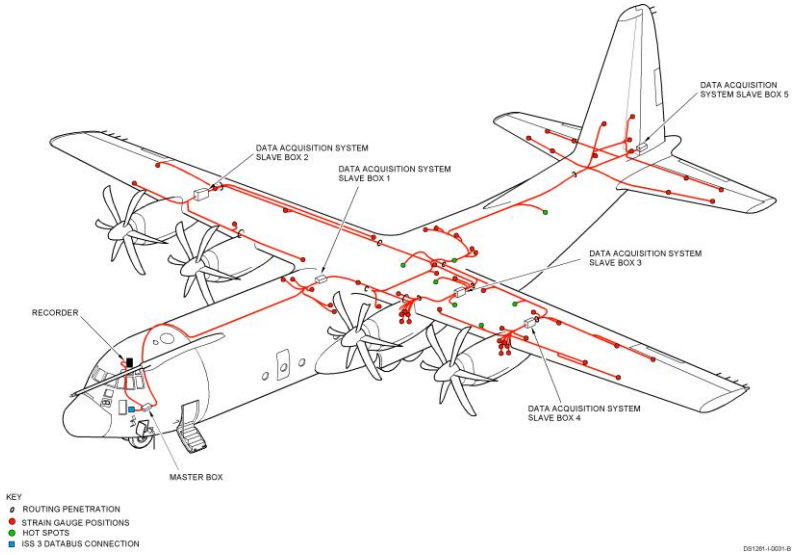

Figure 29: RAAF - Marshall Aerospace OLM Installation

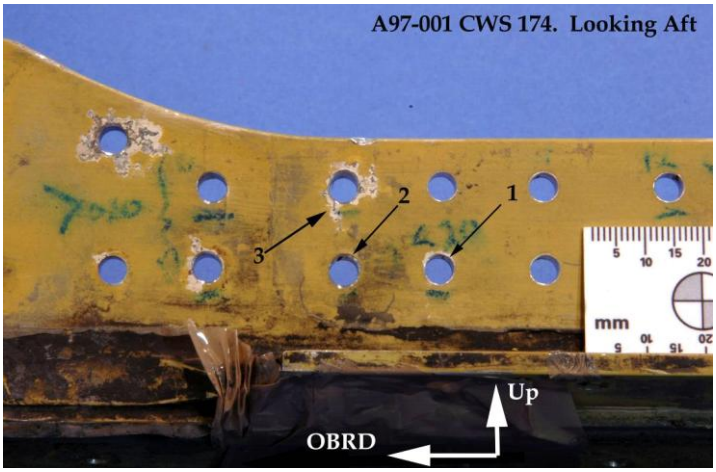

Figure 30: Approximate location of cracks

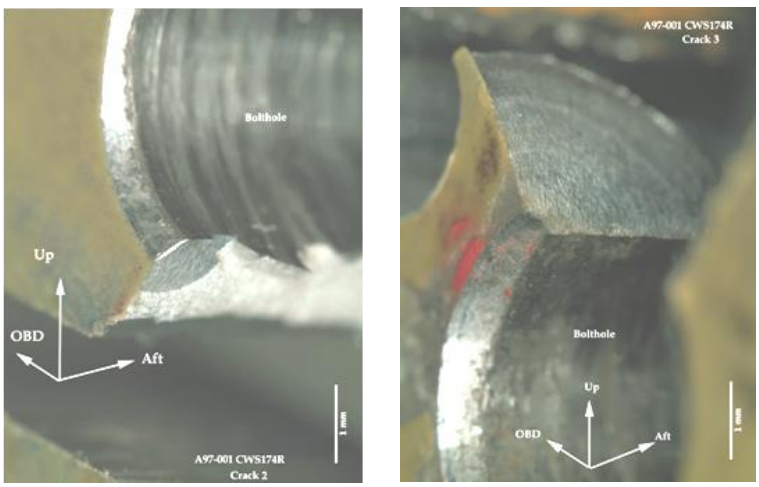

Figure 31: Fracture Surface of Crack 2 (left) and Crack 3 (right) after breaking open. Cracks grew from the chamfer

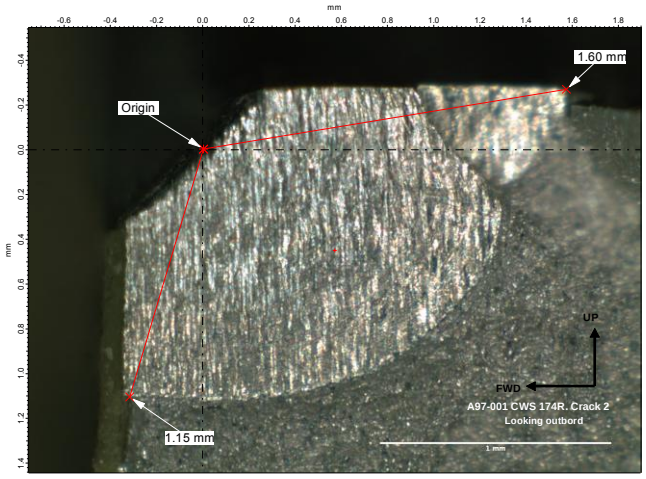

Figure 32: Fracture surface of Crack 2

8.2.19 Lead In Fighter (LIF) Fatigue Test (T.van Blaricum, DSTO)

In 1997, the RAAF formalised a contract for the delivery of 33 Hawk Mk.127 aircraft, to satisfy the requirement for a new Lead-In Fighter (LIF) aircraft. Under the terms of the contract, 12 aircraft were produced at Brough in the United Kingdom, with the other 21 manufactured in Brough and assembled at a purpose built BAE SYSTEMS facility at Williamtown, New South Wales. The first UK-built Hawk Mk.127 made its maiden flight in December 1999, with the first Australian-built aircraft following just five months later.

In comparison with the T Mk 1, the Hawk Mk.127 is approximately: 600 mm longer and 25% heavier (1% weight increase equates to approx 5% reduction in life for unchanged structure). DSTO had been asked to conduct an assessment to determine whether a full-scale fatigue test of the aircraft was required. Fatigue tests on earlier models of the Hawk had been conducted but the DSTO analysis determined that new tests were essential to provide specific information on RAAF operational usage of the Australian version of the aircraft, therefore minimising the possibility of fatigue-related accidents, and potentially increasing the operational life of the RAAF fleet.

Figure 33: LIF Test Rig (left) under construction, and (right) with aircraft installed.

Once the decision had been made to proceed with a comprehensive full-scale fatigue test, DSTO and BAE SYSTEMS entered a commercial business agreement to conduct the test in Australia. Personnel from both organisations are involved in the test, as are several Australian contractors with a range of backgrounds and expertise.

The Hawk Mk.127 fleet has been operational since 2000, under an interim flight clearance that allows for such activity prior to full-scale testing. Fatigue testing commenced in February of 2006. The first objective is for the test to clear the fleet aircraft for 3000 flying hours. To achieve this objective the test needs to reach between 9,990 and 15,000 hours to allow for a range of safety factors between 3.33 and 5 depending on the degree of monitoring afforded by the Fatigue Monitoring System at different locations across the airframe.

The specimen comprises a LIF Hawk production standard Fuselage, Wing and Fin. A production standard Windscreen and Canopy are also fitted to enable cockpit pressurisation to be applied. Some structural items have been, or are being, cleared by an alternative route, and therefore are not fitted to the test specimen. Other items are present in dummy form, which means that the item is not being tested but that it is used to introduce load into the test specimen. Any items, which are regarded as non-structural such as pipework, wiring, avionics boxes, etc, are omitted.

The loads spectrum for the Hawk LIF test is based on a mix computational modeling and actual flight trials data. The test at Fishermans Bend is being complemented by a tailplane test applying both flight manoeuvre and buffet loads. The tailplane test is being conducted in the UK by BAE SYSTEMS.

The test rig is based in a new test laboratory at DSTO's Fishermans Bend site, it is an 8-metre high, three-level test rig designed by BAE SYSTEMS with DSTO input. Key features include:

- a 1st level platform raised 2.0 metres off the ground to allow sufficient headroom and systems installation within the rig footprint;
- additional floor area on all levels surrounding the fatigue article to allow ergonomic work practices and equipment distribution;
- a removable top deck that allows for the installation and removal of the fatigue article as required.

The main control system was developed by MTS Systems Corporation, USA. DSTO provided background intellectual property to enhance the functionality of the system. The system applies and monitors loads to the test article from 84 hydraulic and 6 pneumatic channels simultaneously. It also includes a fully integrated 1200 channel data acquisition system. The hydraulic actuators were designed and manufactured by Moog Australia, while the valve packs, or Controlled Abort Manifolds, which form part of a fully independent controlled abort unload system, were also produced by MOOG Australia, although based on DSTO design principles. The associated unload controllers were developed jointly by Moog and MTS.

Design and construction and commissioning of the test rig was completed in December of 2005. The fatigue test commenced in December 2005 with the application of a simulated Production Flight Acceptance Test (PFAT) load block. Continuous testing commenced in February of 2006 and is expected to continue until 2012, eight years before the fleet's proposed withdrawal date. The fatigue test will be followed by a residual strength test and a full teardown inspection. Overall the project will be completed by 2014.

By April 2007, the test will have achieved 4500 Equivalent Flight Hours and the test article will undergo a major inspection. This will involve removal of the wing to incorporate several modifications that are also to be implemented in the RAAF Hawk LIF fleet.

8.2.20 Helicopter Structural Integrity - Flight Data Recorder (FDR) Trials (C.Knight, DSTO)

Since the late 1990's, the entire Australian Army Black Hawk fleet has been fitted with Flight Data Recorders (FDR). While the primary purpose of the FDR is to provide air safety investigators with information in the event of an accident or incident, previous DSTO work has identified the FDR as a possible source of data for usage monitoring.

Usage monitoring is undertaken to identify how aircraft within a fleet are being used and to compare that against the assumptions made when the aircraft was designed. This information helps aircraft operators to improve the structural integrity management of their aircraft fleets and hence enhance safety.

Currently, usage monitoring is completed by aircrew filling in a standard form after each flight. These forms contain information such as flight time, numbers of landings and rotor starts, and occurrences of extreme manoeuvres.

To quantify the potential benefits of usage monitoring via an FDR, DSTO's Air Vehicles Division conducted a trial using 6 Black Hawks from a training squadron. During the trial, FDR data were downloaded and processed in conjunction with the standard forms.

The analysis of collected data helped to identify several problems related to data retrieval, reliability of the data stream and other data-fusion issues associated with automated data-recording equipment. Also, comparisons between the manual data and the FDR data allowed the fidelity of the manual data to be assessed. Ultimately, though, the trial quantified the benefits of utilising existing sources of automated data gathering, such as the FDR, as part of regular maintenance procedures.

Since most planned maintenance actions are based on flight times, significant savings in aircraft direct operating costs should occur if logged flight hours are greater than those measured automatically. Alternatively, if the aircraft hours and operations are being under-reported then there are airworthiness issues to address.

Trial data was downloaded between December 2003 and February 2005. Across the 8 aircraft involved in the trial approximately 1300 flight hours have been acquired and compared. Results indicated that although most parameters are accurately recorded, some conditions, principally "Number of Landings", are being significantly under-recorded. Of special note is the high correlation between the pilot's and FDR records of flight hours.

The results of this trial provided impetus to extend to all operational Black Hawks. A one-off trial was completed in April 2006. Once again analysis indicated that pilots were generally recording flight parameters accurately. The largest sources of error were in the areas of extreme manoeuvre recording and landings.

References

1. Knight, C.G., "S-70A-9 Black Hawk Flight Data Recorder Trial: Comparative Results of Training and Operational Squadrons", DSTO Report DSTO-TN-0690, April 2006.
2. Knight, C.G., "S-70A-9 Black Hawk Flight Data Recorder Trial", DSTO Report DSTO-TN-0656, August 2005.
3. King, C.N. and Knight, C.G., "S-70A-9 Black Hawk Usage Monitoring by Utilising Output from the Flight Data Recorder", DSTO Report DSTO-TR-143, May 2003.
4. Knight, C.G., "FDR's as HUMS: A Report on Data Issues, Including the Accuracy of Manually Entered Data", Proceedings of the Eleventh Australian International Aerospace Congress, Melbourne, 13-17 March 2005
5. Dore, C. and Knight, C.G., "Flight Data Recorder Information Retrieval Trial", Proceedings of the Eleventh Australian International Aerospace Congress, Melbourne, 13-17 March 2005

8.2.21 Failure Analysis Examples – Military Aircraft (N.Athiniotis, DSTO)

The following sections contain examples of failure investigations conducted in the last two years by DSTO:

8.2.21.1 Bell 206B-1 (Kiowa) Main Rotor Blade Cracking

The aircraft was undertaking a routine sortie when the pilot reported a minor vibration on the ground that disappeared when the aircraft was pulled into hover. A post-flight inspection revealed the presence of a large crack in the Main Rotor Blade, running chordwise through the trailing edge of the blade and located approximately 1.5 metres from the blade inboard root.

The main rotor blade had been in service for 2913 AFHRS. The 'throw away' life of the blade is 3600 AFHRS. Feedback from the OEM revealed that this was the first known occurrence of this type of failure worldwide.

The examination revealed that the blade failed due to the initiation and propagation of a fatigue crack. The crack initiated at the forward face of the trailing edge spar and grew towards the trailing edge of the blade. As the crack grew longer, load shedding resulted in the initiation of further fatigue cracks in the upper and lower skins of the blade. The crack in the spar eventually grew to within 2 mm of the trailing edge before tensile failure of the remaining cross-sectional area occurred. With the trailing edge of the blade no longer structurally intact, rapid tensile tearing of the thin upper and lower skins in the forward direction subsequently occurred, resulting in a final crack length of just over 200 mm prior to discovery of the problem.

The initiating defect for the fatigue crack in the trailing edge spar was found to be a corrosion pit. Examination revealed that the forward face of the spar was extensively pitted, consistent with moisture ingress into the internal structure of the blade. However, the pitting was found to be localised around the area of cracking, suggesting that the entry point for the moisture was probably in the same vicinity. The exact entry point for moisture ingress could not be established.

Figure 34: Photograph of the crack (lower right, vertical on page) in the MRB showing its location in relation to the blade root

Figure 35: Composite photograph showing an overall view of the fracture surface of the crack in the trailing edge spar. Note the presence of progression marks clearly indicating that cracking was due to fatigue. The origin of the crack is indicated by the red arrow

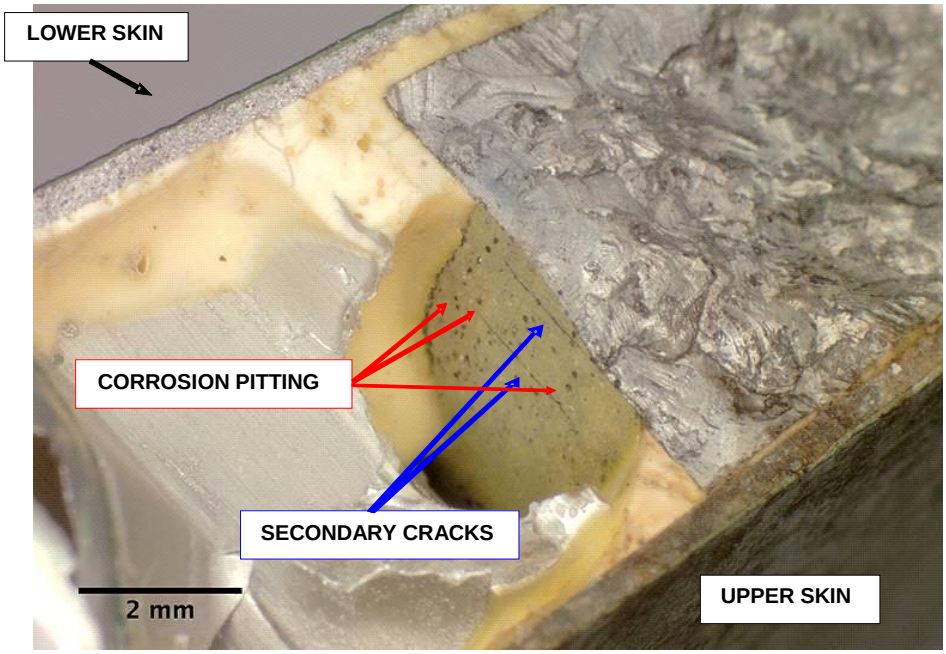

Figure 36: Angled view of the forward face of the trailing edge spar showing the presence of numerous corrosion pits (examples arrowed red), particularly clustered around the lower adhesive boundary and some secondary cracks (arrowed blue)

8.2.21.2 Bell 206B-1 Kiowa Failure investigation of Rolls-Royce 250-C20 Series Engine

The compressor module revealed damage to the blades and vanes comprising the compressor module. In particular, the Stage 3 and Stage 4 vanes were extensively damaged. Examination of the compressor module showed that the liberation of a second stage compressor vane was the cause of the compressor failure.

The service history indicated that the subject compressor case had accumulated 3921.1 hours (time since new). The case was last overhauled 532.5 hours before the incident. Fractographic analysis found that failure of the vane of Stage 2 was by fatigue with the remaining damage to the compressor module appearing to be secondary in nature. Metallographic examination of a cross-section taken through the primary fracture revealed a microstructure that was consistent with other vanes in the compressor module. However, the cross-section did reveal that the vane had suffered a reduction in thickness, predominantly on the vane pressure side; the reduction was a smooth and gradual transition, indicating that the likely mechanism for this loss of thickness was erosion, most likely due to ingested particles entrained in the airstream. The fracture of the vane occurred in the area of reduced thickness. The primary fracture was cross-sectioned and showed a reduced vane profile both above and below the epoxy layer. Reduced cross-section below the epoxy layer indicated that this region was previously eroded and subsequently covered by a new epoxy layer during refurbishment. These cross-sections showed that prior to refurbishment, the vane was at or close to the minimum thickness required by the overhaul manual.

In order to ascertain the extent of the pressure side erosion, a sample of vanes from other locations in the compressor module were examined. These vanes were sectioned at approximately the major vane thickness and the uneroded and eroded thicknesses were measured. Measurements were performed using a calibrated optical stereoscope. The measurement results for the sample of vanes indicated that at the time of the incident several vanes of Stages 1 and 2 of the compressor module had minimum thicknesses below the allowable Operation and Maintenance Manual limits

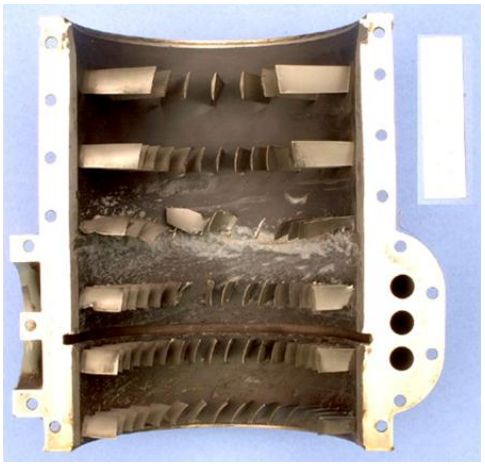

Figure 37: One half of the compressor case showing the extensive damage sustained by the compressor vanes in the incident

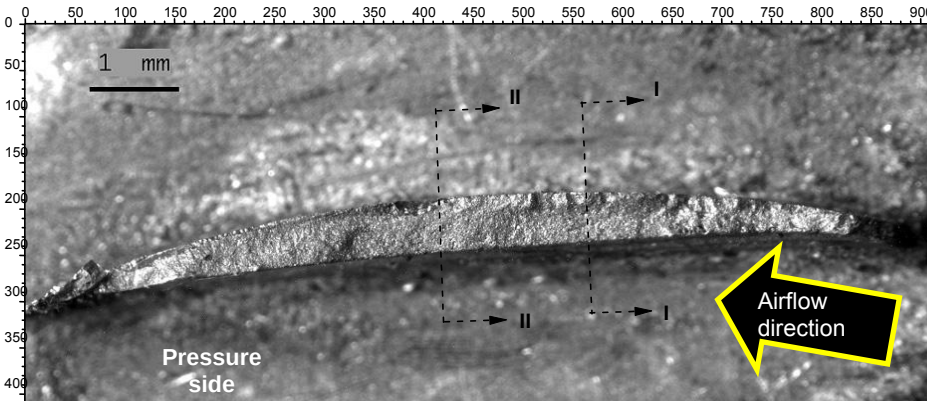

Figure 38: Optical image of the primary fractured vane (Stage 2). A fatigue crack initiated on the pressure side and propagated through the majority of the vane thickness followed by overload of the remaining ligament

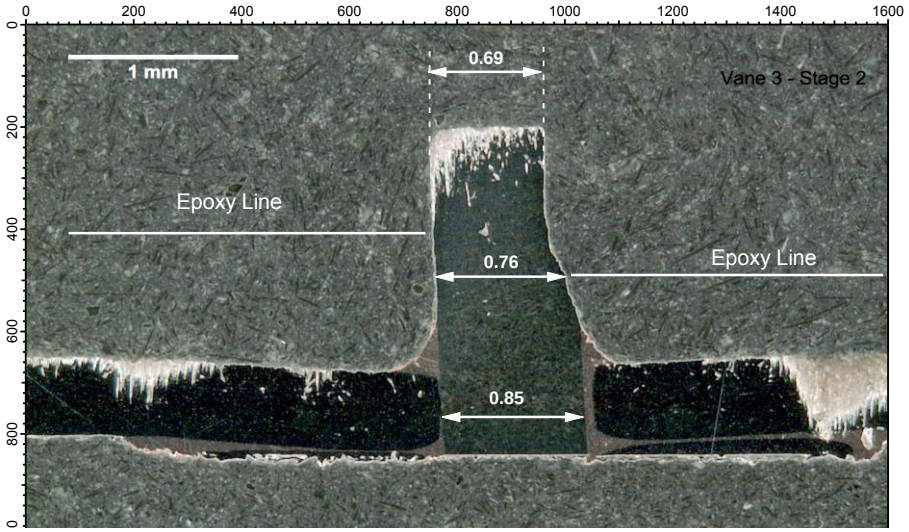

Figure 39: Photomicrograph showing the reduction of the vane thickness below the epoxy line. All measurements are in millimetres

8.2.21.3 Black Hawk Fuel Cell

During investigation of a fuel leak discovered as the aircraft was being returned to service from short term storage, it was found that the fuel system had significant contamination. The contaminant was activated self sealing material (natural gum rubber) of the cell saturated with fuel.

Subsequent investigation by DSTO revealed a crack through the inner liner thickness of the fuel cell's inboard side. The crack was situated in the middle of a repair patch. The patch was found to be severely degraded and had exposed the inner liner crack to fuel. This allowed the fuel to come into contact with the self sealing sealant (natural gum rubber) causing it to activate and swell many times its normal size. This activation and swellingto initiated delamination of the plies of the cell wall, resulting in loss of wall strength and the eventual catastrophic failure of the fuel cell.

The crack in the inner liner material of the cell may have initiated from the surface imperfection that necessitated the repair patch. The cause of the degradation to the patch and crack in the inner liner of the cell was considered to be mostly due to age-related degradation of the elastomers exacerbated by periodic maintenance cycles where the fuel cell would be left dry for extended periods of time.

Figure 40: Photograph of the Black Hawk Port Fuel Cell in the collapsed condition with no external cover or packaging. The cell contained a small amount of water and dirt

Figure 41: (L) The severely deteriorated repair patch located on the inner liner in a corner of the cell, and (R) typical cracking found on the repair patch

8.2.21.4 P3 Orion Turbo Compressor

The Turbine Driven Centrifugal Compressor is the principal component of the Air Multiplier Package (AMP), which provides air to the RAAF P3 Orion air-conditioning system when the aircraft is on the ground. The AMP is powered by bleed air from the aircraft's Auxiliary Power Unit (APU). The AMP reduces the air pressure and increases the weight-flow of the bleed air from the APU making it suitable for use in the aircraft's air conditioning units. Due to a recent increase in the failures of AMPs, DSTO were requested to undertake a comprehensive failure analysis of several failed Turbo-Compressor units to determine the cause of these failures.

The investigation determined that the failures were indicative of the compressors having suffered an over-speed event. Two possible failure sequences may have occurred:

- An over-speed event caused one of the bearings within the compressor assembly to become overheated resulting in the balls within the bearing jamming and skidding on the rolling surfaces of the inner and outer races and the ball retaining cage, causing severe damage. The bearing failure caused the shaft to run out of alignment allowing the compressor shroud to contact the inner surface of the Torus Assembly; or,

- An over speed event has caused separation of the shroud from the vane to shroud brazed joint projecting the shroud onto the inner surface of the Torus Assembly. This caused the compressor shaft to become unbalanced both overloading and overheating the bearing that supported the shaft leading to the destruction of one or both of the bearings.

Regardless of the exact failure sequence that occurred, the primary cause of the failures was an over-speed event.

Figure 42: Photograph showing the compressor inlet (arrowed) in situ on the port side of an aircraft

Figure 43: Photograph showing impeller vane damage from Turbo Compressor

Figure 44: Photograph of severely heat damaged shaft from the Turbo Compressor

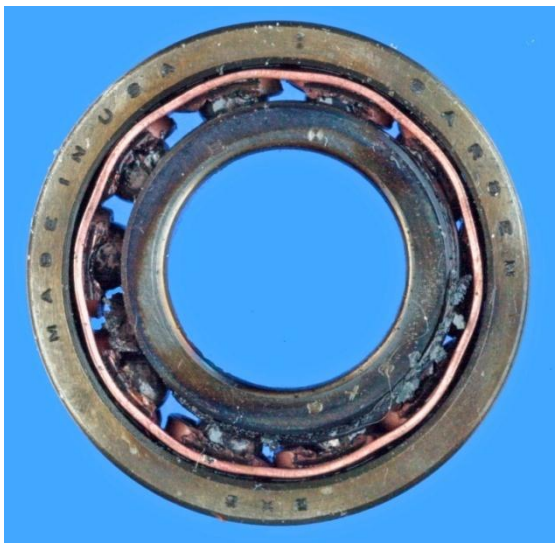

Figure 45: Photograph of a bearing from the Turbo Compressor which had been severely damaged by overheating

8.2.21.5 PC-9 Main Landing Gear Folding Strut

A crack was discovered in the aft flange of the strut during disassembly of the left hand main landing gear of the aircraft. The support strut had accumulated 4961.5 air flight hours and 9826 landings and no previous similar defects were known.

Examination of the aft flange revealed that the crack extended from the end of the flange through to the actuator bolthole; it was gaping towards the end of the flange while towards the actuator bolthole it consisted of multiple fine branches. The crack was broken open to reveal an intergranular fracture surface, with cracking on multiple levels and grains of metal lifting up from the surface, consistent with stress-corrosion cracking.

Testing of the material comprising the strut revealed that it had been manufactured using aluminium alloy AA 2024 in the T3 temper, which is susceptible to stress-corrosion cracking. Cracking in the strut was attributed to environmental exposure and residual stresses from manufacture. It was recommended that the component should instead be manufactured using an alternative material with a greater resistance to stress-corrosion cracking, such as AA 2219-T6.

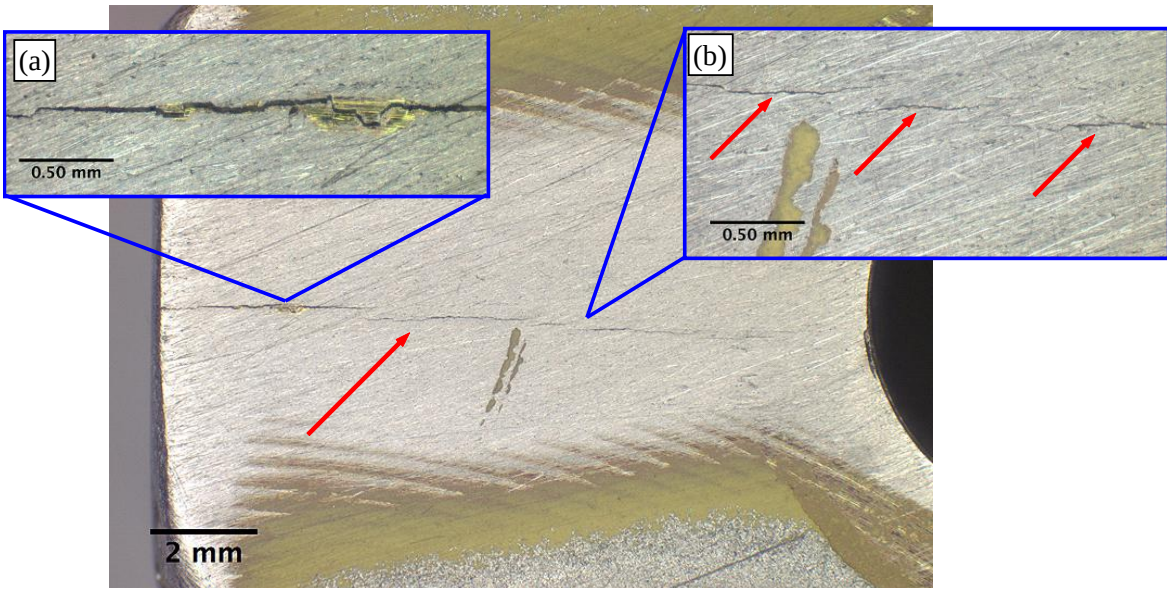

Figure 46: Photograph of the crack in the aft flange of the PC9 MLG folding strut (arrowed). Inset: (a) close up of the crack towards the end of the flange showing the crack to be gaping; inset (b) close up of the crack towards the actuator bolthole showing the presence of multiple crack branches (arrowed)

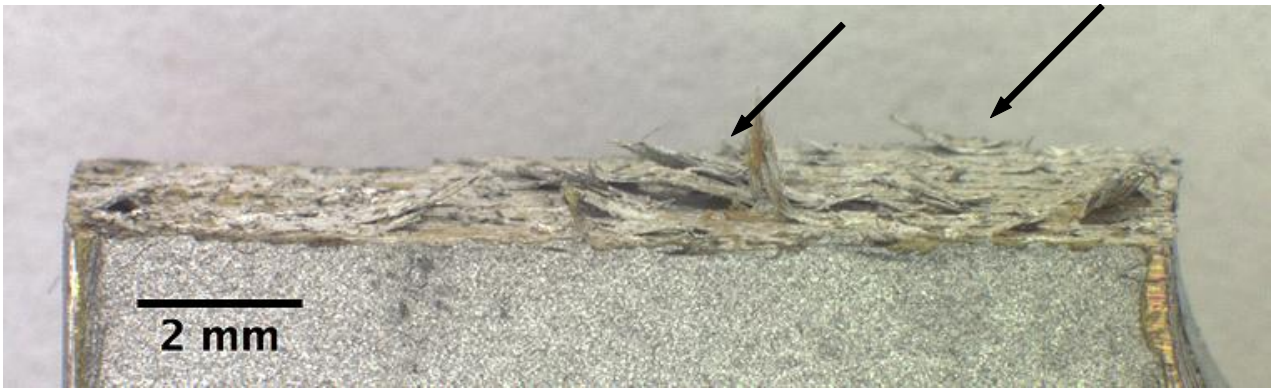

Figure 47: Side view of the support strut fracture surface showing grains of metal lifting up from the surface (examples arrowed), typical of stress corrosion cracking in wrought aluminium alloys

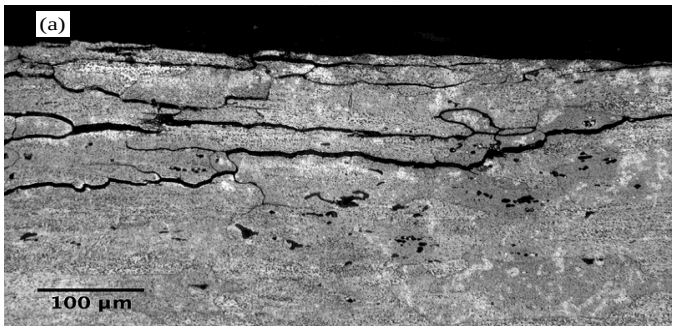

Figure 48: Photograph of an etched cross-section showing the intergranular nature of the cracking

8.2.21.6 Iroquois A02-455 Accessory Drive Gearbox Drive Bevel Gear Failure

The crew of an Australian Army Iroquois experienced a loss of power, with the aircraft entering autorotation and terminating in an engine-off. Prior to landing, the crew had sufficient time to attempt an override of the governor into emergency fuel as well as an in-flight restart. Neither of these was successful. Mayday calls were made to accompanying Iroquois aircraft, which subsequently responded to the forced landing site.

Preliminary investigation indicated that the possible cause of the in-flight failure of the engine could be related to problems with the accessory drive gearbox. Consequently, the engine was removed from the subject aircraft and placed in a safe location for further examination. Disassembly of the engine proceeded to the point where the gear assembly from the accessory drive gearbox was visible.

Visual examination of the accessory drive carrier assembly revealed that the accessory drive bevel gear had failed in three major segments. Visual examination of the fracture surfaces of these segments revealed the presence of a fatigue crack along the root of a tooth. The fatigue crack initiated at the root of the tooth on the pressure side and propagated outwards along the root of the tooth. Final overload fracture of the drive bevel gear ensued when the fatigue crack reached its critical size and the uncracked ligament could no longer carry the applied loads. Seven additional cracks were found during visual examination using a high-powered optical microscope. These cracks were located at the root of the other bevel gear teeth.

Analysis of wear patterns on the bevel gear teeth suggested that off-set loading of the gear teeth was a contributing factor in the initiation of the fatigue cracks that led to failure of the component. Poor tooth load distribution (likely to have been caused by mechanical misalignment of a pinion with the drive bevel gear) resulted in unusually high cyclic loading. The resulting bending moment of the teeth contributed to the initiation of multiple fatigue cracks at the roots.

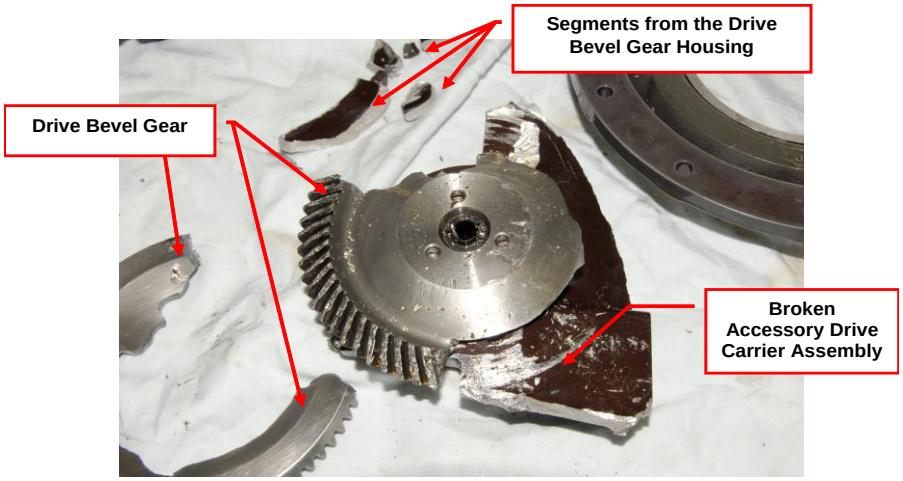

Figure 49: Photograph of the drive bevel gear segments. The largest segment has its respective bearing still attached to the housing

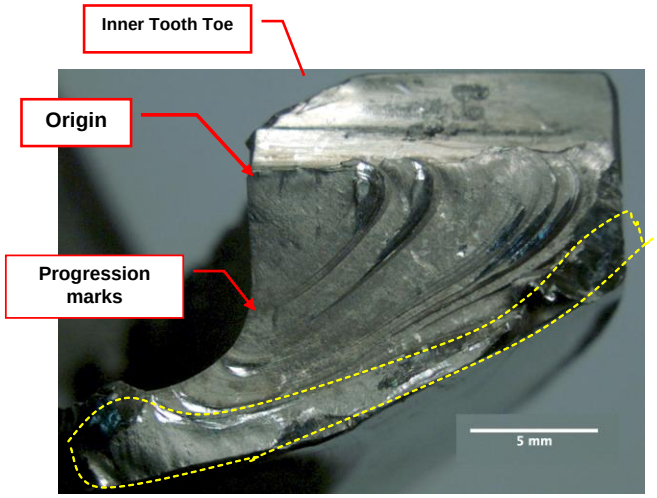

Figure 50: Photograph of the primary fracture surface. The flat almost featureless surface with concentric rings (i.e. progression marks) is typical of fatigue cracking. The direction of the fatigue crack propagation is from top left to bottom right. The approximate location of overload fracture is outlined

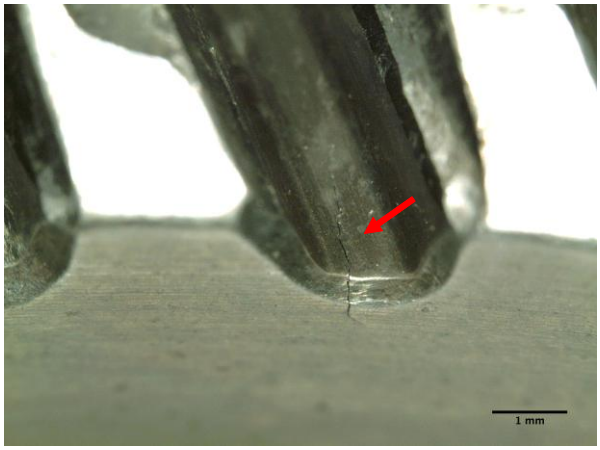

Figure 51: Close up view of an additional fatigue crack located at the root of the bevel gear teeth

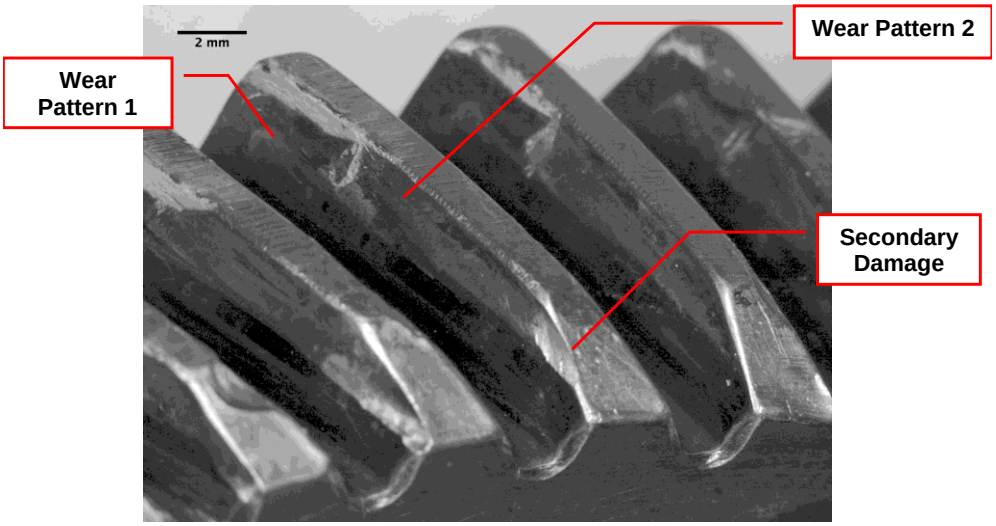

Figure 52: Typical appearance of the wear patterns observed on the face of the gear teeth

8.2.22 Some New Directions for Corrosion Prevention Maintenance (B.R.W.Hinton, DSTO)

With the aging of airframes through extended operating lives, environmental degradation (corrosion) is becoming a major issue for aircraft operators. The gradual breakdown with time of protective paint coatings and sealants means more corrosion is developing in structural components.

RAAF DGTA in response to the increasing development of corrosion in most aircraft types in the fleet recently tasked Aerostructures to develop an Environmental Degradation Management Toolbox (**EDM Tool Box)**. This tool box will provide a rigorous engineering framework to support the following:

- Collection of quality corrosion related data during airframe inspections
- Engineering assessment of that data
- Maintenance decisions based on those assessments to prevent corrosion and to reduce its impact on structural integrity
- Transition of new technologies either developed by DSTO or assessed by DSTO into the aircraft maintenance process.

Use of the tool box will allow the Systems Program Offices to meet the regulatory requirements of Director General Technical Airworthiness, and with more efficient corrosion prevention maintenance increase aircraft availability, thus meeting the needs of the aircraft operators. Major tools for the Box include:

8.2.22.1 Structural Prognostic Health Monitoring

DSTO is developing a Structural Prognostic Health Monitoring (SPHM) System, which will enable the maintainers of Australian Defence Force (ADF) aircraft to manage the prevention and control of corrosion in selected structural aircraft components on a condition basis rather than on the basis of an elapsed number of flying hours.

The development of corrosion in aircraft structural components over their operating life is largely due to the gradual deterioration and breakdown of protective paint coatings, anodised coatings, conversion coatings, metallic coatings and sealants. Unfortunately most of the high strength aluminium alloys and steels used for structural components are susceptible to corrosion. The costs associated with detecting, repairing, replacing and repainting corroded components increase with aircraft age and these costs are important factors in determining the eventual life of the aircraft. While these maintenance costs are readily identified, it is the costs associated with not having the aircraft capability available for operational purposes, that are harder to define, and which may be orders of magnitude greater.

Inspections for corrosion damage are usually time consuming, complex, require aircraft disassembly, and quite often reveal no corrosion damage. In an effort to reduce maintenance costs and to increase aircraft availability, aircraft maintainers are considering condition based maintenance centred around a structural health monitoring system (with a prognostic capability) for aircraft structures, rather than inspections on the basis of elapsed flying hours.

The philosophy of Structural Health Monitoring (SHM) is based on the concept of continually monitoring a structure in order to (i) identify when coatings have broken down, (ii) identify when corrosion has commenced, and (iii) characterise the nature of the environment in a particular area of structure. With this information, a decision can be made as to when and if a component in a structure should be replaced or repaired. The basic tools for effective SHM are (i) corrosion sensors and environment monitors, (ii) corrosion prediction models, and (iii) intelligent decision making software. An extension of a SHM System is a Prognostic Structural Health Monitoring System which should be capable not only of indicating the state of degradation (ie. corrosion) and its effect on structural integrity of the aircraft, but also of predicting when protective coatings will fail, when corrosion is likely to occur in remote areas difficult to inspect, and how those predictions will change depending on aircraft base location and mission type. With this information components could be replaced, before failure due to corrosion or fracture resulting from section loss, thus maintaining structural safety, increasing aircraft availability and recurring maintenance costs.

The DSTO System is based on the concept of locating corrosion sensors and environment monitors in areas of aircraft structure, which are generally difficult to inspect and/or are only inspected at major servicings ie. at 3 to 5-year periods. The output from these sensors and monitors will be inputs into Corrosion Prediction Models (CPMs) and ultimately into Fatigue Prediction Models (FPMs). These Models will predict (i) when protective coatings systems will fail, (ii) when corrosion will occur, (iii) the depth of corrosion and distribution of damage in a given area, (iv) the likelihood of fatigue crack initiation, and (v) the rate of propagation of fatigue cracks. The output from the models will feed into intelligent management software which in conjunction with a database of coating performances, flight and mission details, and materials knowledge will indicate possible maintenance decisions and actions. These decisions may

include (i) inspect component, (ii) repair component, (iii) replace component, or (iv) treat to retard corrosion and leave in place.

Knowledge and information required for the SPHM:

Knowledge of Corrosion Problem Areas

This information is readily available where a fleet of aircraft has been in operation for many years. For a new aircraft, it is difficult to know where corrosion may occur. However a knowledge of aircraft construction, experience in how environments develop within particular areas of structure, and information about local stresses, nature of structural joints, types of alloys and fasteners at these locations and the type of protective coating system, all assist in making judgements on where corrosion may develop.

Operating Environments

It is generally accepted that most corrosion in aircraft structure occurs while the aircraft is on the ground or flying at low altitude. At high altitudes, temperatures are usually too low for the corrosion reaction to proceed. In the vicinity of engines or other onboard heat emitting sources, those low temperatures will not be reached, and corrosion may proceed. A detailed knowledge of what the environment is in the vicinity of particular components, eg. how often the area becomes wet, what contaminants are present and how these factors vary with mission type and base location is probably too difficult to obtain. The location of sensors and monitors in the general area of interest can provide that information.

Paint Coating/Sealant Failure Models

Corrosion will not occur generally until a protective coating fails. This failure may be induced by mechanical damage in the course of maintenance, but it is more usual for a coating on aircraft components to mechanically fail as a result of stress and environmental factors. The stresses arise from operational loads such as those around working joints and fasteners, thermal cycles, (eg. from -30^{o}C to 80^{o}C would not be uncommon), the freezing of moisture absorbed into a paint coating and blistering resulting from moisture accumulating at the paint - metal interface. The environmental factors most relevant to a PHM System, which impact on paint failure and corrosion, are those that develop inside the aircraft. They are condensation resulting from the thermal cycle, the hot box effect associated with enclosed spaces, or prolonged exposure to high temperatures if near an engine or just beneath the outside skin (heated by frictional stress of air flow). Following paint failure, attack on the exposed metal will generally follow when the inhibiting pigment included in the paint coating is depleted by leaching.

Currently, models which will predict coating failure under the combined action of all of these variables do not exist. There have been studies to identify the rate of depletion of inhibitors from primers once the coating has been breached, however these results are empirical and have usually focussed on a particular test environment such as the neutral salt spray test. It is generally accepted that the salt spray test is neither typical nor representative of the environment around an aircraft component, which is more likely to be subjected to condensing droplets of moisture and periods of drying.

While paint coating failure models will be necessary, it will be important also to have some sensors strategically located on board which will detect coating failure, and allow for on board validation of these models. The approach with the DSTO SPHM System is to locate sensors under coatings in an area of interest which will indicate when corrosion on the sensor elements occurs, thus indicating not only when deterioration of the coating has occurred but also when inhibitors in the coating have been depleted.

Corrosion Prediction Models

Once coating failure occurs, and corrosion-inhibiting pigments have been depleted to a level where protection is no longer possible (available from laboratory studies), it is reasonable to assume that corrosion will quickly occur. Corrosion models are required which will predict the depth and distribution of corrosion damage with time, whether it is pitting or intergranular corrosion.

Fatigue Prediction Models

The savings with a SPHM System result from not having to inspect inaccessible areas of structure. Therefore non-destructive inspection techniques (NDI) will not be an option. It will be necessary to have fatigue crack initiation and propagation models to use output from the CPMs. Clearly a detailed knowledge of the stresses in and around joints

where corrosion is suspected of developing is necessary. Finite element models (FEMs) of stress distribution in these areas are usually available. The FEMs will be used in conjunction with corrosion prediction models and stress information to predict where fatigue cracks will develop. With information about location stress and environment, laboratory and handbook data will provide crack propagation rates.

Corrosion Arrest Technologies

If a prediction is made that the corrosion damage will develop and that it represents a low level risk of fatigue crack initiation or none at all, it is envisaged that the corrosion could be treated with appropriate inhibitors to retard further crack growth. Currently, the most appropriate treatment for arresting corrosion involves the use of Corrosion Prevention Compounds (CPCs). CPCs may contain (i) a film former such as an oil, grease or resin, (ii) a volatile, low surface-tension, carrier solvent, (iii) a non-volatile hydrophobic additive and (iv) various corrosion inhibitors eg. sulphonates, which have been shown to have very good corrosion inhibition properties. Some CPCs act by spreading across surfaces and into crevices, displacing any water present. The carrier solvent evaporates and leaves a residue consisting of the film, hydrophobic additive and the inhibitors. Others dry to a waxy or hard resin like finish after application and provide a barrier film. Different CPC products and specifications are appropriate for various locations and with certain effective lifetimes. Empirical data on these properties are available.

Maintenance Decisions

In general the maintenance decisions (ie. Replace or Repair) will be based on structural integrity and safety considerations. The information needed to help make these decisions is available in the aircraft structural repair manuals.

8.2.22.2 Corrosion-based reliability Centred Maintenance (CBRCM)

DSTO has been funded to carry out a CBRCM Pilot Program on the C-130J aircraft. This pilot study will address thirty structural and maintenance significant items on the aircraft. Currently most corrosion related inspections are based on elapsed flying hours, when that corrosion is a time based phenomenon. Furthermore, inspections are geared to looking for corrosion ie. the failed condition. The RCM process is designed to develop inspection intervals which will detect the precursors to corrosion, and thus allow corrosion prevention measures to be applied, and thereby avoid expensive and time consuming replacement or repair. Corrosion only occurs once coatings have failed.

The RCM process follows well defined international standards, and in the pilot study, the US NAVAIR 00-25-403 Guidelines for US Naval Aviation RCM Processes are also used. The process involves identifying the failure pathways and modes associated with corrosion and uses knowledge of coating failure times, corrosion propagation rates and the local environment around the item of interest, to determine the time at which the damage will reach the Material Removal Limits. Using a rigorous analysis and statistical methods set out in the many Standards a new inspection interval is set so as to observe coating breakdown and prevent corrosion just before it starts.

8.2.23 Risk Assessment for Military Aircraft (R.Antoniou, DSTO)

Original equipment manufacturers are particularly conservative in promulgating structural and component lives, especially when there is no prior history (a new design) or where only a limited history exists (early in the service life). Once that structure or component is placed in service, a database of actual performance/lives can be accrued. Subsequently if a fatigue life re-evaluation is required for a particular component or structure, for either logistical, operational or safety reasons, this database can be utilised to provide more accurate estimates of the lives and the associated fleet risks.

A major aim of the risk analysis work in the Air Vehicles Division is to utilise the operating experience of a fleet of aircraft over many years, to compile a detailed and extensive database of component lives that has the potential to be used in assessing airworthiness risk.

Two examples are:

8.2.23.1 Reliability Analysis of F-111C Wing Fatigue Life

The fatigue life validation of the F-111C wing has been a subject of investigation by the RAAF and DSTO for some time, since the failure of the A15-5 wing while under test by DSTO. The interpretation of the A15-5 failure in the outer wing regions had indicated insufficient life in that region of the wing to achieve the planned withdrawal date (PWD) of the F-111C wings fleet. Given that some of the C-model wings had flown well past the indicated life without failure, the RAAF considered that this service life information could be added to that gained from the A15-5 test result, to produce a better estimate of the safe life. Accordingly, the RAAF tasked DSTO to perform a reliability analysis of the service F-111C wing life data.

Three analysis methods were applied to the wing service life data. They were: a DEFSTAN 970 analysis, a Weibayes reliability analysis and a maximum likelihood reliability analysis.

This work demonstrated a useful life increase for F-111 wings (at the outer wing locations) and may be an important contributor to certifying the life of the replacement F&D model wings to achieve the F-111 PWD.

8.2.23.2 Risk Analysis of TF-30 2nd and 3rd Low Pressure Turbine Discs

The TF30 engine is facing significant reductions to the low cycle fatigue (LCF) lives of critical rotating parts a consequence of Original Equipment Manufacturer (OEM) Pratt and Whitney Aircraft (PWA) advice.

The components most affected by these reductions have been the 2nd and 3rd low pressure turbine (LPT) discs. These components are currently being managed using a “safety by inspection” procedure that assumes the components have a crack initiation life of zero and uses a Level 4 fluorescent penetrant inspection of the discs at the designated overhaul interval. If no cracking is found the disc is returned into service. This process is repeated until the safe life of the component, as based on the 2nd most critical LCF location, is reached; thereafter the component is discarded. As a consequence of the OEM recommendations, the discs will now be discarded at a reduced interval that is based on the original overhaul interval less an amount due to the increase in LCF cycles. In order to ascertain whether the required inspection interval is achievable without compromising technical airworthiness of hot section components, DSTO was tasked by the RAAF to conduct a risk analysis.

Based on the results of this risk assessment, the currently available service experience and the RAAF mission, it was recommended that an increased life can be applied to both hot section components.

8.3 FATIGUE OF CIVIL AIRCRAFT

8.3.1 B787 Inboard and Outboard Trailing Edge Flaps Static and Fatigue Tests (P.Hayes, Aerostructures)

Hawker de Havilland, a subsidiary of Boeing, is designing and building the complete trailing edge flap system for the new Boeing 787 Dreamliner.

The two largest components of the flap sets are the inboard and outboard flaps. AeroStructures has been contracted to build and operate the test rigs to conduct structural tests on pre-production and certification test articles, including a full-scale fatigue test on the inboard flap and hot/wet static tests on the outboard flap. These tests are being conducted in the DSTO test facilities in Port Melbourne.

The test rig applies simulated aerodynamic loads via multiple actuators and a two-level whiffle tree. In addition, wing bending is also simulated through displacement control deflections of three of the five flap attachment points.

A program of static tests, both room temperature and hot-wet, incorporating damage and repair schemes, have been successfully conducted on the pre-production outboard flap test article. This program terminated in a successful test-to-failure of the test article.

The test rigs are now being reworked to prepare for the certification static tests, which will be conducted before first flight of the B787 in late 2007.

Figure 53: The Pre-production Outboard Flap Test Rig

8.3.2 "Rusty Diamond" - Could damage Tolerance be as useful for Corrosion as it is for Fatigue? (S.Swift, CASA)

The author has prepared a paper for ICAF 2007, considering whether *damage tolerance* could be as useful for managing corrosion as it is for fatigue. The abstract follows:

"An experienced regulator reviews whether damage tolerance could be as useful for corrosion as it is for fatigue. The answer is 'yes'. Operators, manufacturers and regulators could save time and money while they save lives. Examples, recommendations and draft regulatory guidance show how."

8.3.3 Initial Flaws (S.Swift, CASA)

For many, 'initial flaws' are fundamental to 'damage tolerance'. This ICAF, we ask two questions:

- Are initial flaws in holes always at the corner?
- Are initial flaws a credible safety concern?

8.3.3.1 Are initial flaws in holes always at the corner?

In October 2006, an ex-military jet, a Strikemaster like the one below, crashed in Australia. Both pilot and passenger were killed. The cause was fatigue failure of the lug which attached the right wing.

Figure 54: Strikemaster

Figure 55: Broken lug on the inboard end of the right wing

Above (Figure 55) is the broken lug, on the inboard end of the right wing.
Interestingly, it was the upper lug that broke, not the lower. Strikemasters routinely pull negative 'g' in aerobatics.

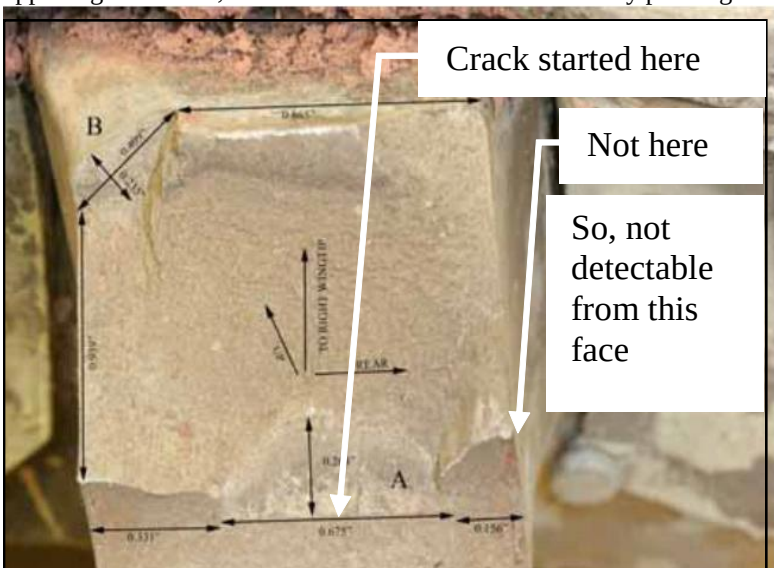

Figure 56: Closer view of the break.

Figure 56 is a closer view of the break. Note how a fatigue crack started *along* the hole in the lug, *not at the corner*, like we often assume. So, it was dangerous before it was detectable by the manufacturer's recommended eddy current inspection of the lug face.

For more information, see the *Preliminary Report* on the Australian Transport Safety Bureau's web site:
http://www.atsb.gov.au/publications/investigation_reports/2006/aair/pdf/aair200605843_prelim.pdf
Also, CASA's *Airworthiness Bulletin*: http://www.casa.gov.au/airworth/awb/02/018.pdf

8.3.3.2 Are initial flaws a credible safety concern?

Figure 57: A Fairchild Metro turboprop airliner.

Figure 57 is a Fairchild Metro turboprop airliner. It seats 19 passengers and is popular with regional airlines.

Figure 58: Supplemental Inspection Document

Figure 58 shows a Supplemental Inspection Document, the latest structural maintenance program, funded by the United States Federal Aviation Administration (FAA). It assumes initial flaws in fatigue-critical structure.

The trouble is, few are doing its inspections, because few airworthiness authorities are enforcing it – even the FAA. It seems there is contentment with the old structural maintenance program, which was based on a normal fatigue test of a production airframe. The old program, of course, has fewer inspections, and they start later.

It seems, in the civil world, for this size aircraft, with good service experience, initial flaws are not yet a credible safety concern.

8.3.4 Comparative Vacuum Monitoring (CVM™) A tool for Structural Health Monitoring of Aircraft (D.P.Barton, Structural Monitoring Systems Ltd, Australia)

The Comparative Vacuum Monitoring (CVM™) technology is able to detect flaws in metals and composites by monitoring the stability of a vacuum level in a confined volume. The confined volume can be produced in the structure under test, or by applying a sensor with micro-channels on its surface to contain the vacuum. Structural Monitoring Systems Ltd is currently working towards certifying the technology with Airbus, Boeing, Embraer and several military organisations for use on aircraft.

Structural Monitoring Systems (SMS) has entered into a Joint Development Agreement (JDA) with Airbus to develop its instrumentation and sensors for use on aircraft. Airbus and divisions of EADS have been involved in a series of benchmarking, environmental robustness, durability and functionality trials of the CVM™ surface sensors to meet the requirements of the DO-160 standard, Airbus internal standards (if there exist greater requirements than the international standards) and a series of Probability of Detection (POD) programs under varying environmental conditions. These trials are designed to test the limitations of CVM™ sensors and their ability to meet the requirements for crack detection whilst surviving in harsh aviation environments. The CVM™ technology has recently been installed on flying aircraft under the umbrella of the JDA program, with the work program outlined in the JDA due to be completed by the end of 2007.

Approximately 140 sensors have been installed on the A380 Full Scale Fatigue Test program in Dresden in Germany. The sensors were installed in July 2005 and consisted of both integral sensors to monitor lap-joints and surface sensors installed throughout the airframe. The sensors are being monitored in real-time over the web in Bremen, and the airframe has currently completed more than one simulated lifetime.

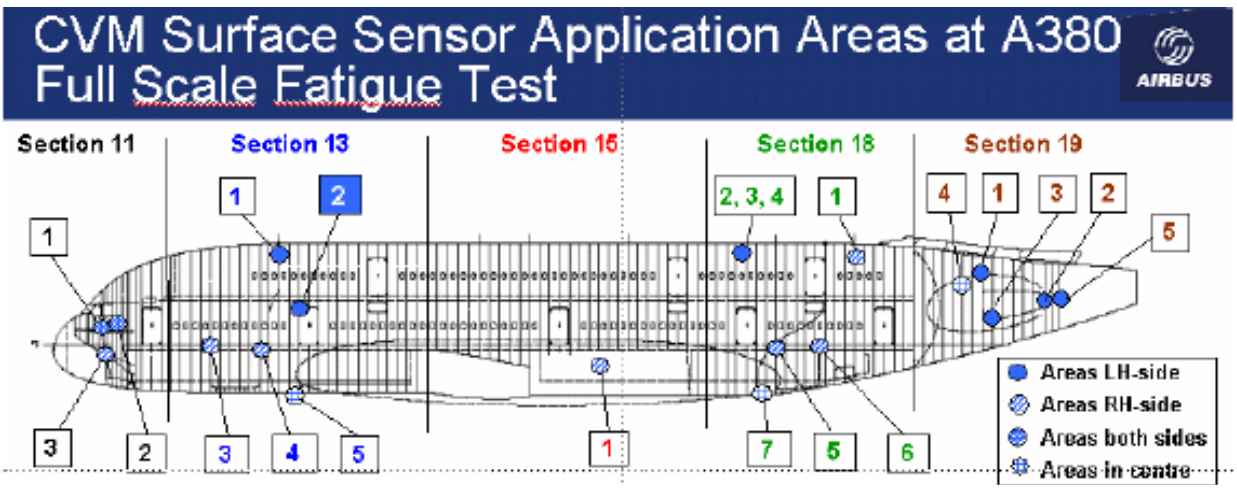

Figure 59: The CVM™ installation on the A2380 FSFT in Dresden Germany

SMS has also progressed significantly through a program with Boeing, Airline Operators and the FAA to have the CVM™ technology entered into the Common Methods NDI (CMN) for Boeing Commercial Airplanes. Once published in the Boeing CMN, the technology will be available for incorporation as a monitoring technique into Service Bulletins for use by operators of Boeing Commercial Airplanes on their aircraft. The program includes a broad range of tests for the CVM™ system including POD, durability (both in the laboratory and on flying aircraft) and defining the effects of contaminants on the system's functionality.

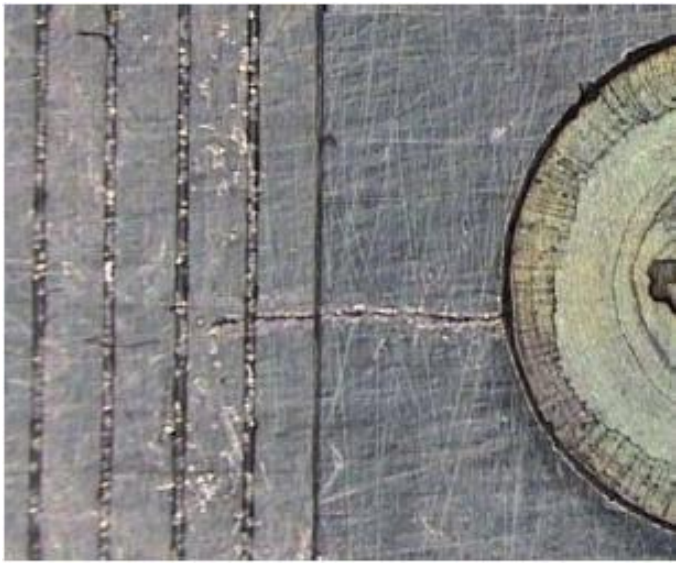

Figure 60: Cracks measured as part of the POD trials within the CMN program

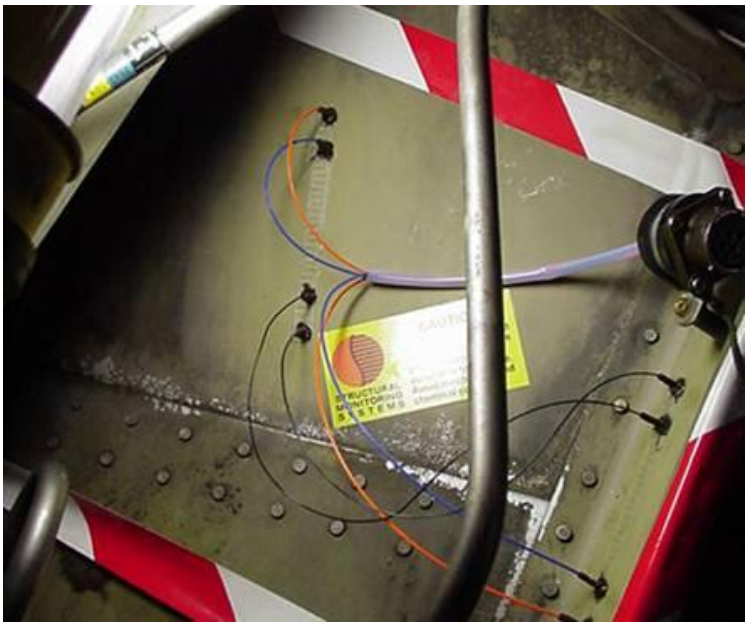

Figure 61: CVM™ sensor durability assessment installation on a USA airline operator aircraft

The company is working closely with the Australian Director General Technical Airworthiness (DGTA) to validate the CVM™ system and SMS to allow the company to supply CVM™ to the Australian Defence Force (ADF). The program builds on SMS' previous trials with the Australian Defence Science and Technology Organisation (DSTO) to demonstrate the functionality and robustness of the CVM™ system; sensors and instrumentation. These programs include laboratory POD and robustness trials and installation on P3-Orion Maritime Patrol aircraft and Blackhawk Helicopters. DGTA is also assessing SMS' internal systems and processes to ensure that the company meets the requirements to be an aerospace supplier to the ADF.

Figure 62: POD test program setup at DSTO in Melbourne.

Figure 63: POD test coupons during fatigue testing

SMS is working with a number of other military programs to validate the technology for use on their fleets of aircraft. SMS has installed sensors on several Royal Navy (UK) Seaking helicopters and a Royal Air Force (UK) Nimrod as part of evaluation trials. There is a close cooperation between the UK Department of Defence and the Australian DGTA for the validation of CVM™ systems for installation on their airborne fleets.

The company continues to work with a number of other Military organisations in North America, Europe and Asia.

SMS has recently expanded its composite programs with a number of organisations including the Cooperative Research Centre for Advanced Composite Structures CRC-ACS in Melbourne, of which it is an Associate Member. The CVM™ system has been reliably used to detect Barely Visible Impact Damage (BVID) using sensors developed from the standard surface sensors, placed on the back face of the impact surface. Bonded structures have also been monitored using Through the Thickness (TTT) sensors (Figure 64), which use blind holes have been drilled through the bond line to monitor the structure with the standard CVM™ equipment. The developments are in a relatively early stage of development, but are showing excellent initial results.

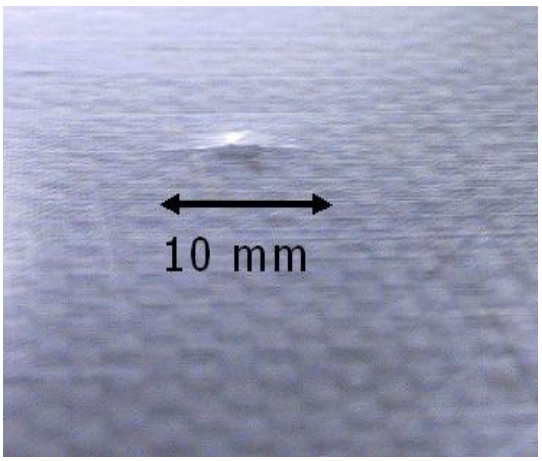

Figure 64: BVID damage detected using surface sensors on the back face of a test coupon

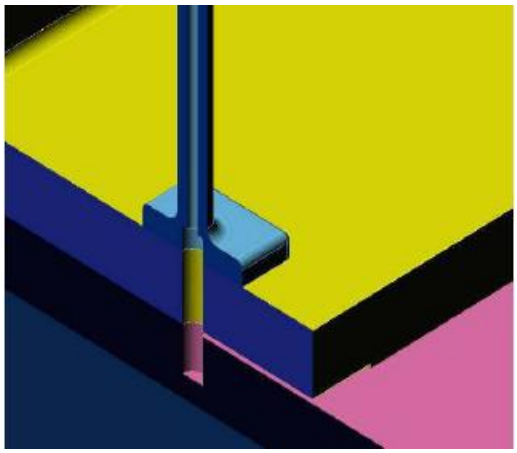

Figure 65: A schematic of a blind hole through the bond line forming part of a TTT sensor.

8.3.5 An Evaluation of a Fatigue Test on a Nomad Aircraft (C.Nicholson, Boeing Australia)

A re-evaluation of fatigue tests completed on a complete Nomad airframe was completed with the aim of developing more suitable inspection techniques. The fatigue test had been completed during the 1980s and had produced apparently anomalous results in respect of one component, the Nomad stub wing, where three components in total failed all at the identical location on the 2024 spar cap, two at approximately 130,000 hours, and one at 37,000 hours, compared to a projected life of 300,000 hours. The failures were significant since the basic aircraft configuration resulted in the stub wing being a primary load path for flight and ground loads. The configuration also resulted in the fatigue spectrum being dominated by a large Groud-Air-Ground (GAG) cycle which also featured large compressive stresses during the ground portion.

Firstly, through analysis of coupon data kindly supplied by FTI in Seattle, it was possible to show that the 130,000 hours was in fact a realistic estimate for the component as the coupon data showed that the compressive stresses in the GAG contributed significantly to the accumulated fatigue damage. Indeed for stress ratios of the order of R=-2, 7075T6 aluminium alloys possessed better fatigue properties than the 2024T3 series alloys.

It was also possible to develop a fracture mechanic approach which could match analysis to the fractographic records which had been produced as a result of the component failures at the time of the fatigue tests. These crack scenarios considered double crack growth from a rivet hole, which when it broke through to near edge transitioned to a single

crack with a much larger characteristic crack length. It was also possible to postulate that the premature failure at 37,000 hours resulted from initial flaws in the holes of the test structure, and that during the first test an unrelated failure in the test rig produced a significant overload, which resulted in crack growth retardation.

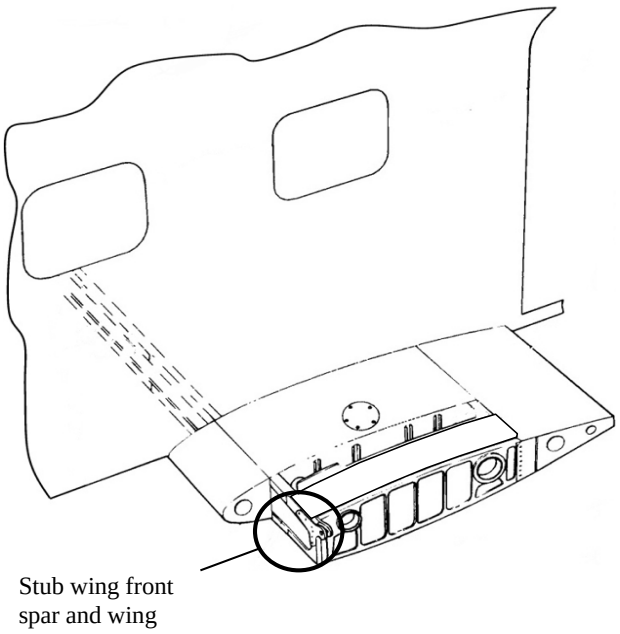

Figure 66: Nomad Stub Wing Structure

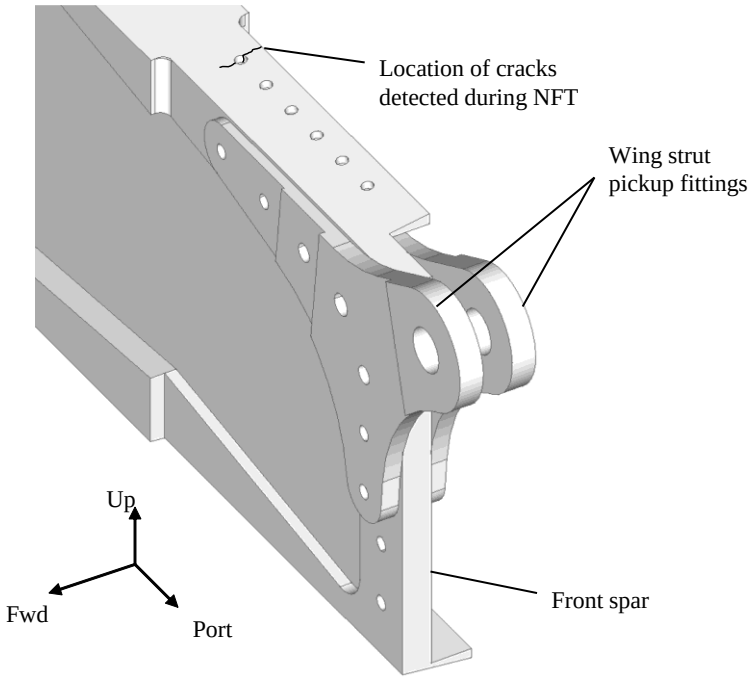

Figure 67: Front Spar

8.4 FATIGUE-RELATED RESEARCH PROGRAMS

8.4.1 A Feasibility Study into the Active Smart Patch Concept for Composite Bonded Repairs (C.Rosalie and N.Rajic, DSTO)

Composite bonded repair technology offers an effective and cost efficient means of restoring strength to damaged metallic aircraft components, with successful repairs applied to a variety of aircraft including Mirage III, C-141 and F-111. One of the most ambitious applications of the technology was to the repair of cracking at Forward Auxiliary Spar Station (FASS) 281.28 in the lower wing skin of the RAAF F-111C aircraft. Involving primary structure and a critical flaw, a stringent substantiation testing program was mandated in order to certify the airworthiness of the repair. While showing that residual wing strength was restored beyond the design limit load (DLL), the substantiation program revealed that certification was both cumbersome and expensive, and thus an impediment to the broader application of the technology.

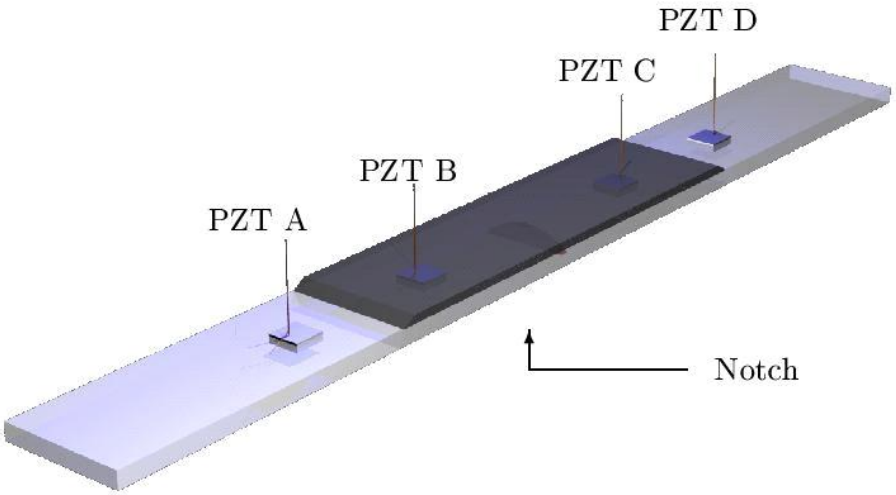

Figure 68: Schematic of ASP-reinforced metallic coupon showing notch location relative to piezoelectric elements

As a potential means of reducing stringent certification requirements a novel form of composite bonded repair was conceived called the Active Smart Patch. The patch combines the fundamental role of a conventional repair with a self diagnostic capability based on a network of embedded piezoelectric elements. With this capability the patch can, in principle, acquire data germane to an assessment of structural condition, both of itself and the structural adherend. Ability to assess the performance of the patch at will obviates the need for an onerous testing program and, once the patch is applied, eliminates the need for routine nondestructive inspection.

Testing of a prototype patch applied to an aluminium coupon with a synthetic crack confirmed that useful indicators of crack growth can be obtained from a network of piezoelectric sensors embedded in the patch. Work is now under way to assess the methodology on coupons more representative of the F-111 Lower Wing Skin structure at FASS 281.28.

8.4.2 A Numerical Model for the Piezoelectric Transduction of Stress Waves (N.Rajic, DSTO)

The contemporary approach to airframe structural management is based largely on routine nondestructive inspection and preventative maintenance, a prescriptive strategy that has underpinned an excellent air safety record, but at an enormously high on-going operational cost. It is generally the case that by the time an aircraft is retired from service, cumulative support costs have far exceeded that of capital acquisition. This has driven an ongoing reassessment of structural management practice, which has led recently to the emergence of in situ structural health monitoring (ISHM) as a prospective new basis for the management of airframes and other high value engineering assets.

One of the most intensely studied forms of in situ structural health monitoring involves the use of piezoceramic disc elements to induce and transduce elastic stress-waves. DSTO has been developing a numerical modelling facility for

axisymmetric acousto-ultrasonic problems where a transversely-isotropic piezoelectric disc element is attached to or embedded in a structural host. The model accounts for both elasto-electromagnetic coupling and viscoelastic material behaviour. Experimental examples are shown to demonstrate good correlation between observed and predicted behaviour. Comparisons show that the predictive accuracy of the model depends profoundly on the quality of the material property data furnished. Where biased inputs are suspected, a remedy is proposed comprising stochastic optimisation guided by observations of the system response.

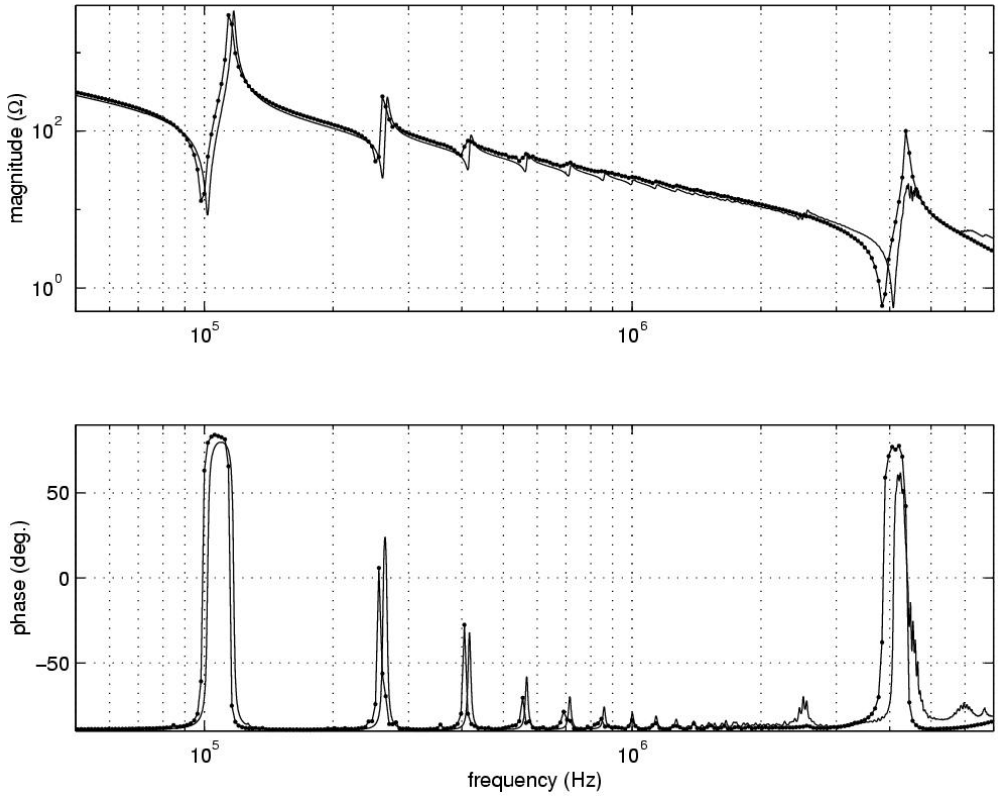

Figure 69: Comparison between measured (solid line) and computed (with symbol) impedance spectra for a Pz27 disc element

8.4.3 Initiation and Growth of Fatigue Cracks from Pits in Pre-corroded Al 7010-T7651 (B.R.Crawford, C.Loader, DSTO)

DSTO, with the Commonwealth Scientific and Industrial Research Organisation CSIRO and BAE SYSTEMS, has been studying initiation and growth of fatigue cracks in corroded 7010-T7651. Fatigue crack growth (FCG) rate tests utilised both centre-cracked tension (CCT) and dogbone coupons. The dogbone coupons contained pitting corrosion, and were fatigued using a marker band (MB) spectrum; after testing, these coupons were examined fractographically. Marker band spacings were measured and used to calculate crack growth rate data. These data differed from 7010-T7651 data collected from the centre-cracked tension coupons and from data available in the literature.

Marker Band Appearance

Marker band data were collected using the optical and scanning electron microscopes. Typically, it was easier to find marker bands optically than in a scanning electron microscope. This is illustrated by examination of Figure 70. Figure 70(a) is an optical deep focus micrograph showing the common appearance of the marker bands produced by a 4, 6 marker band spectrum. Figure 70(b) is a Scanning Electron microscope (SEM) image of marker bands produced by the same spectrum. This latter image was taken at approximately twice the magnification of the previous image. However, the marker bands are not nearly as distinct as in the optical image.

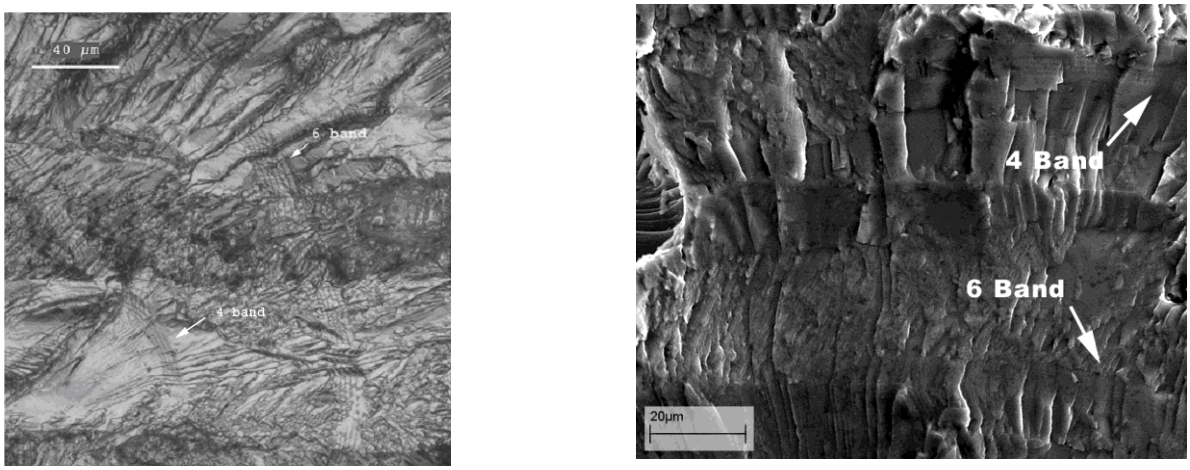

(a) (b)

Figure 70: (a) Deep focus optical micrograph of coupon EMU2-7 showing marker bands. Crack growth is from left to right. The bands were separated by 1000 full load cycles. (b) Scanning electron micrograph of marker bands observed on coupon EMU2-8. Crack growth is from bottom to top

Initiation and Growth of Fatigue Cracks

The initiation and growth of fatigue cracks was mapped in detail on an EDM notched coupon and a corroded coupon. Figure 71shows the results of this mapping. Note the multiple initiation points in each case.

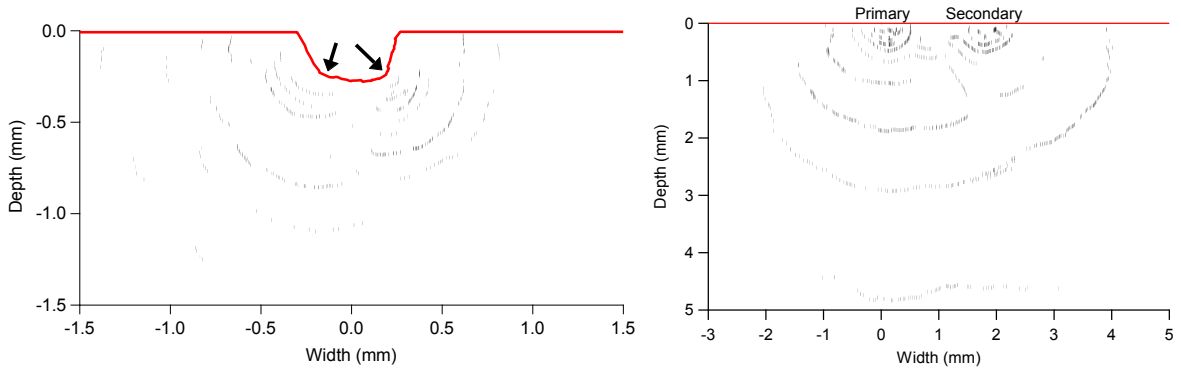

Figure 71: (Left) EDM notched coupon and (Right) corroded coupon. The heavy red line indicates the coupon edge and the profile of the EDM notch. The arrows indicate the crack initiation points

Fatigue Crack Growth Rates from Marker Band Analysis

Figure 72 (left) shows the FCG data collected from marker band observations on dogbone coupons. Most of these data were collected at R = 0.1. These R = 0.1 data range from 2 to 40 MPa√m and exhibit significant scatter at lower ΔK values. This is typical of fatigue crack growth data at low ΔK values and may be indicative of small crack behaviour. The large degree of scatter makes it difficult to distinguish any effect of R on fatigue crack growth.

Fatigue Crack Growth Rates from CCT Specimens

The FCG data obtained from the CCT coupons at R = 0.1 are shown in Figure 72(right) and compared with the R = 0.1 marker band data and data from the literature. The ΔK range of the CCT data is rather limited and starts at a relatively high value of 10 MPa√m. Comparison of the marker band and CCT datasets in the range where they overlap (10-40 MPa√m) shows a significant discrepancy between the two. The crack growth rates are lower for the marker band data than for the CCT data. At a ΔK value of 10 MPa√m, the CCT crack growth rate is 1.7×10^{-7} m/cycle versus a marker band crack growth rate of 6.7×10^{-8} m/cycle. This factor of approximately 2.5 was consistent across the entire overlap in ΔK. However, both sets of data have approximately the same Paris Law exponent.

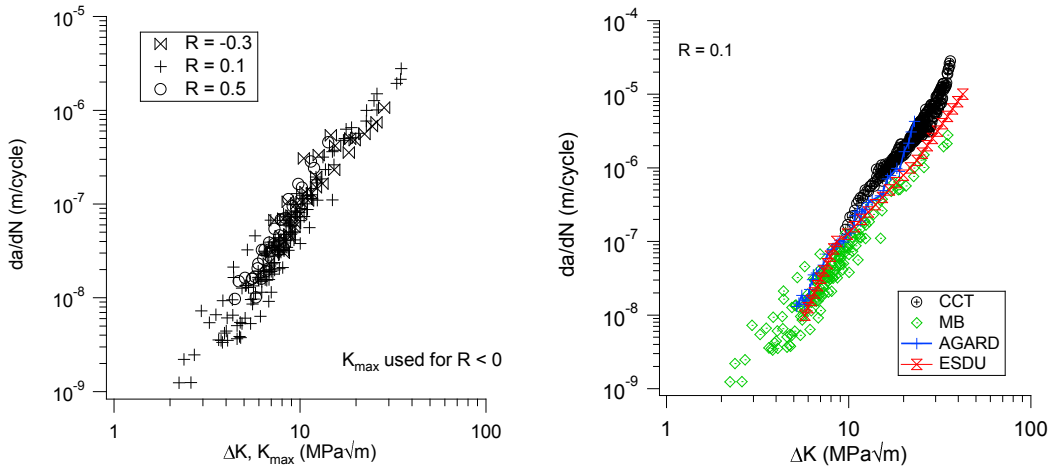

Figure 72: (Left) Marker band FCG data at R=-0.3, 0.1 and 0.5. (Right) Comparison of marker band data with data from CCT specimens and data from the literature

Discussion

The difference in the fatigue crack growth data collected from different coupon geometries is of concern. This difference is unsurprising, however, given the differences in how the two data sets were collected. These include, in addition to the difference in coupon geometry, differences in crack length measurement method and crack growth direction. Note, however, that both datasets are similar to AGARD and ESDU fatigue crack growth data for 7010-T7451. This degree of correlation is unexpected given that ASTM E647-99 states: 'There is no accepted "standard" value for da/dN versus ΔK for any material.' Despite several decades of research there is no guarantee that FCG data collected at one laboratory can be reproduced at another.

The following conclusions can be drawn from this work:

- Marker bands are far easier to detect optically than using a scanning electron microscope.
- FCG rates measured from CCT coupons were faster than FCG rates on the Marker Band coupons by a factor of approximately 2.5 over ΔK values ranging from 10 to 40 MPa√m.

8.4.4 Certification of Retrogressed and Reaged 7075-T6 for use on Australian Defence Force Aircraft (A.Grosvenor, C.H.J.Davies [Monash University], C.Loader, A.Shekhter, P.K.Sharp and B.R.Crawford [DSTO])

DSTO and Monash University have been investigating some of the considerations involved in developing a certification basis for 7075-T6 in Retrogressed and Reaged (RRA) condition. Al alloy 7075-T6 is used extensively in RAAF aircraft such as the C130 Hercules and the P3 Orion. If successful, the RRA treatment of 7075-T6 could significantly reduce maintenance by providing a reduced incidence of corrosion in these aircraft. However, the indiscriminate use of RRA is not without risk as beneficial effects such as the increase in fatigue endurance due to residual stresses can be reduced or eliminated by the RRA treatment process. The aim of the work was to investigate the effect of production route on specimens containing beneficial residual stresses in a laboratory environment to see if the fatigue endurance can be recovered by application of the cold working after RRA treatment.

The 7075 alloy used here was supplied in T6511 temper in the form of two extruded bars with rectangular cross-sections of 19 mm x 101 mm and 12.5 mm x 101 mm. RRA treatments were performed at 195 ±1ºC for retrogression times between 10 and 130 minutes in an air-circulating furnace, followed by a water quenching and storage at less than 4ºC before re-aging at 120±1ºC for 24 hours and air cooling. Table 1 summarizes the experimental matrix for the work reported here. Table 2 lists the codes for each fatigue life test condition reported here.

Table 1: Experimental Matrix

Series	# of specimens	Details
Tensile	61	RRA treatment with retrogression times ranging from 10 to 130 minutes
High-Kt fatigue life	46	See Table 2
Fracture Toughness	26	L-T and T-L orientations

Table 2: Codes defining the test condition of fatigue specimens

Code	Test Condition
AM	As Machined
AM/RRA	As Machined then RRA
AM/CW	As Machined then Cold Worked
AM/CW/RRA	As Machined then Cold Worked then RRA
AM/RRA/CW	As Machined then RRA then Cold Worked

The fatigue life results (Figure 73) indicate that RRA greatly reduced fatigue life. In all instances the fatigue life of specimens when RRA is the final treatment were far shorter than those in the as-machined condition. This decrease in fatigue life indicates a reduction and possible redistribution of residual stresses during RRA. The fact that all RRA specimens have a similar life, less than that of the As-Machined specimens, at the same stress irrespective of pre-processing suggests that RRA relieves both internal and surface stresses. Residual stress measurements showed a decrease in the cold worked compressive stress after RRA, while As-Machined specimens (AM) exhibited small compressive stresses created during machining. A change in failure mode from a single crack initiation site (Figure 74(a)) to multiple crack initiation sites (Figure 74(b)) supports this. Crack initiation at stress concentrators from machining marks is not retarded by residual stresses and competes with corner initiated cracks.

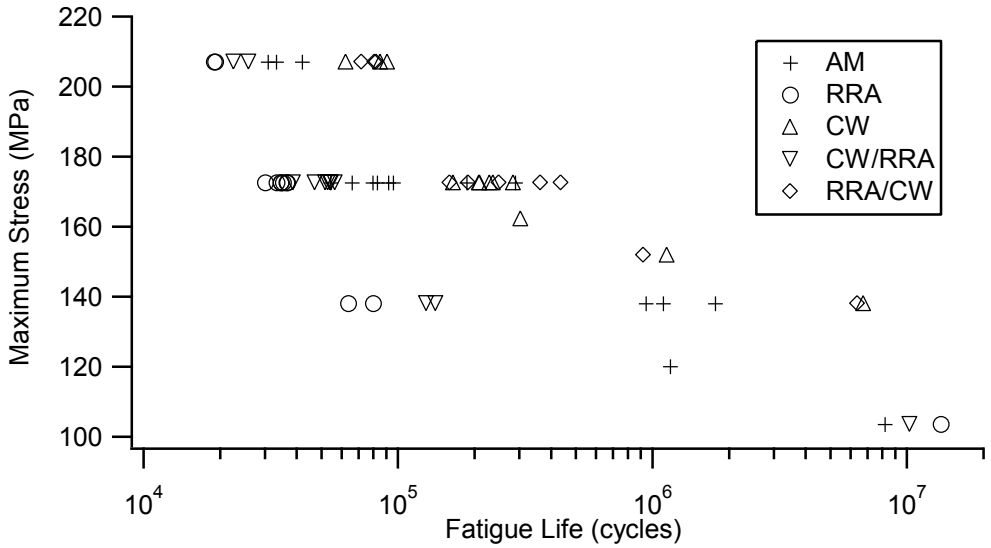

Figure 73: Constant amplitude fatigue life results for all series

Cold working of the holes following RRA treatment (AM/RRA/CW) returns the fatigue life to that of the non-RRA treated cold-worked condition. This provides confidence that the fatigue crack growth and fracture toughness of the RRA treated material is the same as the T6 condition. The initiation loci of the primary crack also return to the corner when cold working is applied after RRA (Figure 74(c)). This suggests that any component in which residual stresses from processing influence the failure of the component must have the stresses reinstated following RRA treatment in order to restore the fatigue life of the component to its pre-RRA level. The use of hardness tests as a quality control mechanism in RRA treatments must be considered carefully as the indentations produced prior to RRA treatment will have their compressive stresses relieved and may produce initiation sites for fatigue crack growth.

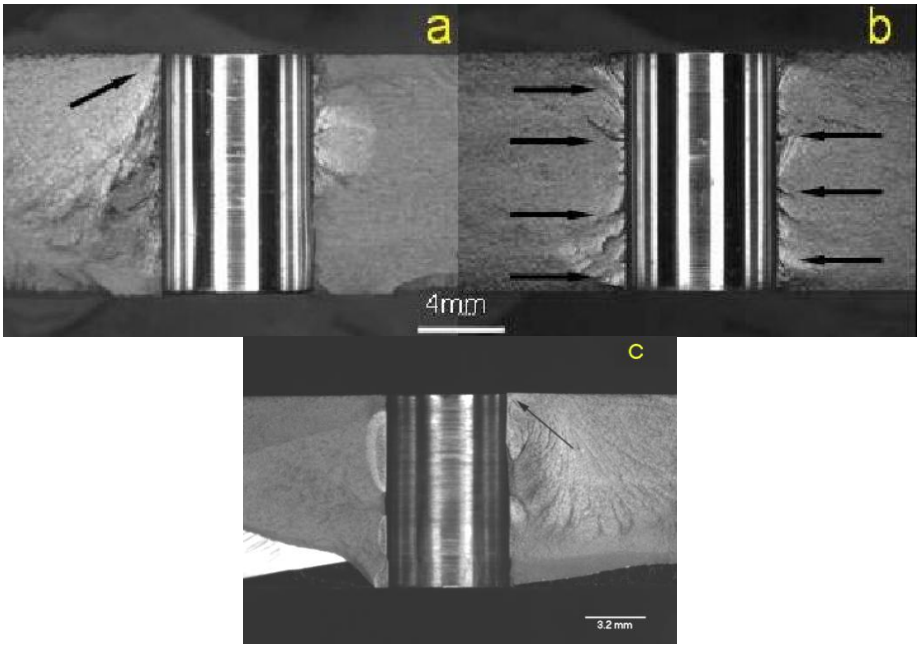

Figure 74: Fatigue fracture surface showing (a) single crack initiation site, indicated by the arrow and (b) multiple crack initiation sites indicated by the arrows after undergoing a RRA treatment, (c) return to corner initiation of the primary crack with application of cold working post RRA treatment

Table 3 presents experimental K_{Ic} results measured at room temperature for 7075-T6 RRA heat-treated material. All tests were valid according to ASTM E399-05. A change in fracture toughness may have little effect on the fatigue life of specimens in this specimen configuration, but can have a drastic effect on the inspectability of in-service components. Fracture toughness was therefore investigated in both the T-L and L-T orientation and compared to the values given for 7075-T6 extrusions in the ASM Handbook, as this property is not covered by MIL-HDBK-5J. The L-T orientation values appear to be higher than that for T-L for both the original and RRA treated materials. It should be noted that the handbook values given are not specific to a particular product form and some variation may occur in extrusions as thickness variations for different extrusion products result in different levels of anisotropy. The statistical summaries of fracture toughness presented in Table 3 show that the minimum value for the T-L fracture toughness for the RRA material is slightly lower than that given by American Society for Metals (ASM). This may indicate that some comparative tests may be necessary to establish and quantify any reduction.

Table 3: Plane Strain Fracture Toughness (K_{1C}) comparison of results with ASM Handbook values. Values in MPa√m.

Orientation	**ASM Published AA 7075-T6**		**RRA-ed 7075-T6**			
	Mean	**Minimum**	**Mean**	**Standard Deviation**	**Sample Size**	**Minimum**
L-T	28	26	28.2	0.61	13	27
T-L	22	20	20	0.34	13	19

The following conclusions can be drawn from this work:

- RRA causes a reduction in the beneficial residual stresses induced by cold working, and to a lesser extent, sample machining.
- RRA increases the number of crack initiation sites around a fastener hole.
- Performing cold working after RRA restores the fatigue endurance and failure loci to the same level as non RRA treated material.
- RRA has little effect on the fracture toughness, but possible reductions in T-L orientation must be investigated to determine its significance.

8.4.5 Risk and Reliability Assessment Methods (R.Melchers, University of Newcastle)

Reflecting increased interest in Australia in linking corrosion management and risk-based approaches to fleet management, University of Newcastle and DSTO have been collaborating on modelling corrosion loss – in the first instance for naval vessels (although the principles may be applicable in some aircraft scenarios). The corrosion modelling is an input to structural reliability modelling for surface vessels. The work is in part experimental, using exposure testing at a tropical site in Queensland.

8.4.6 Fractographic Studies in AA 7050-T7451 (P.White, DSTO)

Studies are continuing of the fracture surface of fatigue cracks in AA7050-T7451 alloy, for a load sequence consisting of a periodic underload (R = -1) in between groups of high stress ratio (R = 0.5) loading cycles. These have revealed a complex fracture surface features that include ridges, depressions and fissures. It has been found that several factors influence these features - the number, magnitude and distance between the underloads. This effect is attributed to elastic compliance produced by a slip band associated with the underload, reducing the tendency for slip in the same direction to occur while the crack tip remains nearby. These slip bands change the path of the crack and result in the production of a ridge. A model of striation formation that explains the formation of the ridges, based on the influence of two or more active slip systems is being developed.

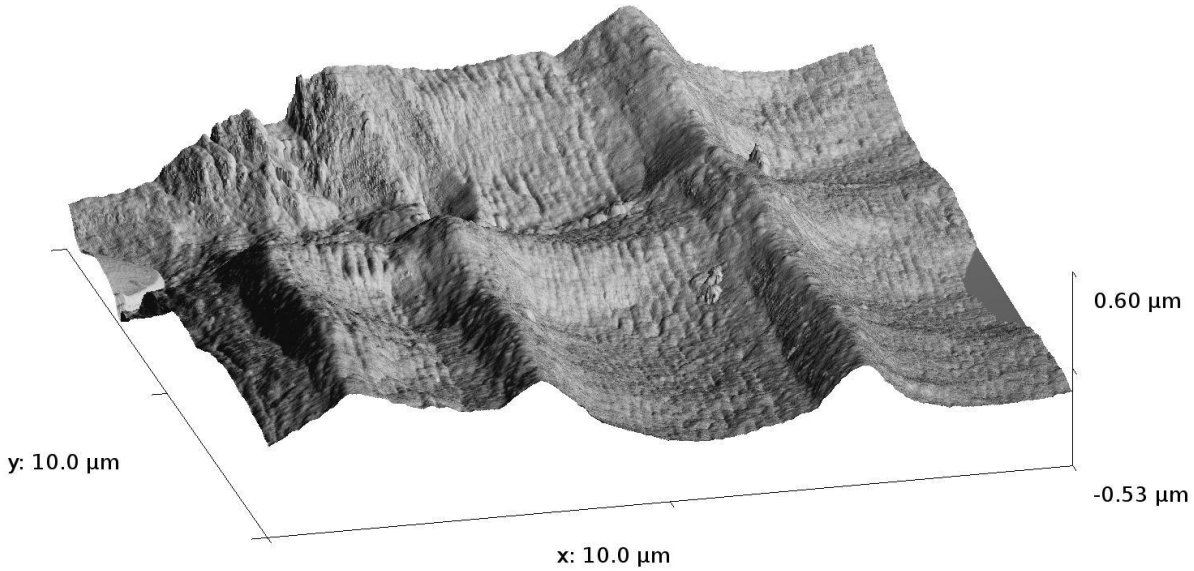

Figure 75: An Atomic Force Microscope (AFM) image of the fracture surface with the crack growing from left to right. Ridges are formed at the position of underloads and consist of a single striation on the face away from the crack and multiple small striations on the face toward the crack

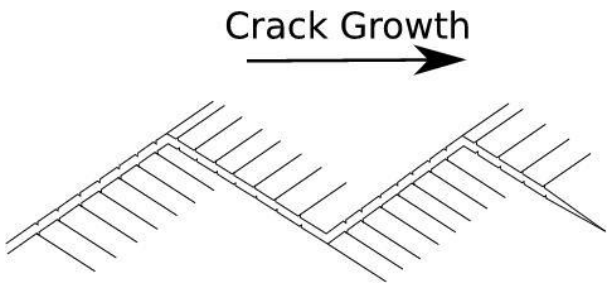

Figure 76: Diagram of the network of fissures formed at the position of the underload. Fissures always point in the direction of the crack growth

8.4.7 Model-Assisted Probability of Detection (MAPOD) Assessment of Nondestructive Inspection Procedures (C.Harding and G.Hugo DSTO)

Maintenance of structural integrity using safety-by-inspection (SBI) requires appropriate intervals to be defined for the nondestructive inspections (NDI). These intervals are normally set using crack growth data (from empirical tests or models) to determine the expected period of usage for a crack to grow from the minimum size at which a crack will be reliably detected by NDI (a_{NDI}) to the size at which the crack poses a risk of structural failure (a_{crit}). The inspection period is then normally derived as a fraction (typically one-half, or one-third) of the expected period of crack growth from a_{NDI} to a_{crit}.

Determination of an appropriate value for a_{NDI} for real inspection procedures is then crucial to enable aircraft structural integrity management by SBI. Airworthiness codes such as JSSG-2006 (USA DoD Joint Service Specification Guide Aircraft Structures) specify that a_{NDI} should be the crack size for which a 90% probability of detection (POD) has been demonstrated with 95% statistical confidence. However, empirical demonstrations of POD are very expensive and the reality is that, to date, very few NDI procedures used for SBI have had the required POD demonstration to determine a_{NDI}. In addition, most empirical POD trials are conducted on simulated defects, such as electric-discharge machined (EDM) notches, rather than real fatigue cracks, and therefore there is a need to understand how POD determined on artificial defects can be translated to detection of typical fatigue cracks.

DSTO is currently developing model-assisted methods to assess the POD for fatigue cracks in aircraft structures. A key part of this research is careful characterisation of the differences in NDI response between EDM notches and real fatigue cracks. These differences are particularly significant for ultrasonic NDI methods, which are the primary focus of the current DSTO research. DSTO have prepared a series of coupon specimens containing fatigue cracks at fastener holes grown using representative flight-by-flight spectrum loading. The ultrasonic sensitivity for these fatigue cracks is being compared to EDM notch defects. The work includes examination of the effects of crack closure due to compressive residual stresses from notch plasticity occurring at the fastener holes during peak loads in the loading spectrum. The results show that the POD for ultrasonic detection of small fatigue cracks (less than 1 mm in depth) is much less than that measured for similar-sized EDM-notch defects. These results confirm previous anecdotal accounts of poor reliability for ultrasonic detection of very small fatigue cracks, when compared to prior demonstrations on EDM notches.

The initial application of the MAPOD methods by DSTO will be for automated ultrasonic inspections to detect fatigue cracks at fastener holes in the lower wing skin of F-111 aircraft. The objective will be to combine through modelling (i) results from an empirical POD trial on EDM notch defects inserted in retired wings, and (ii) data obtained on fatigue cracks grown in laboratory specimens under representative flight-by-flight spectrum loading, to determine the overall POD for detection of fatigue cracks in actual F-111 wing structure.

8.4.8 Local Shape Optimisation for Airframe Life Extension – Example (R.Evans, R.Braemar, W.Waldman, R.Kaye and M.Heller)

Overview: In this investigation, [1], important lessons learned from practical applications of optimal rework shapes for the life extension of F-111 wing pivot fitting (WPF) were reviewed. New enhancements for fully automated 2D and 3D local shape optimization method have also been developed; in one, we minimize the magnitude of the multiple, constant-stress segments around the hole boundary, which typically consist of tensile and compressive stress states. We now include robustness constraints, so that the peak stresses are independent of perturbations in the direction of the dominant loading (within a prescribed range), and/or are optimal for distinct load cases. Thirdly, numerical examples are given to demonstrate the usefulness of the approach, and to quantify the effect of the trade-off between peak stress minimization, hole size constraints, manufacturing constraints, robustness constraints, non-destructive inspection limits, and certification basis. A number of 2D and 3D numerical examples were investigated, with a focus on geometrically constrained holes, which are typical of airframe structures. A simple example is detailed below.

2D example *– Stress and fatigue results for a hole close to an edge in a uniaxially loaded 2D plate*
Figure 77 (left) shows a large rectangular plate subjected to uniaxial loading, *S*, containing a hole near one edge. A key aspect is that the hole cannot grow beyond the bounding constraint line $x = -w/2$. The plate geometry is $W/H = 0.6$, the initial hole width is $w/W = 1/6$, and the hole center is located at $e = w$. Peak K_t and fatigue results for optimized holes

are given for a range of h/w and ρ_{min}, and are compared to an initial circular hole. As a useful limiting case, standard optimization is done to investigate this effect. Figure 77 (centre) shows a typical comparison of the shape of a nominal 2:1 elliptical hole (A) with that of the optimal hole (B), and Figure 77(right) shows the corresponding variation of K_t around the hole boundary, as a function of arc length, μ.

The initial hole has four major stress peaks, which from left to right are K_t = 3.09, -1.51, 2.33 and -1.51. However, the optimal shape reduces these peaks to flat-topped regions that are uniform to within a tolerance of 0.1%, representing reductions in peak K_t for the corresponding ellipse of 24%, 29%, 11% and 29%, respectively.

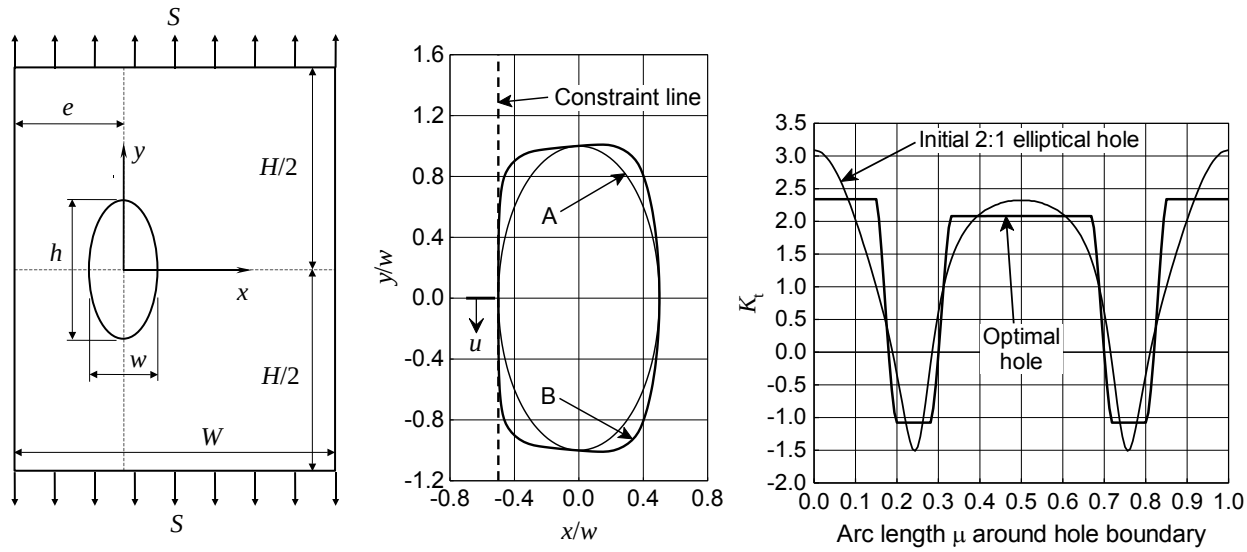

Figure 77: Optimization of a constrained hole near an edge in a uniaxially loaded plate: (left) geometry, (centre) typical comparison of initial elliptical hole (A) with optimal hole (B) for 2:1 aspect ratio case, and (right) variation of K_t *around boundary for initial and optimal hole*

The peak K_t results are summarized in Figure 78a. As h/w is increased, large stress reductions are demonstrated compared to the initial circular hole, and also to the corresponding ellipses. It is also evident that, as h/w is increased, the effect of different ρ_{min} constraints diminishes; however, as expected the peak K_t is always higher for higher value of ρ_{min}. Figure 78b gives stress decay plots along the x-axis, for a typical case of ρ_{min}/w = 0.3. While stresses for optimal holes are reduced at the hole edge, as the distance away from hole edge is increased the stresses for optimal shapes are greater than for the initial circular hole. Fatigue estimates are given for prospective cracking on the left-hand side of the hole, based on a load spectrum typical of a lower wing skin stiffener of a transport aircraft.

The estimates for relative lives as compared to the initial circular hole are summarized in Table 1, where the K_t values are given in parentheses. Even for the large constraint case, ρ_{min}/w = 0.3, (which is desirable for ease of in-situ manufacture), there are very large increases in life, where the benefit increases with increasing aspect ratio. Here a 2:1 aspect ratio is sufficient to provide a six-fold increase in life.

For calculation of the relative inspection intervals, the assumed crack configuration is that of a semi-circular edge crack, starting from the hole edge in a 3D plate. The predicted inspection interval results are summarized in Table 2 for a typical large-hole case with w = 100 mm, where they are normalized with respect to the circular hole case with a_{ndi} = 1 mm. It can be seen that the relative inspection interval increases with increasing h/w, for a given a_{ndi}. As expected for a given h/w, the inspection interval decreases with increasing a_{ndi}. Useful trend plots are given in Figure 79 a and b, which summarizes the required h/w to achieve a doubling of inspection interval as a function of a_{ndi}. Here results for both a small hole (w = 25 mm) and a large hole (w = 100 mm) are given. As expected, a greater h/w is needed for the small hole to achieve a doubling of inspection interval at the same value of a_{ndi}.

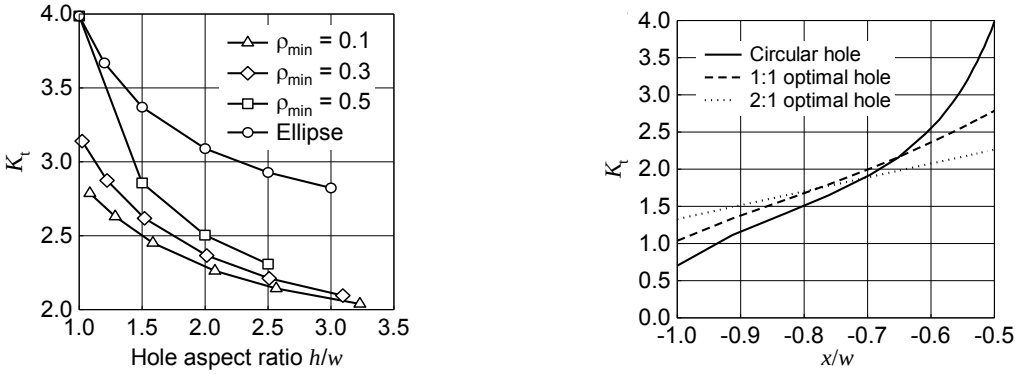

Figure 78: Stresses for optimized constrained hole near edge in uniaxially loaded 2D plate: (a) effect of h/w *and* ρ_{min}*, (b) sample stress decay plots for* ρ_{min}/w *= 0.3, along* x*-axis on left-hand side of the hole*

Table 1: Comparison of relative safe lives, t_{t2}/t_{t1}, and (K_t) for optimized hole near edge

Minimum radius of curvature constraint	Circular hole relative life	Optimal, $h/w \approx 1$ relative life	Optimal, $h/w \approx 1.5$ relative life	Optimal, $h/w \approx 2.0$ relative life	Optimal, $h/w \approx 2.5$ relative life
$\rho_{min}/w = 0.1$	1.00 (3.99)	3.15 (2.79)	4.76 (2.45)	6.16 (2.26)	7.33 (2.14)
$\rho_{min}/w = 0.3$	1.00 (3.99)	2.16 (3.14)	3.85 (2.62)	5.30 (2.37)	6.62 (2.21)

Table 2: Relative inspection intervals, t_{r2}/t_{r1} for optimized hole near edge, compared to circular hole with a_{ndi} = 1 mm; $\rho_{min}/w = 0.3$

Inspection crack threshold, a_{ndi} (mm)	Circular hole relative interval	Optimal, $h/w \approx 1$ relative interval	Optimal, $h/w \approx 1.5$ relative interval	Optimal, $h/w \approx 2.0$ relative interval	Optimal, $h/w \approx 2.5$ relative interval
1	1.00	1.85	2.94	4.32	4.94
2	0.63	1.13	1.86	2.71	3.08
3	0.49	0.82	1.33	2.12	2.23
4	0.42	0.64	1.01	1.71	1.71

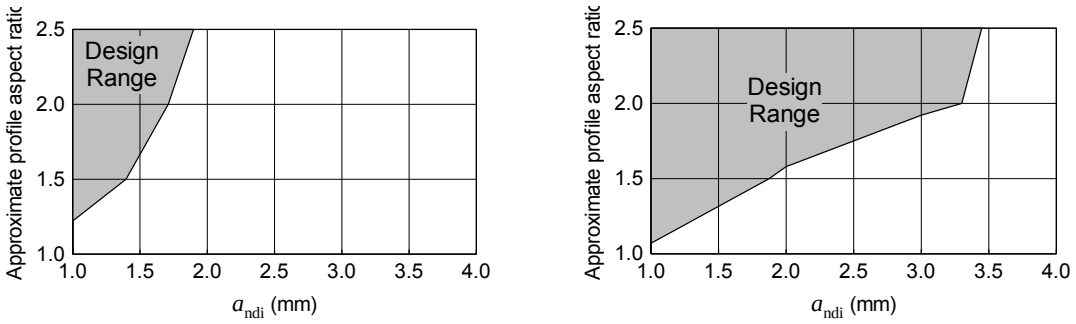

Figure 79: Design range to double inspection interval for optimized hole close to edge in 2D plate: (a) small hole with w *= 25 mm, and (b) large hole with* w *=100 mm*

Reference

1. Heller M, Braemar R, Waldman W, Evans, R, McDonald M, Kaye R.. Local shape optimization for airframe life extension. *Proceedings 6th World Congress of Structural and Multidisciplinary Optimization* 30 May – 03 June 2005, Rio de Janeiro, Brazil.

8.4.9 Verification of Numerical Designs of Optimal Rework Shapes for F/A-18 Y598 Fin Attachment Stub (S.Norburn, R.Wescott, and M.Heller, DSTO)

The purpose of this work, [1], was to undertake further large scale 3D finite element analysis and validation relating to a significantly improved repair design for the F/A-18 Y598 fin attachment stub. The new design could remove existing corner cracks and prevent new cracking by reducing peak stresses in the critical region. Also, the new repair could be used across the F/A-18 fleet to reduce local stress and thereby extend the Y598 stub's fatigue life. There have been a number of previous investigations into various rework profiles that would remove the cracks found in the starboard Y598 stub of FT46. Initial work was for rework profiles of constant radius and showed significant non-uniformity of the stress at the critical region, (ie. significant stress peaks).

Consequently, more recent work in [2] considered optimising the local shape to reduce the non-uniformity of the stress and consequently reduce the peak value at the critical region. The technique implemented in [2], was based upon using 2D optimal profiles published in [1], as a basis for generating 3D profiles without resorting to complex 3D optimisation. This approach (referred to as 'near optimal' shape optimisation) has been shown to be convenient and robust. The work in [2] concluded that a near optimal rework (with a chamfer), could remove existing cracks and reduce the stress there by 25% relative to the FT46 rework. All the approaches mentioned above were based on a simplified model of the stub, which ignored the fin attachment holes and the supporting frame.

Consequently, the following work was undertaken, [1],

(i) address potential shortcomings in the previous modelling methodologies by using a larger scale model that incorporates the stiffness of the supporting frame and includes the fin attachment holes,
(ii) check the validity of the previous results [2],
(iii) investigate the sensitivity of the results to perturbations in loading, to help understand the robustness of the rework profiles, and
(iv) consider a second near optimal rework profile (of reduced length) and determine its suitability.

Figure 80(a) and Figure 80(b) show the new finite element model including the critical region respectively. Here, several rework profiles have been considered, including two near optimal variants (one full length and one reduced length). The geometry of the reduced length optimal is shown in Figure 80(c). Both near optimal reworks were shown to significantly reduce the stress at the critical region of the stub relative to both the baseline and FT46 rework shapes, even though it prospective cracked material is removed to a depth of 0.275 inches. Figure 81 shows that the peak stress at the critical region of the chamfered reduced length near optimal shape was approximately 22% lower than the peak stress in the FT46 rework. Furthermore, the study showed that both near optimal reworks are robust with respect to perturbations in the magnitude of applied loads. Due to the proximity of fin attachment holes, the reduced length near optimal rework is recommended for future practical application. DSTO is currently investigating simplified in-situ machining techniques to support the potential application of such rework shapes for fleet aircraft.

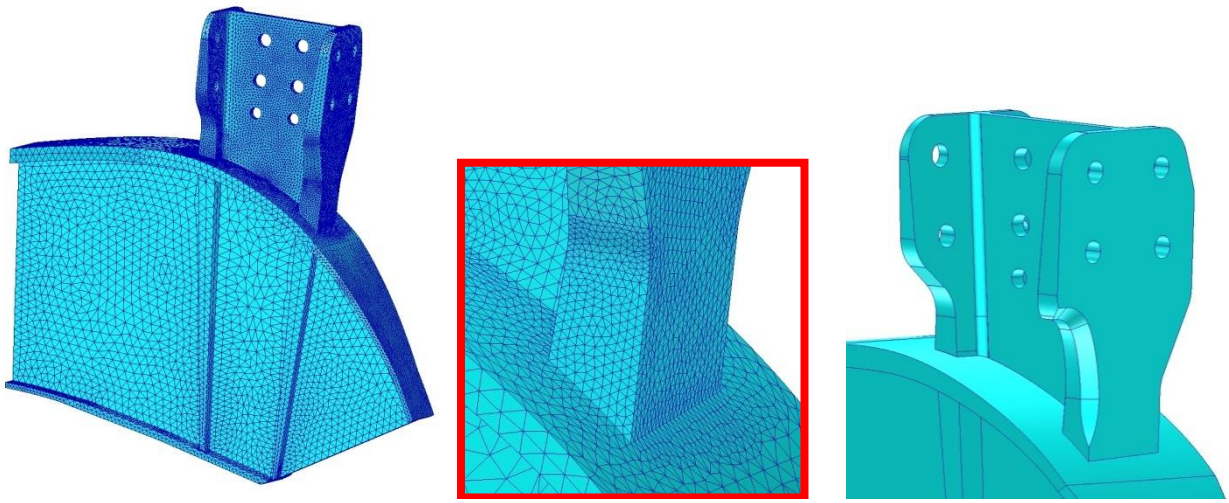

(a) (b) (c)

Figure 80: Typical finite element baseline model and optimised repair shape: (a) overall model, (b) detail at critical region, (iii) solid geometry of reduced length optimal

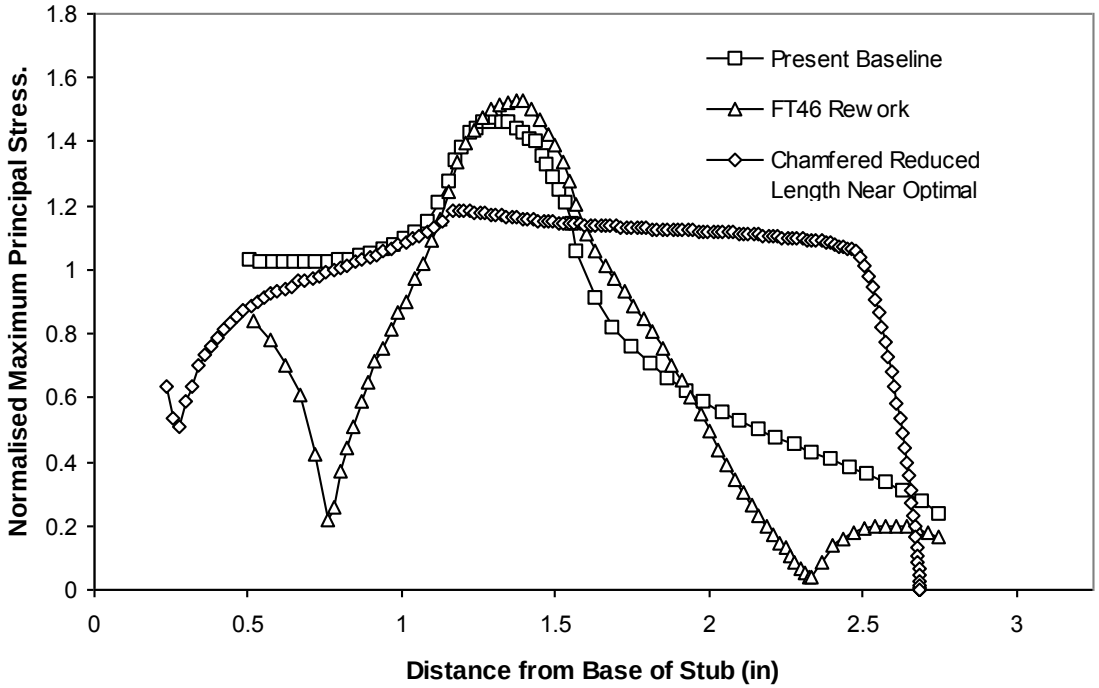

Figure 81: Comparison of predicted stress along edge of the present Baseline, FT46 rework and reduced length near optimal (with chamfer) from finite element analysis

References

1. Norburn S, Wescott R, Heller M, *Verification of numerical designs of optimal rework shapes for F/A-18 Y598 Fin attachment Stub*, Ref. No: B2/129, 10 July 2006.
2. Wescott R, Kaye R, Heller M., *Numerical design of Optimal Rework Shapes for F/A-18 Vertical Tail Stub*, DSTO Minute, Ref. No: B2/129, 22 July 2005.
3. Waldman W, Heller M, and Chen G.X. Optimal Free-Form Fillet Shapes for Shoulder Fillets in Flat Plates under Tension and Bending, International Journal of Fatigue, 23, pp. 509-523, 2001.

8.4.10 Optimal Shape Design for a JSF Demonstrator Geometry (R.Kaye and M.Heller, DSTO)

This research, [1], is the second phase in a series of three, prepared in order to documen "Shape Optimization for Structural Design", (JSTAB-SOSD), an initial one year research program commissioned by the Joint Strike Fighter Science and Technology Advisory Board. The objective is to demonstrate the possible use of DSTO shape optimization technology for specific geometries representing JSF components. Here we consider optimised web penetrations in the JSF496 bulkhead. Two examples are shown where non-circular optimized penetrations are considered in place of circular ones. The optimised shapes used are generic and robust and are aligned with the principal load directions in bulkhead panels. They are unique to a particular biaxial load ratio, and can be used at other airframe locations with the same biaxial load ratio. A number of aspects have been assessed including; peak stress reduction, robustness, fatigue initiation and crack growth, weight saving and buckling strength. In particular there are advantages relating to stress reduction and fatigue performance, and the work has highlighted requirements for the effective use of such generic optimised shapes. To illustrate the concept,

Figure *82*a below shows the stresses around a circular cut-out in a generically loaded plate, while

Figure *82*b shows the significant stress reduction with a robust optimised hole shape. Both holes have the same area.

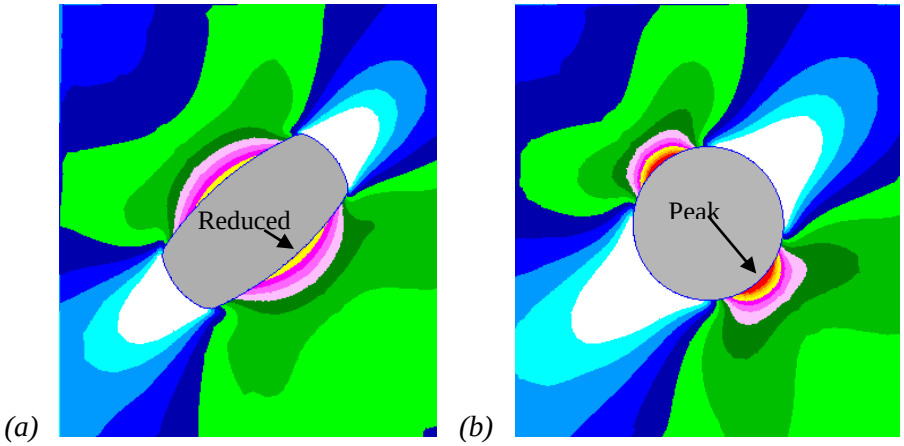

Figure 82: Comparison of stress contour plots for a generic airframe plate, subject to remote biaxial loading: (a) initial circular hole with localised stress peak (red region), and (b) robust optimal shape with 30% peak stress reduction

Reference

1. Kaye R, Heller M, Braemar R. *JSTAB – Shape Optimization for Structural Detail Design: Activity 2 Report: Optimal shape design for JSF demonstrator geometry*, DSTO–TR-1881, July 2006.

8.4.11 Through-Thickness Shape Optimisation of Typical Double Lap-Joints, including Effects of Differential Thermal Contraction during Curing (R. Kaye and M. Heller, DSTO)

Repairs and reinforcements using bonded patches have been shown over a long period of time and in many applications, to be effective and durable. However cracking can occur in the adhesive near stress concentrations when the repairs are applied in certain severe service loading environments. Sensitivity based numerical optimisation coupled with finite element analysis has previously been employed to provide free-form through-thickness shapes for the patch and the adhesive layer. These shapes reduce adhesive stress concentrations by evenly distributing the load transfer along the bond-line.

In this program, automated and iterative finite element based shape optimisation methods were used to determine optimal shapes which account for the effects of the different thermal expansion coefficients of boron/epoxy patches and the aluminium alloy parent structure, [1]. The adhesive stress was considered to have a static component due to thermal effects and a cyclic component due to service loading. The benefits of optimising for minimal cyclic component have been compared to benefits of optimising for minimal combined component. How to best configure the optimisation problem in view of the mixture of cyclic and static loading has been addressed.

The initial double lap joint arrangement is shown below in Figure 83. The shape of the adhesive layer and patch are optimised in the taper and joint/crack regions. The main optimisation constraint is that the crack opening should not increase due to the shape changes of the patch or adhesive, as compared to the nominal configuration.

Some typical results for one optimisation case are given in Figure 84. Overall this work has shown that for the taper region it is better to optimise using combined thermal and remote loading, as lower static and cyclic adhesive stresses result. In the crack region similar reductions in cyclic adhesive stresses are achieved whether or not both loadings are applied during the optimisation. When both loadings are included however, static adhesive stress can be traded off against static crack opening.

Reference

1. Kaye R, Heller M. Through-thickness shape optimisation of typical double lap-joints including effects of differential thermal contraction during curing. *Int. J Adhes Adhes*, 25, pp 227-238, 2005.

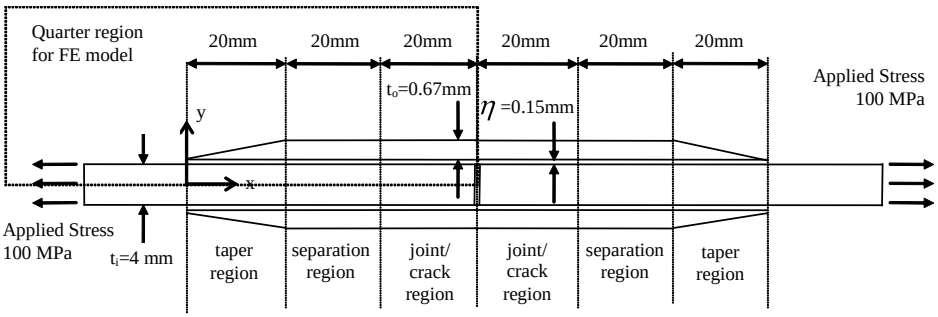

Figure 83: Dimensions and loading arrangement for nominal double lap-joint

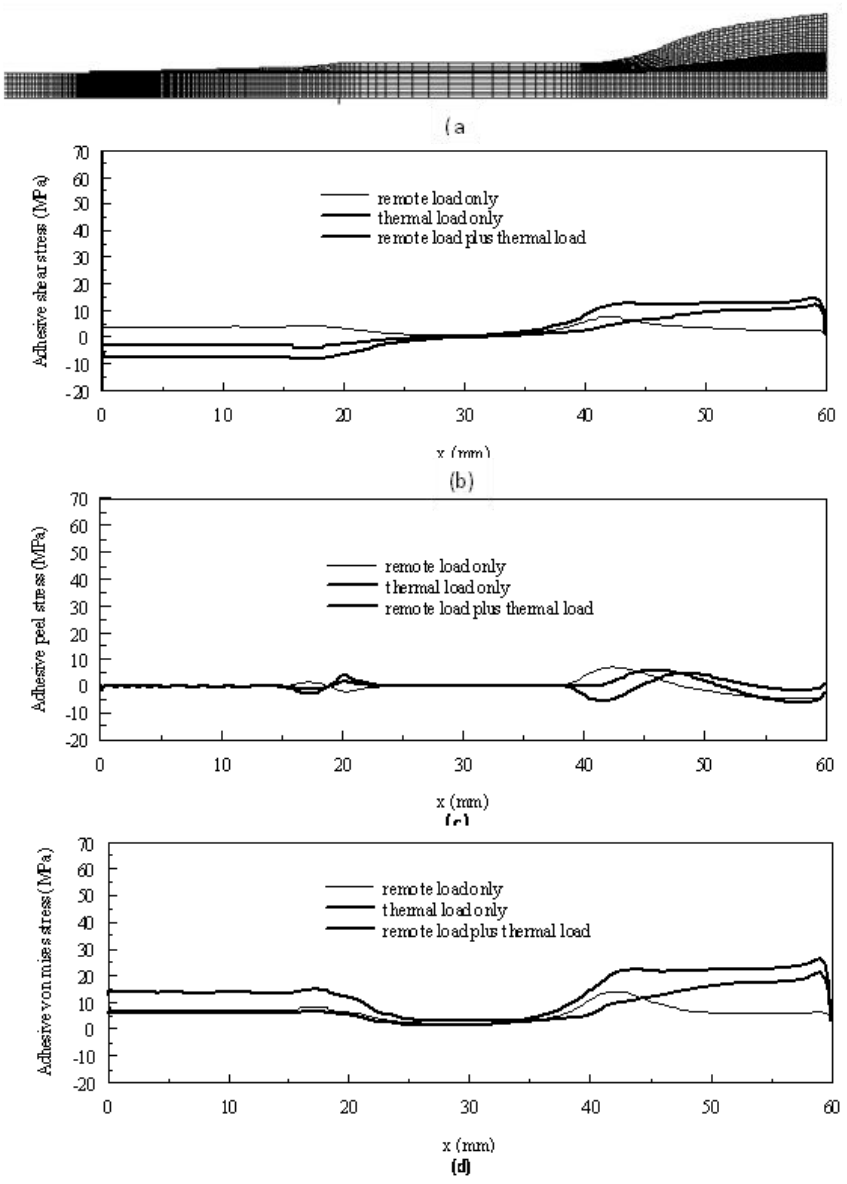

Figure 84: Adhesive stresses for double lap-joint optimised with thermal and remote load applied together but with larger crack opening restraint: (a) shape and mesh, (b) adhesive shear stress distribution, (c) adhesive peel stress distribution, and (d) adhesive von Mises stress distribution

8.4.12 Finite Element-based 3D Stress Analysis of Composite Bonded Repairs to Metallic Aircraft Structure (R.Kaye and M.Heller, DSTO)

The use of high modulus bonded patches has been shown to be a very useful life extension strategy when used to reinforce damaged or damage-prone aircraft structural components. When applied to aircraft skin panels such as fuselage and wing skins, the patch attracts load up through the thickness of the panel, as well as from the wider in-plane regions, creating a stress concentration on the surface of the panel at the ends of the patch. The main objective of this work is the numerical evaluation of this stress concentration for a single layer patch, a multilayer patch equivalent stiffness patch with uniform stepping, and a multilayer patch with non-uniform stepping based on shape optimisation principles [1].

Modelling of the residual thermal effects caused by heat curing of dissimilar materials has been included, as well as comparison of the through-thickness and in-plane 2D results with the 3D results. In this work higher order p-elements were used, to reduce the number of elements in the mesh. Figure 85 shows the distribution of the key stress quantities for the patch, adhesive and plate respectively. It was found that the plate stress concentration factor for a typical 3D boron/epoxy patch configuration (see Figure 85c) is 1.34. This can be reduced to 1.23 by the use of a long first patch step. Further 2D analysis indicates that the value can be reduced to 1.16 by also using a first patch layer of carbon/epoxy instead of boron/epoxy. As expected, the peak adhesive stresses are similarly reduced by these patch lay-up changes.

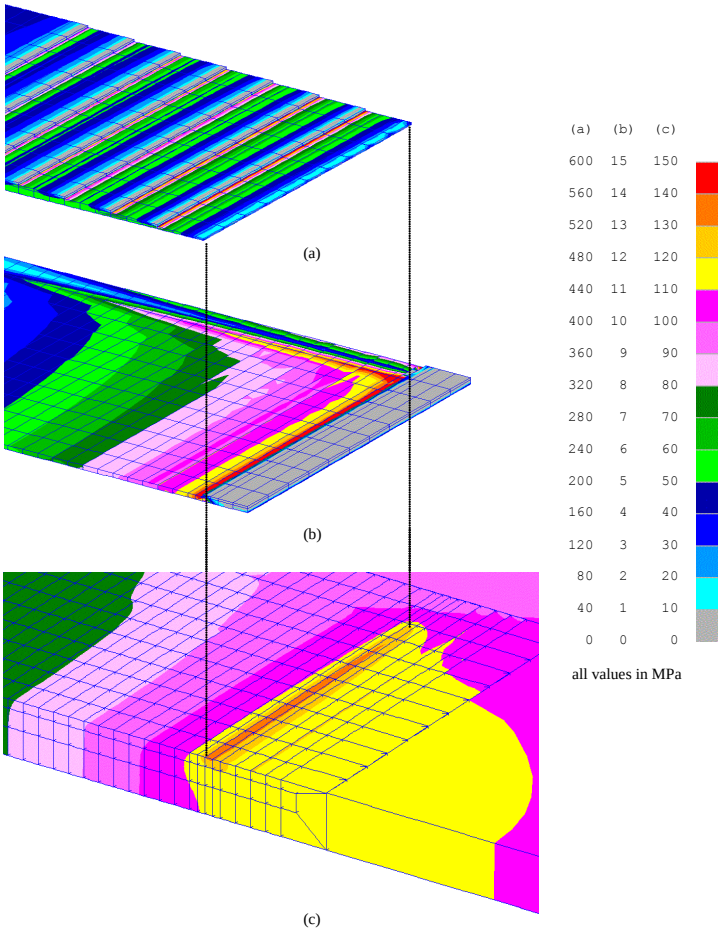

Figure 85: Stress distribution near end of doubler for 8 layers boron/epoxy patch with uniform stepping: (a) major principal stress in doubler, (b) shear stress in adhesive, and (c) major principal stress in plate

Reference

1. Kaye R, Heller M. Finite element-based three-dimensional stress analysis of composite bonded repairs to metallic aircraft structure. *Int. J Adhes Adhes*, 26, pp 261-273, 2006.

8.4.13 On the Selection of Test Factors for the Determination of Safe Life (G.Habermann, Boeing Australia Limited) - Paper to be presented at ICAF 2007 Symposium

"A persistent danger when engaging in engineering activity is the selection of methods of analysis that are inappropriate for resolving the problem at hand. With the passage of time, "tried and tested" methods tend to be taken for granted and the assumptions and limitations that underpin these techniques are frequently forgotten. Whilst it is prudent to periodically reinforce one's understanding of these techniques, it is particularly important to do so when pushing the boundaries of traditional wisdom. With the increased use of composite materials in aerospace structures, the traditional techniques that underpin the certification of structural durability qualify as an area that warrants special attention.

Historically, the lack of agreement by regulatory authorities on the choice of test factors used to certify the structural durability of metallic structures is one indicator of the need for greater understanding of this topic. The growing trend by airworthiness regulators of placing the onus for the selection and justification of test factors on the applicant seeking design certification further reinforces this need.

This paper revisits the theoretical and empirical origins of the test factors applied to the results of fatigue tests in the certification of structural durability. In particular, it identifies the basic limitations and assumptions that should be considered when applying these techniques. To further assist analysts in their selection and comprehension of test factors this paper outlines a simple statistical method for calculating test factors based upon user-specified parameters such as the standard deviation of the parent population, sample size, acceptable probability of failure and required confidence levels.

Whilst the physical testing of full-scale test articles provides much information on the sequence and location of fatigue failures under test conditions, the common practice of conducting a single full-scale test due to cost and time constraints, limits the statistical confidence that can be placed in estimates derived from a single test. Although these tests are frequently augmented by supporting programmes of lesser assembly, component and coupon tests; the traditional approach by analysts of full-scale fatigue test data has been to draw upon prior knowledge of the behaviour of the structural materials and systems being tested to minimise the cost and duration of these test programmes.

Half a century of in-service and test experience with metal fatigue in the aerospace industry since the tragic Comet jet airliner accidents has resulted in the development and validation of statistical models, which have underpinned the initial certification and continuing airworthiness management of the majority of aircraft produced over this period. Of fundamental importance to the success of these techniques is the observed consistency in the statistical distribution of fatigue life, particularly the lognormal distribution of both test and in-service data with a standard deviation that is largely independent of load spectrum and structural configuration. Despite the repeated verification of these observations and the numerous papers that have been written on this topic, the analyst's interpretation of the test factors mandated or recommended by a broad range of sources – including airworthiness regulations – has been hampered by the dearth of detail on the techniques used to derive these test factors.

Against a backdrop of early teachings that "composite materials do not fatigue" (at least not in the manner demonstrated by metallic structures) it is not clear that techniques derived from a statistical understanding of the accumulation of fatigue damage in metals should be used when certifying the durability of composite aerospace structures. Even if it can be demonstrated that the limitations and assumptions inherent in these models apply to composite structures, there exists a need to select appropriate test factors based upon a statistical understanding of the behaviour of specific composite materials and structural configurations under representative load and environmental conditions. "

8.4.14 Investigation of Corrosion Fatigue Interactions in Aluminium Alloy Joints Used in Aerospace Applications (K.Shankar[ADFA], S.Russo, B.R.W.Hinton [DSTO])

During the past 10 years Corrosion Preventative Compounds (CPCs) have come into regular use in both the military and civilian aircraft. The effect of these CPCs on load transfer joint fatigue life is not well understood. In many cases, the fatigue life results are inconclusive and depend on a range of factors including the type of CPC, the joint design and load level. Recent work at ADFA and DSTO on $1^1/_2$ dogbone specimens with interference fit Hi-Lok fasteners showed a reduction in fatigue life in the presence of CPC at 144MPa under constant amplitude loading. The CPC had no effect at a higher stress of 210MPa. The addition of the CPC had a marginal effect on the location of the Fatigue Crack Initiation Site (FCIS) and prevented fretting at the faying surfaces. The present work involves a more extensive test program to investigate these effects in relation to a typical joint on a RAAF aircraft which is prone to corrosion. A single-shear lap joint specimen that is typically found on the Boeing 737-700/800 is used in this test program. This aircraft/joint was chosen as it is representative of joints on the fuselage of the new RAAF AEWCs to be based at RAAF Williamtown, and it has a history of corrosion/fatigue problems. The loading conditions reflect the stresses and secondary bending moments typically found on the front fuselage lap joint of these aircraft. Fatigue tests will be performed using tension-tension constant amplitude sinusoidal loading at an axial stress of 14.3ksi (98.6MPa). The stress equates to approximately 90% of the gross hoop stress experienced by Boeing 737 fuselage lap joints at 35,000ft.

The initial series of tests consisted of lap joint specimens tested in dry air and under 95% humidity with and without the application of CPCs. The results showed that the application of CPC reduced the fatigue life of the joints about 260,000 cycles to about 100,000 cycles in dry air, and about 200,000 cycles to about 89,000 cycles in humid air, ie. reductions of the order of 60% and 55% respectively, in dry air and in humid environment (see Figure 86).

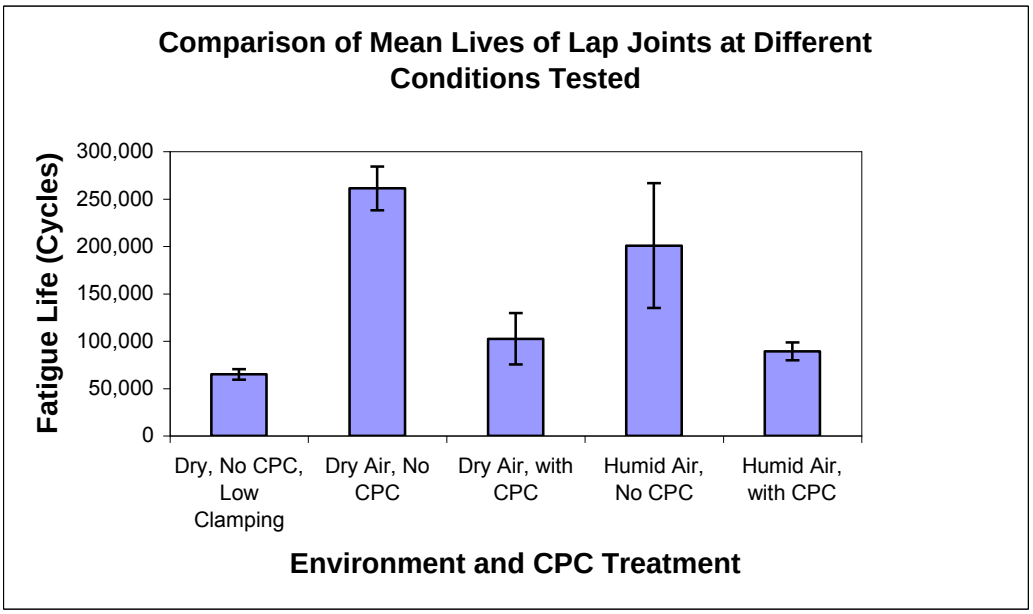

Figure 86: Fatigue test results

Currently tests are under way to investigate the effect of CPCs on pre-corroded lap joints in dry and humid conditions. The general approach is to measure and compare the fatigue lives and crack initiation features of an artificially corroded lap joint, both with and without the application of a CPC. They will follow conditions that are to be adopted by the collaborative program between DSTO, APES Inc and NRC. A total of 15 lap joint specimens are being tested. These involve specimens with pre-corrosion to be tested in dry air to investigate the stress raiser effect of corrosion, specimens with pre-corrosion in humid environment to investigate the effect of continuing corrosion in operation, and specimens treated with CPC after with introducing pre-corrosion to assess the ability of the CPC in arresting the growth of lap joint corrosion under fatigue loading in humid conditions.

8.4.15 Automatic Synthesis of Transfer Functions to Predict Helicopter Dynamic Component Loads from Fixed System Parameters (L.Krake, DSTO)

The rotor and its attachments contain most of the fatigue-critical structural components in a helicopter; however, quantifying the loads in these components requires slip rings or rotating telemetry systems that currently lack the reliability and maintainability needed for everyday fleet usage. An alternative is to use transfer functions to predict the loads in dynamic components from loads (and other parameters) measured on the airframe. Traditionally, such transfer functions have been derived from mathematical models of the rotor system; however, owing to the complexities involved, this approach has had limited success.

The focus of some current work in DSTO is investigation of the ability of machine learning techniques to automatically synthesize transfer functions for dynamic component load prediction. The techniques being investigated - namely Genetic Programming (GP) and Artificial Neural Networks (ANNs) - are domain-independent problem-solving approaches borrowed from computer science. GP 'evolves' computer programs (e.g. mathematical expressions) to solve problems and ANNs can be trained to solve problems. Both methods are data-driven and computationally intensive. However, they have an advantage over direct mathematical modelling in that they do not require any detailed physical insights into the system being modelled. This is especially helpful given the inherent difficulty of modelling helicopter rotor systems. A further advantage of GP is that it generates complete mathematical expressions as output, which means that it has the potential to provide novel physical insights into the system being modelled.

The GP and ANN approaches are utilising Black Hawk helicopter data obtained during the joint USAF/ADF flight loads measurement program, which was conducted in 2000 and reported in previous ICAF reviews. The application of the GP and ANN methods to the helicopter load synthesis problem has so far concentrated on implementation of the GP and ANN methods in code and offline data pre-processing and analysis, which are crucial to the success of machine learning techniques. With these activities nearing completion, experimental runs will soon be carried out to evaluate the performance of GP and ANN in the selected problem domain.

The current research complements work done in previous years [1], [2], and [3], which was based on a more traditional mathematical modelling approach. [4] briefly describes some of the ANN-related work carried out to date.

References

1. Polanco, F. G., Estimation of Structural Component Loads in Helicopters: A Review of Current Methodologies, DSTO Technical Note, *DSTO-TN-0239*, December 1999.
2. Polanco, F. G., Development of a Stress Transfer Function for an Idealised Helicopter, DSTO Research Report, *DSTO-RR-0171*, March 2000.
3. Polanco, F. G., Determining Beam Bending Distribution Using Dynamic Information, DSTO Research Report, *DSTO-RR-0226*, January 2002.
4. Cheung, C & Krake, L., Helicopter Loads Synthesis using a Neural Network, fifth DSTO International Conference on Health and Usage Monitoring (HUMS2007), March 2007.

8.4.16 Effect of Thermal Damage on the Mechanical Properties of 7050-T7451 Aluminium Alloy. (J.Calero, DSTO) - Paper to be presented at ICAF 2007 Symposium

Abstract

"It is not uncommon that Military aircraft structures and components made from 7050-T7451 aluminium alloys are accidentally exposed to temperatures above the ageing temperature for this alloy. As a consequence, depending on the temperature and exposure time, thermal damage may occur. Although localised thermal damage is often indicated by visual signs of thermal distress, such as paint discoloration and deformation, these signs do not provide a clear indication of the degree of damage. Furthermore, in some cases heat affected areas might not show any visual evidence that heat distress has occurred.

To overcome the limitation of visual inspections, hardness and electrical conductivity tests are normally used to assess the extent of thermal damage by measuring relative variations of these properties within the affected regions with respect to a reference value. Assessment of affected areas is usually required to formulate a strategy to manage affected areas that may require repair actions or limitations to the performance envelope of the aircraft. However, the available data on thermal damage is usually limited to very specific conditions. Consequently, DSTO has developed and conducted an extensive experimental test program to quantify the time-temperature effects of exposure to elevated temperatures on hardness, electrical conductivity, strength, fatigue life and fracture toughness properties of 7050-T7451 aluminium alloy. The test program investigated temperatures ranging from 205 °C to 350 °C and exposure times ranging from ten minutes to five hours.

The test program explored the use of hardness testing as a means to estimate residual properties at room temperature after thermal damage. The data presented in this paper quantify time-temperature variations in strength and fatigue life and correlate changes in these properties with hardness. The fatigue testing was performed using a spectrum loading developed from flight data collected from the wing root strain gauges from F/A-18 aircraft and which was modified to replicate the Royal Australian Air Force (RAAF) fleet service conditions.

The testing has shown that there is a direct relationship between hardness, strength and fatigue life and consequently, hardness testing could be used to estimate residual properties. Currently, fracture toughness testing, using Single Edge Bend specimens to determine J1c, is being conducted to determine whether hardness testing could be used to assess fracture toughness after thermal damage."

8.4.17 Fatigue Cracks Emanating from Notches: A Survey and Assessment of Predictive Methodologies (W.Hu and P.Jackson, DSTO) - Paper to be presented at ICAF 2007 Symposium

"While numerous experimental and numerical studies have been carried out to characterize and model the behaviour of fatigue crack growth in notch-affected zones, the modelling of fatigue crack growth in this region still lacks accuracy and robustness. In particular, the observed fast growth in the notch zone followed by slow growth is not well captured by the general predictive tools, even when complicated numerical calibration is introduced.

A recent critical review of aircraft structural lifing methodologies and tools carried within DSTO has identified notch effect as one of the key areas for improvement of the overall structural integrity assessment, and this paper extends that work by surveying and critically assessing the current methods and approaches used in aircraft structural integrity management community and those under active study in the general scientific community.

In particular, detailed assessment will be carried out on two distinctly different approaches: the explicit modelling of notch plasticity using discreet elements and the implicit modelling of notch effect by self-equilibrated internal stresses. The key features of the explicit model include the determination of the notch root stress-strain response history, the approximation of the elastic-plastic stress distribution ahead of the notch root along the crack plane, and the calculation of an effective stress intensity factor range, when the specimen is subjected to external cyclic load. The near-notch stress-strain field will be determined using a Chaboche-type nonlinear kinematic hardening plasticity model and the Neuber rule, and the evolution of the stress-strain field monitored on a cycle-by-cycle basis for constant amplitude and spectrum loading.

The implicit model is based on the internal stress method developed by Dong, P., J. K. Hong, et al. (2003, International Journal of Fatigue 25: 811-825), in which a system of self-equilibrated internal stresses is introduced to modify the stress intensity range in the near-notch zone.

Based on the outcome of the survey and detailed assessment, the paper will present recommendations for the appropriate and effective use of existing tools for the estimation of fatigue crack growth life of notched components, and identify research directions."

8.4.18 Modelling of Defects and Damage in Aerospace Composite Structures (R.Thompson, CRC-ACS)

The Cooperative Research Centre for Advanced Composite Structures (CRC-ACS) is a full partner in the European Commission Sixth Framework Programme project COCOMAT ("Improved **MAT**erial Exploitation at Safe Design of **CO**mposite Airframe Structures by Accurate Simulation of **CO**llapse"). COCOMAT is a four-year project that started in January 2004 and aims to develop advanced damage models for composite materials, to allow more efficient and damage-tolerant postbuckling composite designs for aircraft fuselage structures (www.cocomat.de). The CRC-ACS has developed a comprehensive modelling strategy to predict interlaminar damage initiation in intact structures, interlaminar crack growth such as delamination and skin-stiffener debonding, and degradation due ply damage mechanisms. The analysis methodology, embedded in a commercial finite element code, was extensively validated using experimental results for coupons, verification structures and large multi-stiffener panels.

Figure 87 below is an example of the advanced capabilities of the developed approach. Within COCOMAT, a five-stiffener curved panel representative of composite fuselage designs, manufactured by Aernnova and tested by DLR, was first loaded cyclically into the postbuckling region for 3700 cycles before a static loading until collapse.

The cyclic loading introduced debonding between the skin and stiffener, which can be seen in the image at zero load. A numerical model was created using the developed approach that included this pre-damage, and this model was able to represent the crack growth of these pre-damaged regions in combination with ply-based damage mechanisms such as matrix cracking and fibre fracture.

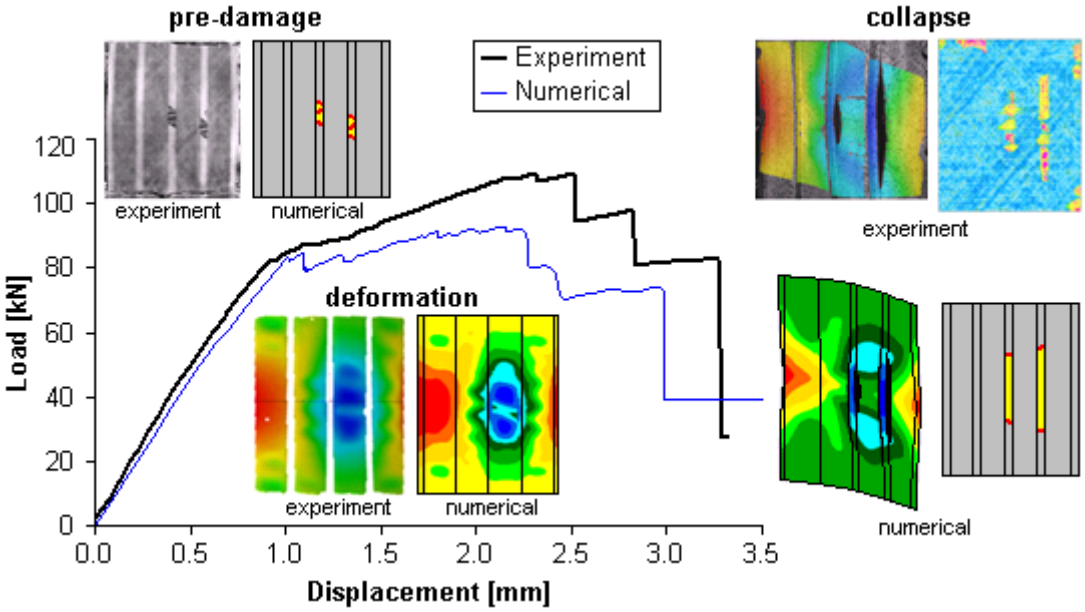

Figure 87: Load-displacement curve of a curved stiffened compression panel showing experimental and predicted postbuckling behaviour and damage development

8.4.19 Fatigue Life recovery in Corroded Aluminium Alloys Using Bonded Composite Reinforcements (A.A.Baker, DSTO).

Results of research into recovery of fatigue life in corroded aluminium alloys, using bonded composite reinforcements, has been published [1]. The conclusions from this were:

Bonded reinforcements provided a useful life improvement in specimens damaged by severe exfoliation. Possibly due to the presence of tensile residual stresses, the boron/epoxy reinforcement performed somewhat less well than an aluminium alloy reinforcement, but this loss in repair efficiency does not outweigh the many other benefits of composite reinforcement. The fatigue life improvement results from the strain reduction provided by the reinforcement and possibly the bonding heat treatment. The adhesive was unable to penetrate into the exfoliated region so did not provide significant improvement.

Grit blasting was not able to modify the deep exfoliation damage so was ineffective.

A combination of more energetic grit blasting to remove much more corrosion product and adhesive penetration would almost certainly be highly beneficial. Thus it is anticipated that considerable further life extension would be obtained by using a more fluid (uncured) adhesive and possibly vacuum assistance to aid penetration of the adhesive deep into the exfoliated region. An alternative would be to use a low viscosity epoxy resin to impregnate the exfoliated region prior to bonding.

Unless bonded reinforcements are used only as a temporary measure for the repair of severely exfoliated aluminium alloys, there is an obvious need to remove most the damaged region, particularly since some corrosive product remains trapped in the parent material after patch application. Fortunately, based on the observed benefits of bonded reinforcements for repair of small corrosion pits the need to remove all the corrosion damage is much less stringent than would be the case in the absence of the reinforcements. For example, small pits in the area surrounding the main area of attack or at the base of the grind out may inadvertently remain after treatment.

For relatively mild corrosion pitting, boron/epoxy reinforcement can fully restore the original undamaged fatigue life if the considerable benefit of strain reduction is considered. The life recovery in the aluminium alloy in the absence of strain reduction is associated with the patching process, most probably the adhesive coating. This coating would be highly effective in isolating the pits from the humid test environment. Generally, bonded composite repairs have excellent potential to allow recovery of components when in the process of corrosion removal local thickness of the component falls under allowable limits, even if some pitting remains. High-stiffness non-conducting patches, such as boron/epoxy, could be used effectively in the repair of damage to faying surfaces, as the reinforcing layer will provide a corrosion-resistant insulating layer and minimise fit-up problems."

Reference

1. Fatigue Life recovery in Corroded Aluminium Alloys Using Bonded Composite Reinforcements, A.A.Baker, Applied Composite Materials (2006).

8.4.20 Fatigue and Fracture Research (R.Jones, Monash University)

In the past few years:

We have shown how for constant amplitude loading the concept of similitude, which underpins most crack growth laws, is invalid in Region I. We have also seen how this similitude is invalid under variable amplitude loading in both Regions I and II.

We have also explained how the generalised Frost-Dugdale crack growth law is linked to fractal concepts, the two parameter crack growth law, dislocation based crack growth laws, Tomkins' crack growth law and to notch mechanics based growth laws.

We have shown how crack growth under a composite repair follows the generalised Frost-Dugdale law and how this formulation can be used to predict crack growth from near micron sized defects to 10's of mm's. We propose that this approach to analysis of composite repairs to cracked metallic structures is consistent with the experimental data, and is a more effective interpretation than existing analyses.

As an aside the mathematics underpinning the methodology is now firmly in place and the generalised Frost-Dugdale crack growth law can be derived either from first (mechanics) principles, or via a dislocation approach, or using fractal mechanics. Furthermore, we are able to show where Paris and co-workers made their mistakes in their initial 1960's papers. We are currently preparing an invited paper on this topic, and that paper also forms part of chapter of a USAF special publication on the state of the art in fatigue crack growth analysis. The outcome is that the Paris law, and its variants, only holds for constant amplitude loading, and then only in Region II.

8.4.20.1 Similitude and the Frost-Dugdale Crack Growth Law.

It has now been shown [1] that the concept of similitude, that underpins current crack growth concepts, is invalid in Region I. It has been shown [1] that da/dN is a function both of ΔK and the crack length, see Figure 88 and Figure 89

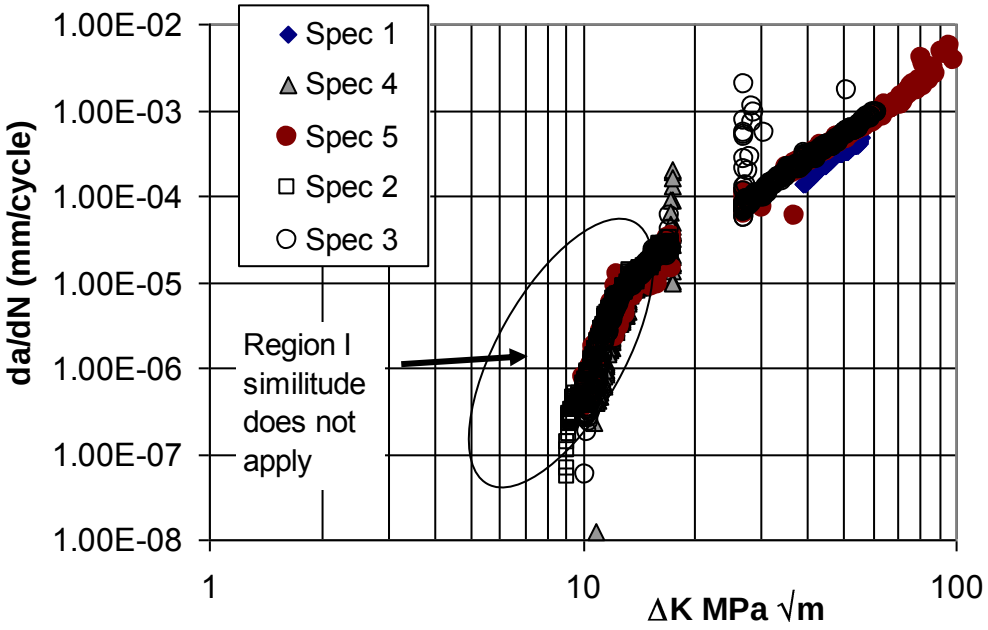

Figure 88: Crack Growth in L6B-2, from [1]

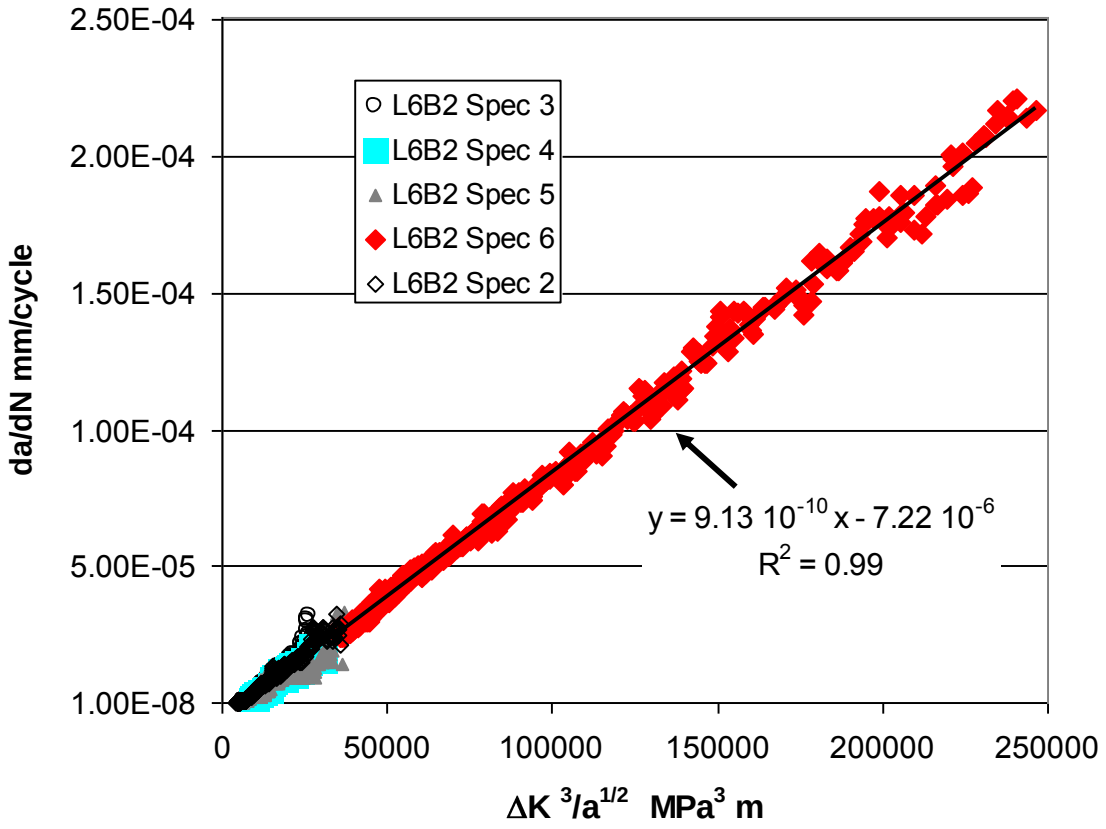

Figure 89: Crack growth in Region I in L6B-2, [1]. Note the linear scale in this figure

This finding was expanded in [2] which presented crack growth data for a wide range of steels; in each case crack growth was found to follow the generalised Frost-Dugdale crack growth law [3-5], viz:

$$da/dN = C^* \Delta K^{\gamma}/a^{\gamma/2-1} + (da/dN)_0 \qquad (1)$$

where in this case ΔK is the crack driving force, C^* and γ are constants, and $(da/dN)_0$ reflects the nature of the initial defect from which the crack grows.

The ability of generalised Frost-Dugdale crack growth law to predict crack growth from near micron size up to of the order of 10 mm's is illustrated in [1, 4, 5] both for laboratory coupon tests and for full scale aircraft fatigue tests. Application to F/A-18 aircraft was presented in [1] where it was shown that unlike FASTRAN it accurately reproduced test data, see Figure 90. Application to cracking in F-111 aircraft was presented in by Jones, Molent, Pitt, and Siores [5].

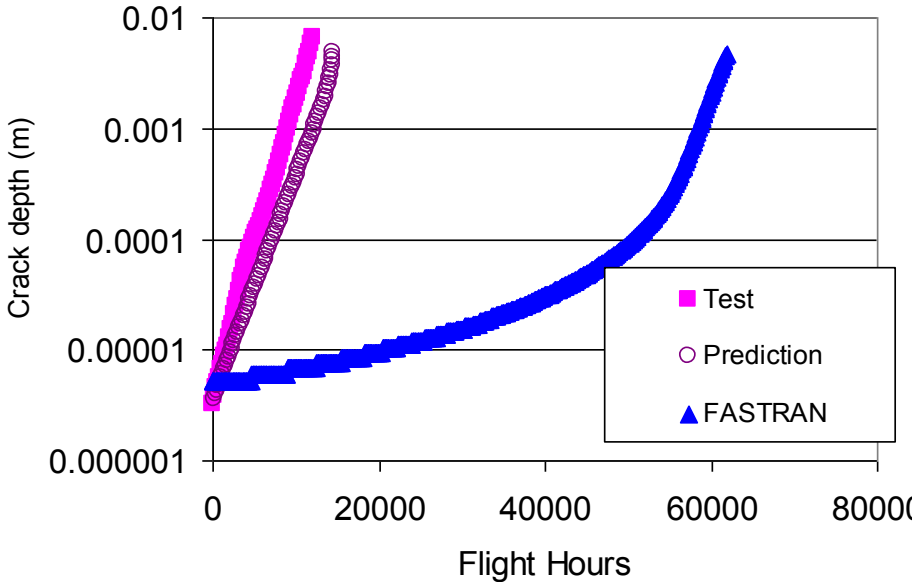

Figure 90: Experimental and predicted crack growth histories in the DSTO F/A-18 Centre Barrel test

Jones, Molent, Pitt, and Siores [5] also showed that the results of the Boeing 767 and 757 Materials Characterization Test program [6] followed the generalised Frost-Dugdale crack growth law. In this work Miller et al [6] presented the Boeing centre cracked panel test data, derived for B767 and B757 aircraft, which compared crack growth in various aluminium alloys, viz 6.3 mm thick 2024-T3, 3.2 mm thick 2324-T39, 3.2 mm and 12.7 mm thick 7150-T651, under constant amplitude loading, see Figure 91. In all of the cases shown we see that crack growth follows the generalised Frost-Dugdale crack growth law, which for the test geometry studied results in a linear relationship between ln(a) and the number of cycles, see Figure 91.

Variable Amplitude Loading

Miller et al [6] also presented data comparing crack growth in a 6.3 mm thick and 610 mm wide centre cracked panel for 2324-T39, 2024-T351, 7075-T651, 7150-T651, and 2024-T3 aluminium alloys tested under representative spectra, termed Transport spectra A, B, and C. A summary of the experimental results is presented in Figure 91. From this figure we see that crack growth was essentially log linear and that when presented in this fashion Spectrum B and C appear similar. They also presented crack growth data for a range of 7150-T651 thicknesses tested under Transport spectra B. These results are shown in Figure 92 where we see that when presented in this fashion the thickness effect was also minimal.

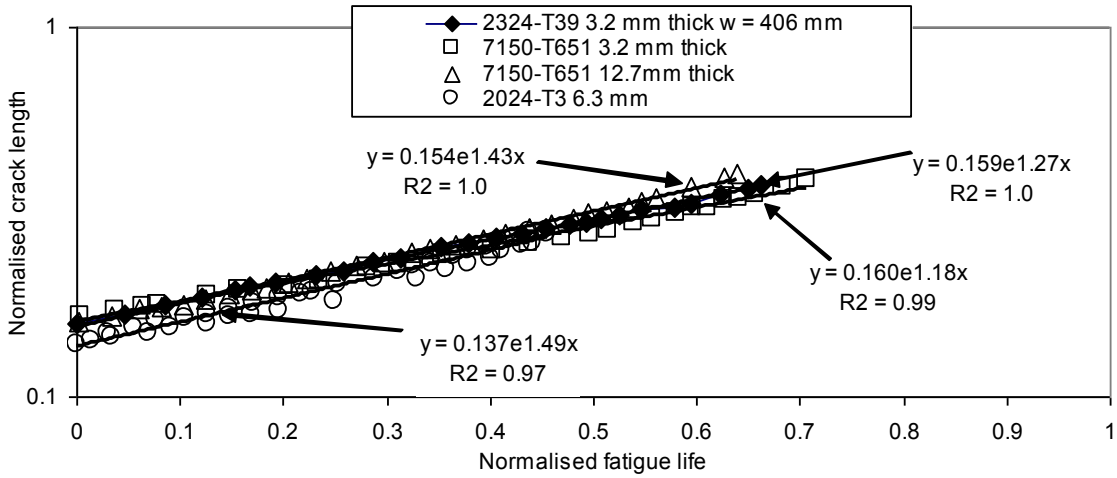

Figure 91: Boeing constant amplitude crack growth data, adapted from [6]

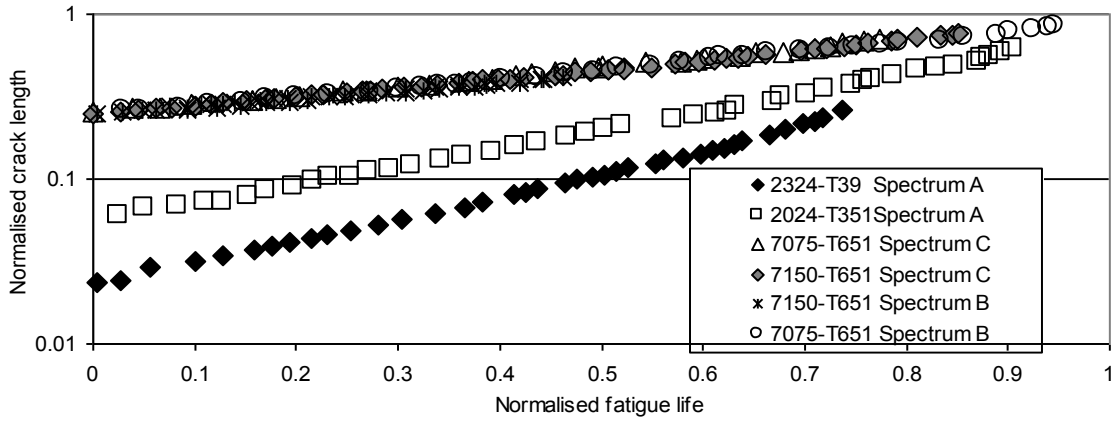

Figure 92: Boeing crack growth data for tests under various transport load spectra, adapted from [6]

Jones, Molent and Pitt [1] also demonstrated how the generalised Frost-Dugdale crack growth law can be related to:

a) The two parameter crack growth law [7];
b) dislocation based crack growth laws as presented by Ding Hong-Zhi and Xing Xiu-Sa [8];
c) Tomkins' crack growth law [9],
d) Fractal based crack growth laws as developed by Carpinteri [10] , Carpinteri and Spagnoli [11] and Spagnoli [12].
e) Notch mechanics based growth laws, see Sih, Tang [13] and Wnuk [14].

Composite Repair Technology

It has also been shown [15-17] that crack growth under composite repairs also follows the generalised Frost-Dugdale crack growth law. An example of the predictive capability is presented in Figure 93. An equivalent block formulation for crack growth in both patched and unpatched structures has been developed [17] and its application to the C-5A repair is presented in Figure 94.

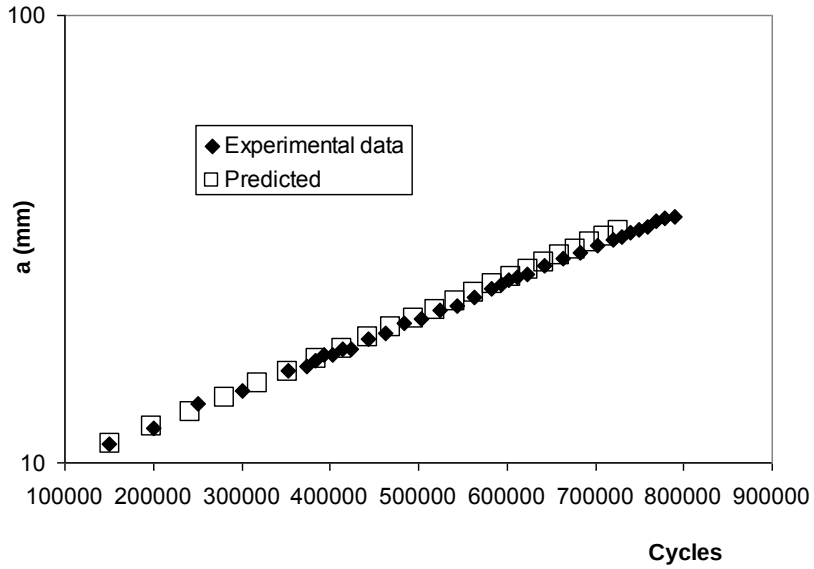

Figure 93: Crack depth versus number of cycles for the edge cracked 2024 T3 aluminium plate, repaired with a seven ply boron epoxy patch, under variable R ratio from [15]

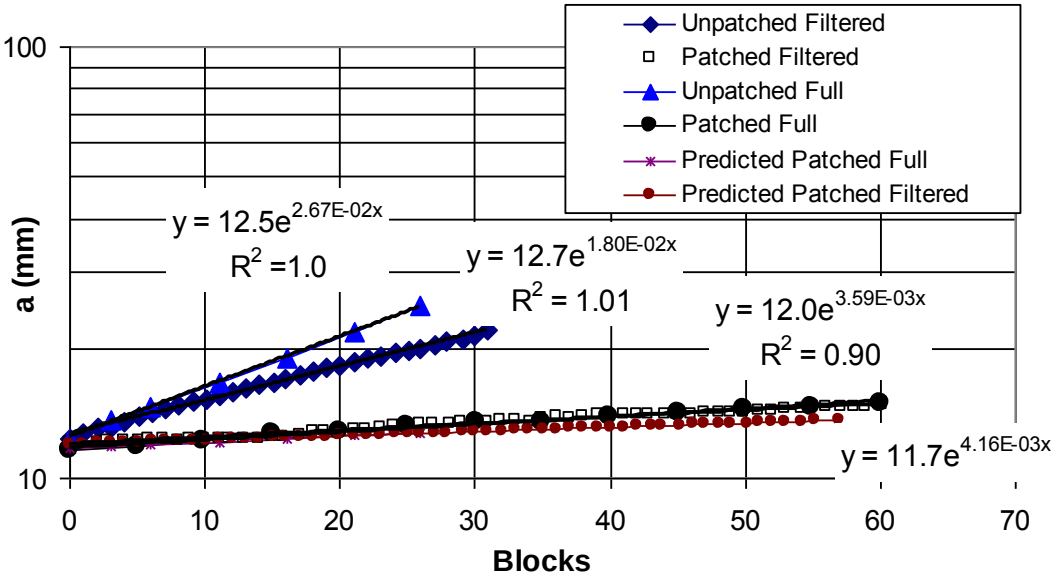

Figure 94: Crack growth under a representative C5A load spectrum, from [17]

Earlier studies into fatigue crack growth under a composite repair were predicated on the assumption that the stress intensity factor rapidly reaches a constant value [18, 20] supported by experimental study [21]. In [16], it is proposed that this hypothesis, ie. that the stress intensity factor rapidly reaches a constant value, is invalid.

Fatigue Crack Growth Under Variable Amplitude Loading

In the review paper on crack growth and similitude Davidson [21] concluded that similitude was lost during fatigue crack growth under variable amplitude loading. This conclusion is consistent with the findings presented in [1, 5, 15, 16] that crack growth under variable amplitude loading is best described using the Frost-Dugdale law, or its equivalent block variant [16, 23].

This can be best observed by considering crack growth in the Round Robin helicopter fatigue study. The objective of this study, as devised by Cansdale, Perret, Irving and Bristow [23], was to assess the capability of current structural analytical tools to predict fatigue crack growth. The round-robin test specimen was chosen to represent a complex aerospace component, subjected to a typical rotorcraft spectrum (Asterix).

Interest in this problem was kindled due to the conclusions reached by US Army researchers Vaughan and Chang [24], who used AFGROW and NASGRO to predict the crack length history for this problem, who stated:

i) "It is evident that the crack growth was under-predicted for the crack length below 5 mm and is over-predicted when crack length is more than 10 mm."

ii) "We believe more research; especially in the area of modeling crack growth near the crack growth threshold and determining experimentally the crack growth threshold values are needed."

Indeed, the generalised Frost-Dugdale crack growth law, and its equivalent block variant, was specifically formulated to address point (ii). This problem was analysed using the (non-similitude) equivalent block approach variant presented in [16, 23], viz:

$$da/dBlock = \tilde{C}\ a^{(1-\gamma/2)} K_{max}^{\gamma} \qquad (2)$$

where $\tilde{C}$ is a spectrum dependent constant and K_{max} is the maximum stress intensity factor in the block. The resultant predictions obtained using $\tilde{C} = 0.92\ 10^{-15}$ and $\gamma = 3$ are shown in Figure 95, where we see an excellent agreement between the predicted and the measured crack length histories. This example supports Davidson's conjecture [21] that similitude is lost under variable amplitude loading. Advantages of this approach are:

a) Its simplicity.
b) Only two constants are needed, and they remain unchanged throughout the analysis.

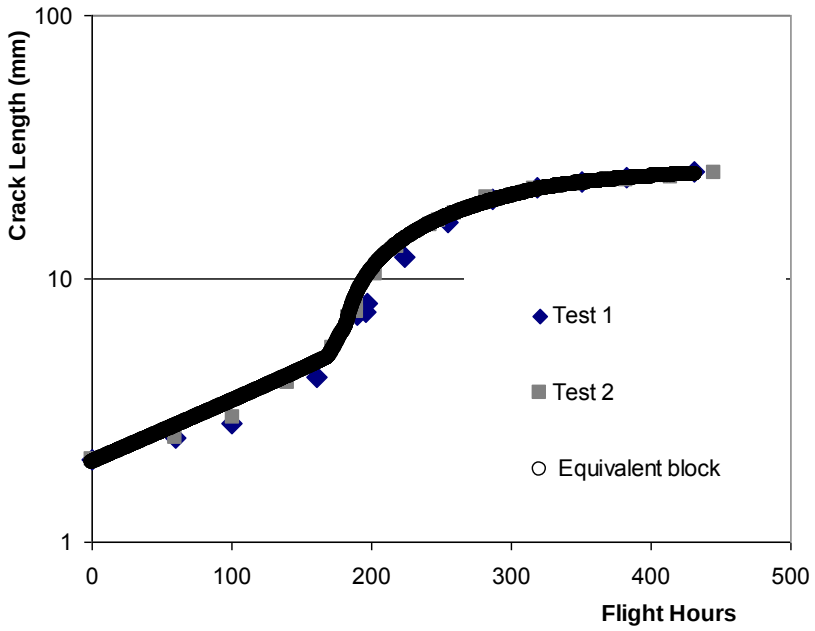

Figure 95: Computed and measured surface crack length histories

8.4.20.2 Crack Closure

Jones and Pitt [26] used D-mode infra-red thermography to investigate crack tip closure during fatigue crack growth. This revealed that the near crack tip region was always open and led to the two parameter crack growth model as formulated in Noroozi, Glinka and Lambert [7]. An example of this is shown in Figure 96, where it can be seen that the crack tip region is open. This finding is supported by the results shown in Figure 97, where we see closure related energy dissipation away from the crack tip region. However, immediately behind the tip there was no closure, and hence minimal energy dissipation. The geometry of the test specimen is shown in Figure 98.

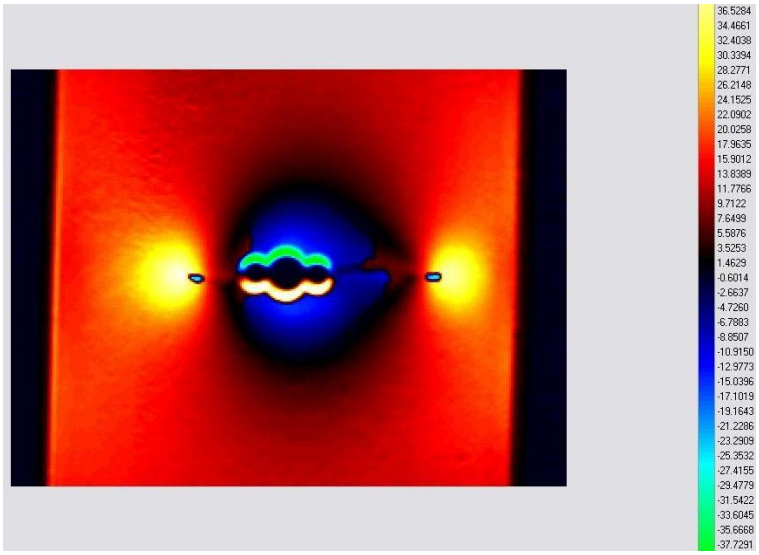

Figure 96: Stresses around the crack, from [26]

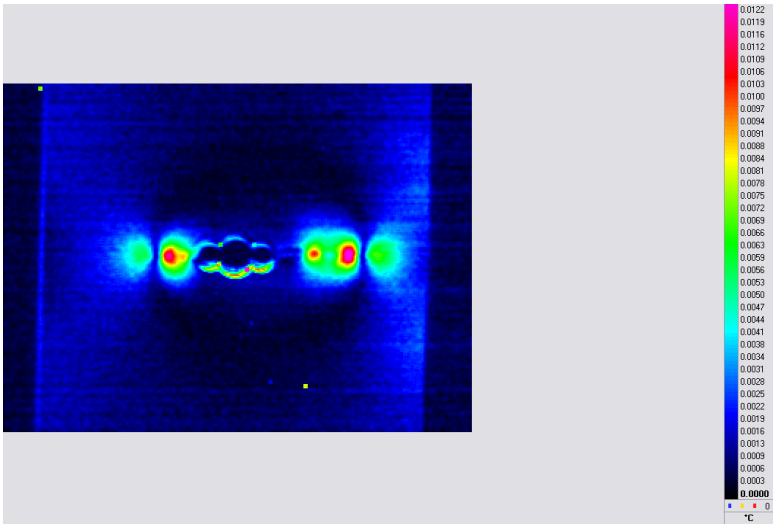

Figure 97: The energy dissipation field, from [26]

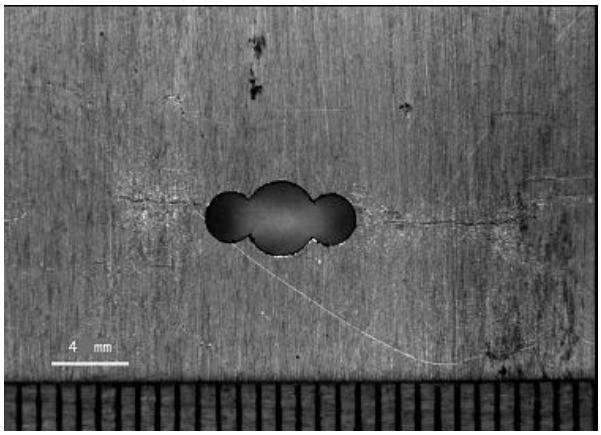

Figure 98: Test specimen with central holes, from [26]

Conclusion

In the past few years we have shown how for constant amplitude loading the concept of similitude, which underpins most crack growth laws, is invalid in Region I. We have also seen how this similitude is invalid under variable amplitude loading both in Regions I and II.

We have also explained how the generalised Frost-Dugdale crack growth law is linked to fractal concepts, the two parameter crack growth law, dislocation based crack growth laws, Tomkins' crack growth law and to notch mechanics based growth laws.

We have shown how crack growth under a composite repair follows the generalised Frost-Dugdale law and how this formulation can be used to predict crack growth from near micron sized defects to 10's of mm's. We propose that this approach to analysis of composite repairs to cracked metallic structures is consistent with the experimental data, and is a more effective interpretation than existing analyses.

References

1. Jones R, Molent L, and Pitt S., "Crack growth of physically small flaws", Proc Int. Conf on Fatigue Damage of Structural Materials VI, Hyannis, USA, September 2006. Int. Journal of Fatigue, Elsevier website: http://dx.doi.org/10.1016/j.ijfatigue.2007.01.031
2. R. Jones, B. Chen, and S. Pitt, Similitude: cracking in steels, Theoretical and Applied Fracture Mechanics, (accepted for publication).
3. Barter SA., Molent L., Goldsmith N. and Jones R., An experimental evaluation of fatigue crack growth, Journal Engineering Failure Analysis, Vol 12, 1, pp 99-128, 2005.
4. Jones R., Barter SA., Molent L., and Pitt S., A multi-scale approach to crack growth, Multiscaling in molecular and continuum mechanics: biology, electronics and material science, Edited by G. C. Sih, Springer, 2007.
5. Jones R., Molent L., Pitt S and Siores E., Recent developments in fatigue crack growth modelling, Proceedings 16th European Conference on Fracture, Alexandropoulos, Greece, July 2006.
6. M. Miller, V. K. Luthra, and U. G. Goranson, "Fatigue crack growth characterization of jet transport structures", Proc. of 14th Symp of the Intl Conf on Aeronautical Fatigue (ICAF), Ottawa, Canada, June 10-12, 1987.
7. Noroozi A.H., Glinka G., Lambert S., A two parameter driving force for fatigue crack growth analysis, International Journal of Fatigue 27 (2005) 1277–1296.
8. Ding Hong-Zhi, Xing Xiu-San. A plastic flow-induced fracture theory for fatigue crack growth, Journal Of Materials Science, 1996, 31, 4099-4103.
9. Tomkins, B. (1968) Fatigue crack propagation—an analysis, "Phil. Magazine ", 18, 1041–1066.
10. Carpinteri, Al., 1994. Scaling laws and renormalization groups for strength and toughness of disordered materials. Int. J. Solids Struct. 31, 291–302.
11. Carpinteri An., Spagnoli A. A fractal analysis of size effect on fatigue crack growth, Int. J. Fatigue, 2004, 26, 125–133.
12. Andrea Spagnoli An. Self-similarity and fractals in the Paris range of fatigue crack growth. Mechanics of Materials 37 (2005) 519–529.
13. Sih GC., Tang XS., Form-invariant representation of fatigue crack growth rate enabling linearization of multiscale data, Theoretical and Applied Fracture Mechanics 47 (2007) 1–14.
14. Wnuk M.P., Yavari A., A correspondence principle for fractal and classical cracks", Engineering Fracture Mechanics 72 (2005) 2744–2757.
15. R. Jones, K. Krishnapillai and S. Pitt, "Crack patching: Predicting fatigue crack growth", Theoretical and Applied Fracture Mechanics 45, 79 – 91, 2006.
16. Jones R, Pitt S. Crack patching revisited, Composite Structures, 2006; 76: 218-223.
17. R.Jones, S.Barter, L.Molent and S. Pitt , "Crack patching: an experimental evaluation of fatigue crack growth", Composite Structures, Volume 67, Issue 2, February 2005, Pages 229-238.
18. L.R.F. Rose, "Theoretical Analysis of Crack Patching," Chapter 6, Bonded Repair of Aircraft Structures, Editors A.A Baker and R Jones, Martinus Nijhoff, pp 107-173 1988.
19. A.A.Baker, "Crack patching: experimental studies, practical applications", Chapter 6, Bonded Repair of Aircraft Structure, A. Baker and R. Jones, Martinus Nijhoff Publishers, The Hague, 1988. (Book), pp 107- 173.
20. Bayram Aktepe and Alan Baker, "Validation of stress intensity estimations in patched panels", Chapter 18, "Advances in the Bonded Composite Repair of Metallic Aircraft Structure", A. Baker, L. R. F. Rose and R. Jones, Elsevier Applied Science Publishers, 2002. ISBN 0-08-042699-9.

21. Davidson, D. L., "How Fatigue Cracks Grow, Interact with Microstructure, and Lose Similitude," Fatigue and Fracture Mechanics: 27th Volume, ASTM STP 1296, R. S. Piascik, J. C. Newman, and N. E. Dowling, Eds., American Society for Testing and Materials, 1997, pp. 287-300.
22. L. Molent, M. McDonald, S. Barter and R. Jones, Evaluation of Spectrum Fatigue Crack Growth using Variable Amplitude Data, Int. Journal of Fatigue (2007) in press.
23. Cansdale R. and Perrett, B., The Helicopter Damage Tolerance Round Robin Challenge, Workshop on Fatigue Damage of Helicopters, University of Pisa, September 12-13, 2002.
24. Vaughan RE. and Chang JH., "Life predictions for high cycle dynamic components using damage tolerance and small threshold cracks," presented at American Helicopter Society 59th Annual Forum, Phoenix, Arizona, 2003.
25. U. H. Tiong, R. Jones, and L. Molent, Analysis Of Fatigue Crack Growth In A Helicopter Component Using The Generalised Frost-Dugdale Law, In preparation.
26. R. Jones and S. Pitt, "An Experimental Evaluation Of Crack Face Energy Dissipation", Int. Journal of Fatigue, Volume 28, Issue 12, December 2006, Pages 1716-1724.

8.4.21 A critical Evaluation of Unified Approaches for Analysing Short and Long Fatigue Crack Growth (K.Walker and W.Hu, DSTO) - Paper to be presented at ICAF 2007 Symposium

Abstract

"The analysis of structural fatigue life and crack growth is an essential component in the management of the structural integrity of military aircraft fleets. For structures that were designed according safe life methodology the total life may be modeled as a combination of crack initiation life and (long) crack growth life, or just as crack growth life, starting from very short cracks. With the advancement in experimental and computational techniques, there is a trend to push crack growth analysis into the arena of traditional crack initiation, ie. modelling the growth of cracks on the scale of micrometres. In the latter approach, a critical issue is the use of long crack growth rate data to model the short crack growth behaviour (short cracks may continue to grow below the long crack threshold; short cracks grow faster than long cracks under the same stress intensity range), as it is difficult and expensive to obtain short crack growth rate data. Various models have been proposed to account for the short crack effect with different degree of success, and three of them are critically evaluated in this paper.

Firstly, the approach proposed by Molent, Jones et al., known as the C method was assessed. In this approach, the Paris-type crack growth relationship was modified by dividing the stress intensity range by the square root of the crack length "a".*

Secondly, the El Haddad model (1979) was examined, in which a crack size dependent on the threshold stress intensity range is added to the physical crack length.

Thirdly, the method currently implemented in FASTRAN was evaluated. The FASTRAN method is similar to the El Haddad model, except that the fictitious crack length added to the physical crack is dependent on plastic zone size associated with the current load cycle. The inherent properties of the analytical crack closure model built into FASTRAN also deal with the short crack effect to some extent.

All three models aim to achieve a similar desirable effect, ie. increasing the crack growth rate when the crack is short while diminishing the effect when the crack becomes longer, but the models appear to be substantially different over a long range of crack lengths. The objective of this paper is, therefore, to critically evaluate the capability of these three models in treating short and long crack growth in a unified manner, and to suggest the boundaries of applicability of each approach. The first two models have been implemented in a DSTO-developed crack growth computer code, CGAP, and the code was used to evaluate the performance of the approaches. Based on the outcome of the evaluation, recommendations are made on the selection of different models for the task of fatigue crack growth assessment."

8.5 FATIGUE INVESTIGATIONS IN NEW ZEALAND

8.5.1 C-130 Life Extension Program (L3 Communications Spar Aerospace, and S.K.Campbell, DTA, New Zealand)

The Royal New Zealand Air Force (RNZAF) operates a fleet of five C-130H Hercules aircraft. In December 2004 The New Zealand Ministry of Defence awarded L-3 Communications Spar Aerospace a contract to conduct a Life Extension Program (LEP) on the RNZAF fleet. The scope of this project includes the replacement of specific mechanical, avionic and structural components as well as the design and installation of a modern communications and navigation system. The first aircraft to be upgraded was inducted into Spar's Edmonton facility in October 2005.

One aspect of the LEP that is of specific interest to the aeronautical fatigue community is the replacement of a number of critical wing structural elements and the embodiment of a Fatigue Improvement Modification (FIM) package for those wing components not being replaced. The replaced components include the center wing lower skin, caps and webs of both the front and rear center wing beams and the rainbow fittings. The areas subject to FIM have been designed by Spar to provide increased durability. The FIM includes an extensive fastener hole cold working, the installation of oversized fasteners (damage removal) and an extensive bolt hole and surface scan eddy current inspection programme. The goal of the FIM is to increase the durability of the RNZAF fleet wings and accordingly minimise the likelihood of future fatigue related maintenance.

Figure 99: The first RNZAF aircraft undergoing upgrade in Edmonton

8.5.2 C-130 Operational Usage Monitoring (M. J. Hollis, S. K. Campbell, DTA, New Zealand)

The RNZAF are in the process of performing a Life Extension Programme (LEP) for their C-130 fleet. This is to include a significant enhancement of the flight deck and mission systems installed on the aircraft. As a precursor to the LEP, the Defence Technology Agency (DTA) has been conducting usage monitoring trials on one of the pre-LEP aircraft. The trials utilize commercial data recorders (Reported to ICAF 05).

While the statement of operating intent for the upgraded fleet is not significantly different to the current fleet, it was decided that a comparison between pre- and post-upgrade mission profiles is needed. Consequently, a data collection

phase was initiated in late 2006 aimed at capturing the pre-upgrade baseline mission profiles for RNZAF C-130 operations.

After initial ground and flight calibration, the RNZAF system has been cleared for operational use and is currently fully functional and collecting data, including GPS based groundspeed and altitude, airspeed, absolute cabin pressure, wing strains at four locations, normal acceleration and a number of other parametric data. The strain and normal acceleration data is being collected at 100 Hz to allow for the identification of lower frequency dynamic events.

8.5.3 Autonomous Processing of Aircraft Usage Data (S.K.Campbell, DTA, New Zealand)

The development of an Operational Usage monitoring system utilizing commercially available digital data recorders has presented a number of challenges for the processing, analysis and display of the collected data.

In its current configuration, the RNZAF usage monitoring system is recording approximately 25 channels of data, sampled at rates varying between 1 Hz (GPS based altitude) and 100 Hz (strain gauges, normal acceleration). Typically this produces approximately 25 MB of data per flight hour. The RNZAF sought to develop an autonomous data processing system that performs data checking and initial analysis with minimal operator input.

A data analysis and processing system has been developed using a combination of commercially available tools. Primarily, the processing is conducted using nCode's GlyphWorks toolsets for data analysis, open standards (XML, HTML) report generation. The scripting language Python is used to integrate the processing steps. The data processing system is capable of detecting and correcting anomalies such as sensor drift, sensor failure, data "flat lines", signal spikes, signal noise and invalid (outside limits) data. While these anomalies are detected and corrected automatically, a copy of the original un-corrected data is retained and archived to retain integrity. Once the data anomalies have been corrected a number of automated reports are generated and published in either XML or HTML format. These include flight by flight mission profiles (Figure 100), strain and 'g' traces (Figure 101) and the normal acceleration exceedance curve is updated (Figure 102).

The initial data processing is fully automated working in batch mode from the data storage location with the results published directly to an intranet web server.

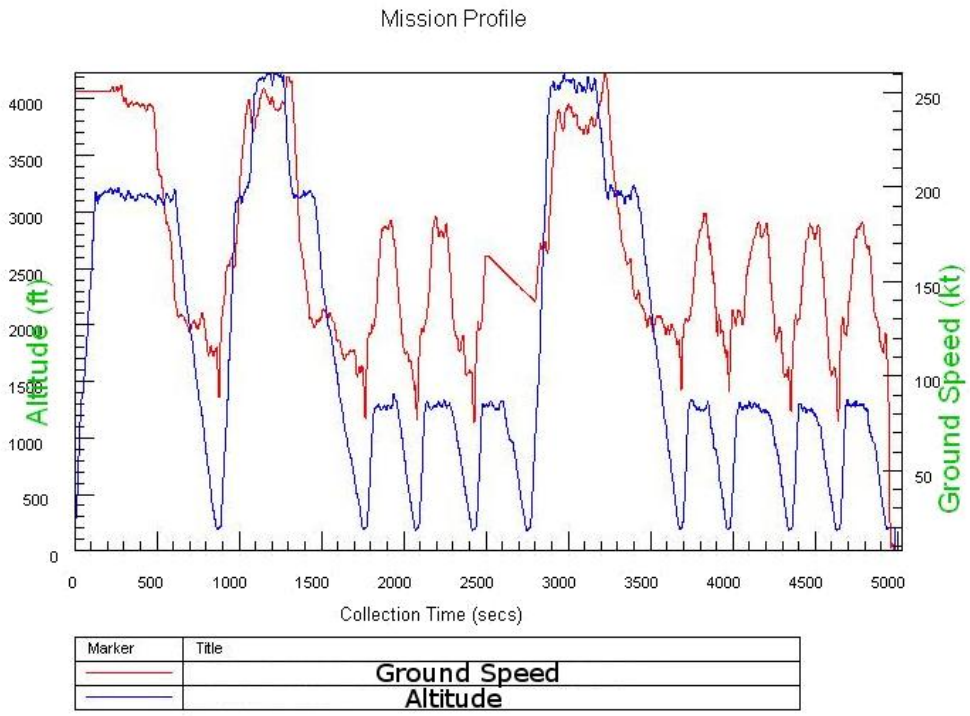

Figure 100: A typical Mission Profile graph showing GPS measured groundspeed (Red) and Altitude (Blue)

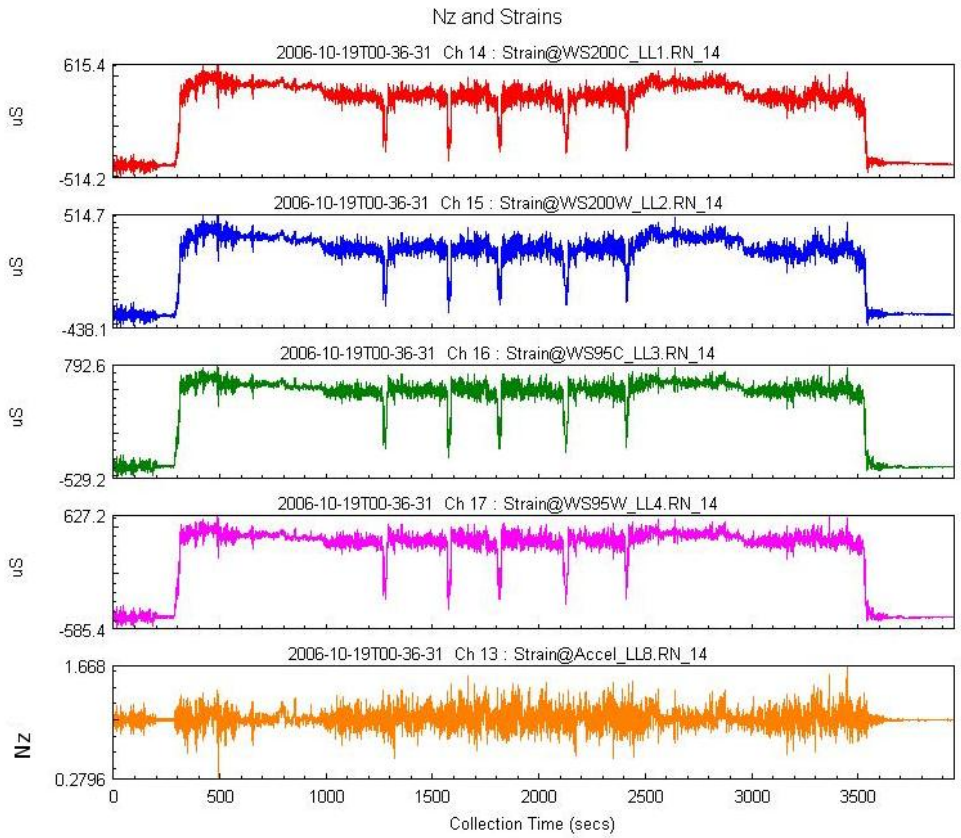

Figure 101: Typical strain and normal acceleration traces

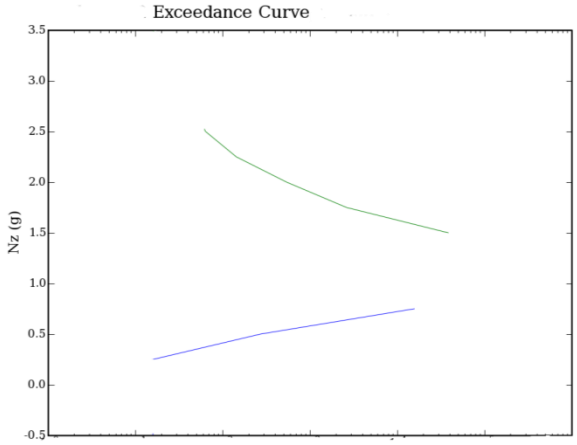

Figure 102: Normal Acceleration Exceedance curves are updated after each flight

DEFENCE SCIENCE AND TECHNOLOGY ORGANISATION
DOCUMENT CONTROL DATA

1. PRIVACY MARKING/CAVEAT (OF DOCUMENT)

2. TITLE

A Review of Australian and New Zealand Investigations on Aeronautical Fatigue During the Period April 2005 to March 2007

3. SECURITY CLASSIFICATION (FOR UNCLASSIFIED REPORTS THAT ARE LIMITED RELEASE USE (L) NEXT TO DOCUMENT CLASSIFICATION)

Document	(U)
Title	(U)
Abstract	(U)

4. AUTHOR(S)

Graham Clark

5. CORPORATE AUTHOR

Defence Science and Technology Organisation
506 Lorimer St
Fishermans Bend Victoria 3207 Australia

6a. DSTO NUMBER	6b. AR NUMBER	6c. TYPE OF REPORT	7. DOCUMENT DATE
DSTO-TN-0747	AR-013-873	Technical Note	April 2007

8. FILE NUMBER	9. TASK NUMBER	10. TASK SPONSOR	11. NO. OF PAGES	12. NO. OF REFERENCES
M1/8/1709	A20227B (AE/MGT - TTCP)	CAVD	91	60

13. URL on the World Wide Web

http://www.dsto.defence.gov.au/corporate/reports/DSTO-TN-0747.pdf

14. RELEASE AUTHORITY

Chief, Air Vehicles Division

15. SECONDARY RELEASE STATEMENT OF THIS DOCUMENT

Approved for public release

OVERSEAS ENQUIRIES OUTSIDE STATED LIMITATIONS SHOULD BE REFERRED THROUGH DOCUMENT EXCHANGE, PO BOX 1500, EDINBURGH, SA 5111

16. DELIBERATE ANNOUNCEMENT

No Limitations

17. CITATION IN OTHER DOCUMENTS Yes

18. DEFTEST DESCRIPTORS

fatigue, fatigue tests, military aircraft, civil aircraft, research projects, Australia, New Zealand

19. ABSTRACT

This document has been prepared for presentation to the 30th Conference of the International Committee on Aeronautical Fatigue scheduled to be held in Naples, Italy, 14th and 15th May 2007. Brief summaries and references are provided on the aircraft fatigue research and associated activities of research laboratories, universities, and aerospace companies in Australia and New Zealand during the period April 2005 to March 2007. The review covers fatigue–related research programs as well as fatigue investigations on specific military and civil aircraft.